

**INTRAFASCICULAR MULTIELECTRODE STIMULATION
STRATEGIES FOR NEUROPROSTHETIC APPLICATIONS**

by

Brett Ross Dowden

A dissertation submitted to the faculty of
The University of Utah
in partial fulfillment of the requirements for the degree of

Doctor of Philosophy

Department of Bioengineering

The University of Utah

May 2012

Copyright © Brett Ross Dowden 2012

All Rights Reserved

ABSTRACT

Paralysis can be ameliorated through functional electrical stimulation (FES) of the intact peripheral nerves. The Utah Slanted Electrode Array (USEA) can improve FES systems by providing selective access to many independent motor unit populations. This dissertation includes three studies that expand the role of USEAs in FES applications.

The first study leverages the selectivity of the USEA to independently activate the hamstring muscles. Because the different biarticular hamstring muscles can either flex or extend the limb (at the knee or hip), the ability to selectively activate each one independently is required to evoke functional movements such as stance and gait. USEAs implanted in the muscular branch of the sciatic nerve were able to selectively activate each muscle of the hamstring group. Activation of these muscles was graded with increasing stimulus strength, and provided ample dynamic range to allow for fine control of muscle force.

The second study demonstrates the ability of the USEA to selectively block neural activity. Upper motor neuron damage can cause hyperreflexia and spasticity as well as paralysis. By delivering high-frequency sinusoids through electrodes of the USEA, fiber subsets in a nerve were blocked while allowing the remainder of the nerve to function normally. Sinusoids delivered through different electrodes allowed for deactivation of different muscles. The ability to selectively interrupt activity in fiber subpopulations within a nerve will provide new therapeutic options for the positive symptoms of upper motor neuron damage.

The final study addresses the practical difficulty of choosing the appropriate stimulus parameters to evoke functional movements. In a USEA-based FES system, the electrodes and stimulus parameters that evoke the desired responses must be identified empirically. USEAs were implanted into three different hind limb nerves,

and the response evoked by each electrode was measured noninvasively using 3-D endpoint force. Each electrode was classified as evoking limb flexion or limb extension, and a range of stimulus intensities was identified that evoked a graded force response. Excitation overlap between selected electrode pairs was quantified using the refractory technique. This method will allow for electrode and stimulus parameter selection for use in an FES system using minimal, noninvasive instrumentation.

To everyone living with neural deficits who hopes for something better.

CONTENTS

ABSTRACT	iii
LIST OF FIGURES	ix
LIST OF TABLES	x
ACKNOWLEDGMENTS	xi

Chapter

1. INTRODUCTION	1
The Neuromuscular System	2
Nerve Anatomy	3
Excitation-Contraction Coupling	4
The Motor Unit	6
Injury to the Neuromuscular System	7
Spinal Cord Injury	8
Stroke	9
Spasticity	9
Electrical Activation of Muscles and Nerves	10
Surface Electrodes	11
Epimysial Electrodes	11
Intramuscular Electrodes	12
Peripheral Nerve Electrodes	14
Epineural Electrodes	14
Intrafascicular Electrodes	17
Research Outline	21
Selective Activation of Hamstring Muscles	21
Selective Block of Muscle Activation	22
Noninvasive Selection of Stimulus Parameters	23
References	25
2. SELECTIVE AND GRADED RECRUITMENT OF FELINE HAMSTRING MUSCLES WITH INTRAFASCICULAR STIMULATION	36
Abstract	36
Introduction	37
Methods	38
Animal Preparation and Surgery	38

Stimulation and Recording Setup	39
Experimental Design	40
Data Analysis	41
Results	43
Surgical Access	43
Hamstring Activation at Perithreshold	43
Musculotopic Organization	43
Validation of EMG Normalization	45
Selective Muscle Activation	46
Stimulus Dynamic Range and Recruitment Width	50
Discussion	50
Conclusion	52
References	54
3. MUSCLE-SELECTIVE BLOCK USING INTRAFASCICULAR HIGH-FREQUENCY ALTERNATING CURRENT	57
Abstract	57
Introduction	57
Methods	59
Surgical Preparation	59
Stimulation and Recording Setup	60
Block Using HFAC	61
Classification of Responses to HFAC	62
Results	64
Nonselective Neuromuscular Block Using a Cuff Electrode	64
Selective Neuromuscular Block Using USEA Electrodes	66
Simultaneous Neuromuscular Block and Muscle Activation Using USEA Electrodes	68
Prolonged Muscle Block Using USEA Electrodes	71
Conduction Block Using USEA Electrodes	71
Discussion	76
Copyright	79
References	80
4. NONINVASIVE METHOD FOR SELECTION OF ELECTRODES AND STIMULUS PARAMETERS FOR FES APPLICATIONS WITH INTRAFASCICULAR ARRAYS	82
Abstract	82
Introduction	83
Methods	84
Surgical Preparation	84
Stimulation and Recording Hardware	88
Data Analyses	89
Excitation Overlap	91
Results	93
Determining the Stimulus Range for Each Electrode	94

Classifying Flexor or Extensor Activation	96
Excitation Overlap of Electrode Pairs	98
Discussion	98
Conclusion	105
References	106
5. CONCLUSION	110
Summary of Major Findings	110
Technological Developments	111
Limitations	112
Future Work	114
References	118

LIST OF FIGURES

1.1 Nerve Cross Section	3
1.2 Epimysial Electrodes	12
1.3 Intramuscular Electrodes	13
1.4 Spiral Cuff Electrodes	16
1.5 Flat Interface Nerve Electrode	17
1.6 Longitudinal and Transverse Intrafascicular Electrodes	19
1.7 Utah Slanted Electrode Array	20
2.1 Muscular Branch Implantation	40
2.2 Perithreshold Activation of Hamstring Muscles	44
2.3 Threshold Map From 1 Animal	45
2.4 EMG Recruitment Curve	46
2.5 Selective Activation of Each Muscle	47
2.6 Selectivity Indices at Three Levels of Muscle Activation	49
3.1 Experimental Setup	60
3.2 Nonselective Block Using a Cuff Electrode	65
3.3 Block Using an Intrafascicular Electrode	67
3.4 Sustained Activation and Block	69
3.5 Block and Activation Using 2 USEA Electrodes	72
3.6 Activation was Unaffected by Block on Another Electrode	73
3.7 Block for 30 minutes	74
3.8 Conduction Block	75
4.1 Limb Position and Load Cell Axes	87
4.2 Characterization of Two USEA Electrodes	95
4.3 Force Vectors Evoked by Intramuscular and USEA Stimulation	97
4.4 Classification of USEA Electrodes Using IM-Evoked Forces	99
4.5 Excitation Overlap Using Force Vectors	101

LIST OF TABLES

3.1 Classification of HFAC Trials	63
3.2 HFAC Block with USEA Electrodes	66
3.3 HFAC Parameters Tested Using USEA Electrodes and the Evoked Effects	70
4.1 Instrumented Muscles	85
4.2 Number of Electrodes Activating each Muscle	100

ACKNOWLEDGMENTS

This work would not have been possible without the funding provided by the American taxpayers through the National Institutes of Health grants R01-NS039677 and R01-NS064318-01A1, as well as the Defense Advanced Research Projects Agency grant N66001-06-C-8005.

CHAPTER 1

INTRODUCTION

The ability to move our body throughout our surroundings with precision and power is something that most of us take for granted. Even the simplest motor task is the result of a complex orchestration of neural and muscle activity that usually goes unnoticed until it is disrupted by injury or disease. Injury to the neuromuscular system, such as spinal cord injury or stroke, can result in paralysis and have devastating consequences on physical and psychological health. Many congenital disorders disrupt the normal function of the neuromuscular system and leave the individual with little or no control over their movements.

Although each injury and disease is different, in many cases, impaired motor function can be partially restored through electrical stimulation of muscles or the nerves that innervate them. The objective of restoring impaired motor function through electrical stimulation has been a pursuit of scientists and physicians since the discovery of electricity. Armed with modern electronics and manufacturing processes, researchers in the field now known as functional electrical stimulation (FES) have been able to restore some function to people with neuromuscular deficits. FES systems have been created that enable control of a paralyzed arm for reaching and grasping [1, 2], that control paralyzed lower limbs for sit-to-stand transitions and gait [3], and allow for bladder voiding [4]. Although a boon to many people living with paralysis, the functionality of current FES systems is poor compared with the coordination and endurance of natural movement [5]. The implementation and performance of FES systems will be described in greater detail below.

Each muscle in the human body is made up of hundreds to thousands of motor units—independent sets of muscle fibers, each of which is innervated by a single motoneuron [6]. An intact central nervous system controls the timing and frequency

of activation of each motor unit to produce smooth, controlled movements with the force required for any given task. Although a single peripheral nerve may innervate several muscles—and each muscle may have hundreds of individual motor units—conventional peripheral nerve electrodes are capable of exciting at most a handful of independent motor unit populations within a nerve [7, 8]. At best, this allows activation of one or two muscles individually and at worst, simultaneous activation of all muscles innervated by the nerve. This poor selectivity to the neuromuscular system permits only gross motor control. The functionality of FES systems could be greatly improved if selective access to individual motor units began to approach that of the central nervous system.

The work described in this dissertation attempts to improve upon the successes of current FES systems by leveraging the highly selective interface with the peripheral nervous system afforded by penetrating microelectrode arrays. Before the specifics of the research are presented, relevant anatomy and physiology of the neuromuscular system will be described as well as several disease states that impair its function. Next, various electrical interfaces to the peripheral nervous system will be described, followed by a brief outline of the research presented.

The Neuromuscular System

The neuromuscular system consists of the central nervous system, the peripheral nervous system, and the smooth and skeletal muscles. Command signals are sent from the motor centers of the brain and spinal cord to the muscles through peripheral nerves leading to muscular contraction. Sensory nerve fibers in the muscles and tendons relay muscle force and length information back to the central nervous system, creating a closed-loop feedback system. When trauma partially or completely severs the spinal cord, the control signals from the brain can no longer reach the muscles and effect movement. However, the peripheral circuitry for movement and sensory feedback remains intact, allowing for the possibility of external control of the paralyzed musculature. The use of external devices to replace lost neural function is called neuroprosthetics.

Nerve Anatomy

Nerves are a collection of individual axons (also called fibers), each of which has a specific target. Axons within the nerve, along with supporting glial cells, course in bundles called fascicles, which are surrounded by perineurium. These fascicles and associated vasculature are bound together by a tough and flexible sheath of connective tissue called epineurium (Figure 1.1). At a proximal location, a single nerve contains fibers innervating many different targets; as the nerve approaches those targets, it eventually branches into smaller nerves. Microdissection of the human femoral [9]

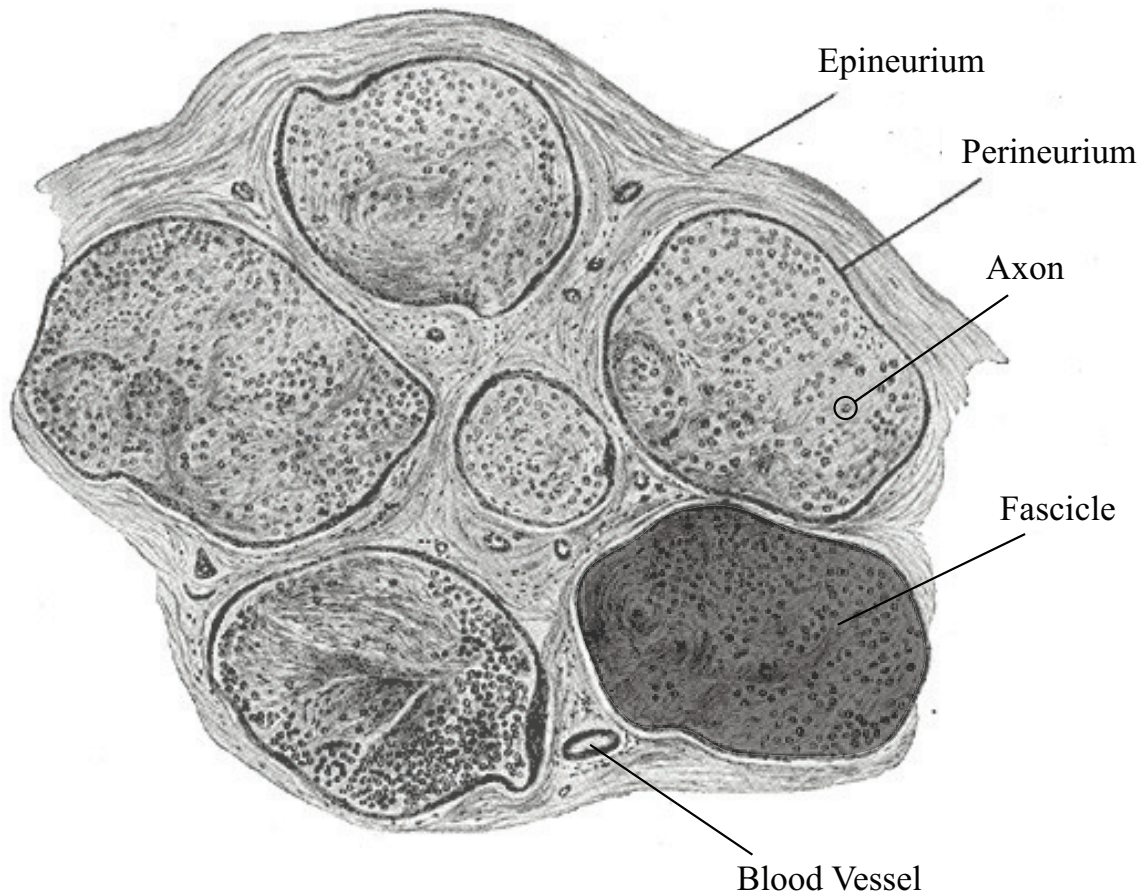


Figure 1.1: Nerve Cross Section

A stained cross section of a peripheral nerve shows the bundles of axons called fascicles. Individual fascicles are surrounded by connective tissue called perineurium, and the fascicles and vasculature are bound together by the epineurium. (Modified from Gray's Anatomy, public domain)

and pudendal [10] nerves suggests that the location of nerve fascicles within a main nerve trunk is similar to their eventual branch locations. Similar studies in cat sciatic nerve show a functional grouping of fascicles within the proximal nerve trunk that is similar to its eventual branches [11, 12, 13]. This grouping of nerve fibers with similar targets makes the demands for selectivity of a nerve interface somewhat less stringent because many fibers surrounding an electrode are likely to have similar targets. Therefore, as stronger stimuli are delivered and the charge spreads farther from the electrode, the fibers that are excited will likely innervate similar targets, and thus the evoked effects will be similar.

A single nerve may contain motor fibers innervating several different muscles, as well as contain sensory fibers from those muscles and also cutaneous receptors from surrounding skin. For example, the sciatic nerve of the cat contains motor fibers that innervate all the musculature of the lower leg and digits. Thus, ankle plantar-flexion, ankle dorsi-flexion, inversion and eversion of the foot, as well as flexion and extension of the digits are all mediated via fibers contained in the sciatic nerve. A neural prosthetic system hoping to control foot motion would have access to motor channels to effect movement as well as sensory feedback channels to modify outgoing control commands. In the example of the sciatic nerve, a sufficiently selective peripheral nerve interface along with an appropriately designed control system would allow for near-natural control of the ankle joint and foot.

Excitation-Contraction Coupling

The nerve cells that innervate skeletal muscles are called alpha-motoneurons. The initiation of an action potential in an alpha-motoneuron faithfully leads to a muscle contraction through a well-understood series of events. The specifics of this process are not crucial to understanding the research presented in this dissertation and thus are described only briefly. However, one step of the process, synaptic vesicle release and recycling, is of particular relevance to Chapter 3 and will be presented in greater detail.

The synapse between an alpha-motoneuron and a muscle cell is called the neuromuscular junction (NMJ). Depolarization of the presynaptic terminal by the incoming

action potential triggers the opening of voltage-gated Ca^{2+} channels. The incoming Ca^{2+} ions act to release a pool of docked synaptic vesicles through action on the SNARE (soluble N-ethylmaleimide-sensitive fusion protein attachment protein receptor) protein complex [14, 15]. This pool of vesicles ready for immediate release is called the readily releasable pool (RRP), and represents about 1-2% of the total number of vesicles in the presynaptic terminal [16]. Although the exact details of vesicle storage and reuptake are not fully understood, a review by Rizzoli and Betz [16] presents evidence that suggests there are three pools of synaptic vesicles in the NMJ—the readily releasable pool, the recycling pool, and the reserve pool—each of which has different release and reuptake characteristics. During periods of normal synaptic activity, the RRP and recycling pool mediate transmitter release. Vesicles from the RRP pool dock with the membrane and then undergo rapid endocytosis to rejoin the recycling pool, which in turn replenishes the RRP. Vesicles in the reserve pool are only mobilized during sustained intense activity in which the recycling pool becomes depleted. Reserve pool vesicles are reclaimed through a slow process of endocytosis that likely involves a large reclamation of membrane and subsequent division into individual vesicles once inside the cell.

The acetylcholine (ACh) released from these vesicles diffuses across the synaptic cleft to bind to nicotinic acetylcholine receptors in the muscle fiber membrane. Na^+ ions enter the cell through these receptors and depolarize the muscle cell. The depolarization of the muscle fiber in response to binding of ACh is called an end-plate potential. A special feature of the NMJ is that, under normal circumstances, the amount of ACh released by a single presynaptic action potential always evokes an end-plate potential that is sufficiently large to trigger an action potential in the muscle cell. The action potential in the muscle fiber propagates along the muscle fiber membrane and into the T-tubule network inside the cell where it triggers the release of Ca^{2+} from the sarcoplasmic reticulum. The Ca^{2+} enters the cytoplasm and binds to troponin C causing a conformational change in the troponin complex, which exposes cross bridge binding sites on the actin filaments. With the binding sites now exposed, the head of myosin filaments bind to actin filaments and pull the two

ends of the sarcomere towards each other, thus generating muscle force. Repeated excitation from the alpha-motoneuron results in repeated Ca^{2+} release and increased force generation. This graded force production in response to repeated activation eventually saturates, and further increases in muscle force require activation of a larger number of alpha-motoneurons and their corresponding muscle fibers. Thus, exogenous generation of muscle force through the use of electrical stimulation of peripheral nerves can be graded by activating different numbers of alpha-motoneurons, or by activating them at different frequencies.

The Motor Unit

Sir Charles Sherrington coined the term motor unit in 1925 to represent a single alpha-motoneuron and the collection of muscle fibers it innervates [17]. An action potential in the motoneuron reliably results in activation of all the muscle fibers it innervates, making the motor unit the smallest discrete unit of motor function. Although the term motor unit was created in 1925, the quantal nature of muscle twitch force was demonstrated by direct electrical activation of efferent fibers in 1913 [18], and also for reflex activation via stimulation of afferent fibers in 1923 [19]. These experiments showed that a single motor unit responds in an all-or-none fashion, and that the twitch forces produced by different motor units are not necessarily equal.

Histological examination of cat hind limb nerves by Eccles and Sherrington revealed a dispersion of motor axon diameters, and the authors hypothesized that axons with larger diameters innervated a greater number of muscle fibers than axons with smaller diameters [6]. This hypothesis was lent experimental support when Henneman and colleagues showed that the force produced by a motor unit was proportional to its axonal conduction velocity, and thus axon diameter [20, 21]. Henneman and colleagues continued to investigate the characteristics of motor units of different sizes and determined that there is an orderly recruitment of motor units based on their size. Using the stretch reflex in the cat triceps surae, they found that the first motor units to be recruited were always small and that additional forces were produced by progressively larger motor units [22]. Although this phenomenon was

first reported by Denny-Brown and Pennybacker in 1938 [23], it is referred to as the Henneman size principle due to his statistical characterization and identification of cellular mechanisms.

Variations in axon diameter and twitch force are not the only differences amongst different motor units. The time course of the twitch response, fusion frequency, and fatigue characteristics vary as well. Fusion frequency is the rate of activation that produces a smooth, ripple-free contraction. These differences correlate well to the myosin heavy chain (MHC) isoform present in the muscle fibers of a given motor unit. Four MHC isoforms have been identified: Type-I, Type-IIa, Type-IIb, and Type-IIx—though not all isoforms are present in each species [24]. The Type-I isoform is present in slowly contracting motor units called slow-twitch motor units. Slow-twitch units express large amounts of oxidative enzymes and are very slow to fatigue. Type-II isoforms are present in rapidly contracting motor units called fast-twitch motor units. The various Type-II motor units vary in their time to fatigue. Type-IIb and Type-IIx units produce very strong forces and fatigue rapidly. Type-IIa units produce an intermediate amount of force and are slower to fatigue than the Type-IIb/x units [25, 26]. In part because Type-I motor units are innervated by small diameter axons, they are recruited first during muscle contractions according to the size principle stated above. These fatigue-resistant fibers sustain the contraction unless greater force is needed, at which time the larger, fatigable units are recruited. As contraction force increases, motor units that are active increase their firing rate and new motor units are added [27]. This orderly recruitment serves to produce smooth contractions of graded force and to minimize fatigue during natural movement.

Injury to the Neuromuscular System

Under normal circumstances the brain, spinal cord, peripheral nervous system, and muscles act in concert to control movement. Damage to any of these components of the neuromuscular system can cause loss of motor function ranging from weakness or discoordination to complete paralysis. Although this system can malfunction in

many ways, I will present three major causes of motor deficit that have potential to be improved by FES: spinal cord injury, stroke, and spasticity.

Spinal Cord Injury

Trauma to the spinal cord can interrupt communication between the brain and the periphery, resulting in loss of volitional motor control and sensation. The specific functions affected depend on the level and severity of the injury. The cervical spinal cord innervates the neck, arms, and diaphragm, and injuries to this region usually result in partial or complete tetraplegia. Injuries at the third cervical vertebra and above can result in loss of diaphragm innervation and the inability to breathe without an external ventilator. Thoracic spinal cord injuries spare arm and hand function but can result in paralysis of the legs. Regardless of the level of injury, 81% of persons with spinal cord injury (SCI) report problems with bladder function and 63% report problems with bowel function [28]. Along with loss of sexual function, bladder and bowel function rank as the most problematic symptoms for SCI patients [29, 30].

According to the National Spinal Cord Statistical Center, there are approximately 265,000 people in the United States living with SCI, and there are about 12,000 new cases each year [31]. A study done by the Christopher and Dana Reeve Foundation places the estimate much higher at 1,275,000 people living with SCI [32]. In most countries across the world, motor vehicle accidents are the leading cause of SCI [33]. In the US, the most common causes of SCI are motor vehicle accidents (40.4%), falls (27.9%), and acts of violence (15%). Since 2005, the average age at the time of injury is 40.7 [31]. The life expectancy after injury and the total cost of medical care depend greatly on the level and severity of the injury. A 25-year-old with high tetraplegia could expect to live another 35 years and have lifetime medical expenses in excess of 4 million dollars, whereas a 40-year-old with a motor incomplete injury would have virtually no change in life expectancy and lifetime medical expenses of 1 million dollars [31]. In the past, the leading cause of death for persons with SCI was renal failure, but improvements in urologic management have mitigated much of this

risk and now the leading causes of death for persons with SCI are pneumonia and septicemia [31].

The paralysis often accompanied by SCI results from severed connections between the brain and lower spinal circuits and musculature. However, the peripheral nerves and muscles, as well as many spinal circuits are spared and remain somewhat functional. This leaves open the possibility of electrically stimulating these peripheral tissues and artificially controlling movement.

Stroke

Stroke is the leading cause of disability in the United States [34]. A stroke occurs when vasculature in the brain becomes blocked or ruptures. This lack of blood flow causes ischemic tissue damage and corresponding loss of normal brain function. Because stroke can damage any portion of the brain with varying degrees of severity, the outcome can be as devastating as death or locked-in syndrome—where a person is conscious but unable to move or communicate—to as mild as dizziness. Although spinal cord injury is a well-known cause of paralysis, more people suffer from paralysis caused by stroke than by spinal cord injury [32]. Each year, approximately 795,000 people in the United States have a stroke and half of stroke survivors experience hemiparesis or hemiplegia [35, 34]. As with the paralysis caused by SCI, strokes damage the central motor pathways, and spare the peripheral nerves and musculature, leaving open the possibility of functional restoration through electrical stimulation of the paralyzed muscles.

Spasticity

Unlike paralysis, spasticity is a pathological increase in muscle activity. It is defined as a velocity-dependent increase in the tonic stretch reflex with exaggerated tendon jerks, clonus, and spasms resulting from the hyper-excitability of the stretch reflex [36, 37]. Spasticity arises from upper motor neuron lesions, which can result from a variety of causes including stroke, spinal cord injury, cerebral palsy, multiple sclerosis, and traumatic or anoxic brain injury. The mechanisms of spasticity are different for different types of upper motor neuron lesions. Spasticity arising after stroke

appears to be largely due to changes in the tendon and intrinsic muscle stiffness with some degree of hyperreflexia, whereas spasticity arising after SCI is predominantly neurological in origin [38, 37]. Normally, the monosynaptic stretch reflex receives presynaptic inhibition from supraspinal fibers. After SCI, this inhibition is removed which can lead to overactivity of the stretch reflex and is thought to contribute to spastic muscle tone [37].

The incidence of spasticity is not well documented, in part due to the various metrics used by different studies, and the different combinations of motor impairments caused by different types of upper motor neuron lesions [39]. It is estimated that 17% to 38% of stroke survivors and 40% to 78% of people with SCI have some degree of spasticity [40, 39]. Available data suggest that 2,584,000 people in the United States have spasticity and for just over 1,000,000 people, spasticity impairs activities of daily living and requires some form of treatment [39].

High-frequency electric currents have been shown to block action potential conduction in peripheral nerves [41]. Because some spasticity is thought to arise from overactivity of the stretch reflex, it may be possible to prevent spastic muscle activity by blocking action potentials somewhere in these reflex circuits. The blockade could be delivered to the sensory fibers, thus removing their excitation of the motoneurons, or the blockade could be delivered to the motoneurons themselves. Although the mechanisms of spasticity and their effects on motor function vary widely, it is possible that some patients could benefit from this type of block.

Electrical Activation of Muscles and Nerves

Paralyzed muscles can be activated to restore movement by means of electrical stimulation. Both nerve and muscle tissue conduct action potentials and are thus both excitable by extrinsic electric currents. However, the stimulation current required to activate muscle cells is considerably larger than that required to activate nerve cells [42]. For this reason, nearly all electrical activation of muscle is elicited by exciting action potentials in the nerve that innervates the target muscle and allowing the nerve to distribute the excitation throughout the muscle. Many different types of electrodes

have been used to deliver electric stimuli in FES applications, and each has a different balance between invasiveness and selectivity.

Surface Electrodes

The simplest and least invasive type of electrode for FES is the surface electrode. These electrodes consist of a conductive pad placed on the surface of the skin over a targeted muscle or nerve. An electrolytic gel is usually applied to maintain a conductive contact between the electrode and skin. Surface electrodes have been used extensively in FES applications for foot drop [43, 44, 45], standing and walking prostheses [46, 47, 48, 49], and upper limb prostheses [50, 51, 52, 53]. The current amplitudes used with surface electrodes range from 25 mA up to 140 mA. Although surface electrodes are simple and effective, they suffer several drawbacks for use in FES systems. Surface electrodes are unable to selectively activate deep muscles or nerves, and they must be regularly placed and removed, causing variations in the input-output relationship between stimulus strength and muscle force. Also, patients are often dissatisfied with the visual appearance of externally placed electrodes [30]. Thus, to improve the cosmetic appearance of the electrodes and to create a more selective and permanent interface to evoke muscle activation, several types of implantable electrodes have been developed for FES.

Epimysial Electrodes

Epimysial electrodes are placed on the surface of the targeted muscle, beneath the skin (Figure 1.2). This subcutaneous placement allows for epimysial electrodes to be fully implanted within the body, and eliminates the need for transcutaneous connectors if the stimulation and control circuitry is also implanted. Epimysial electrodes are placed near the motor point of the muscle, which is an empirically determined site where the stimulus strength required to activate the muscle is least. Activation usually requires 10–30 mA of current [55, 56]—less than half the current required for surface electrodes. The electrodes are usually sutured in place to prevent motion during muscle activation and movement. Epimysial electrodes have been used as part of a fully implanted system to restore hand grasp in tetraplegic patients with

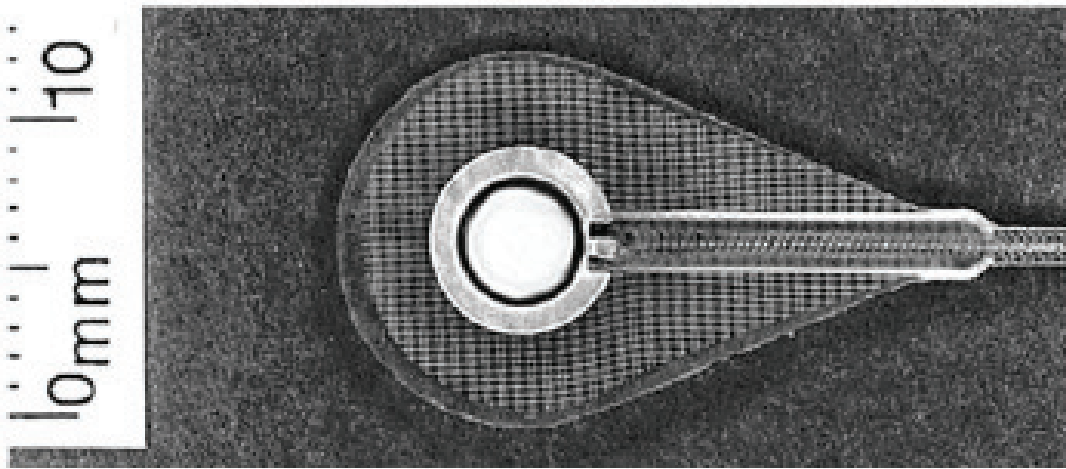


Figure 1.2: Epimysial Electrodes

Epimysial electrodes are implanted beneath the skin and sutured to the surface of the target muscle. This allows them to be fully implantable. (Reproduced with permission from Uhlir and colleagues [54])

excellent results [1]. Because epimysial electrodes are sutured to the muscle surface, the targeted muscle must be surgically exposed. This makes epimysial electrodes difficult to place on some deep muscles without extensive surgical dissection.

Intramuscular Electrodes

A versatile and commonly used electrode for FES is the intramuscular (IM) electrode. These electrodes are small, insulated wires with a portion of insulation removed, constituting the electrode surface (Figure 1.3). Intramuscular electrodes are inserted into the belly of a muscle using a hypodermic needle; a small bend in the wire at the tip acts as a barb to keep the electrode in place when the needle is removed. Intramuscular electrodes can be inserted through the skin for temporary experimentation, or implanted subcutaneously for long-term FES applications.

A common failure mode for chronically implanted IM electrodes is wire breakage due to repeated bending resulting from muscle contractions. To circumvent this problem, the wire is commonly wound into a coiled structure prior to implantation.

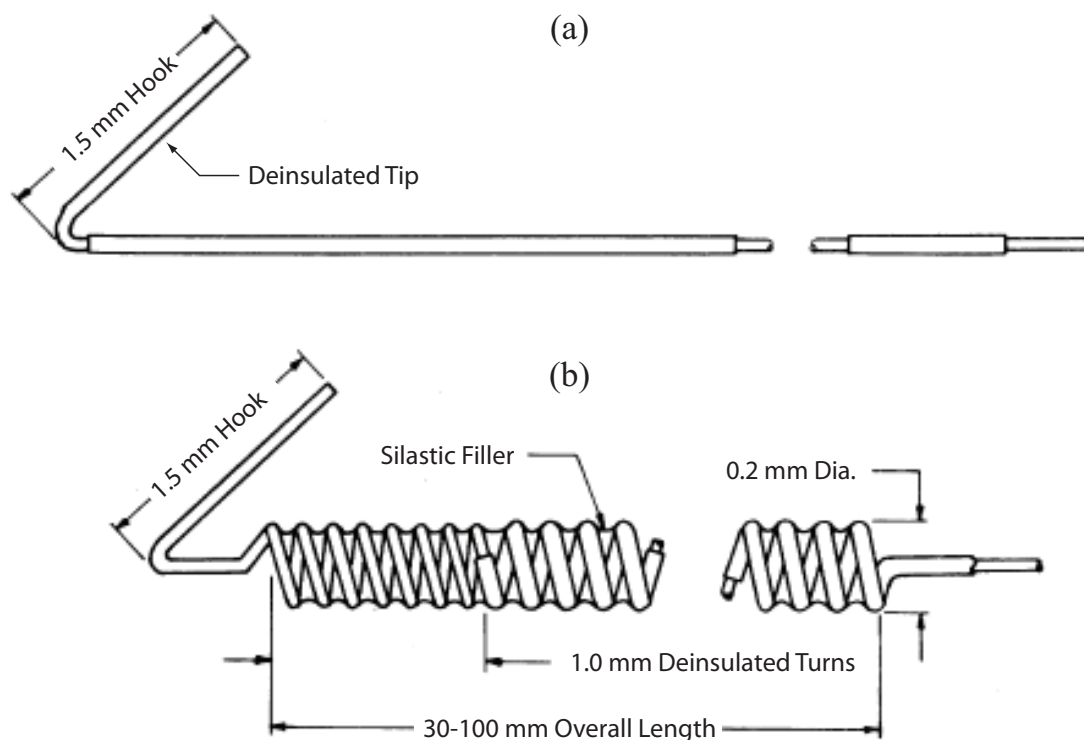


Figure 1.3: Intramuscular Electrodes

(a) Straight wire and (b) coiled wire intramuscular electrodes. A portion of the wires are deinsulated to serve as the active portion of the electrode. A sharp bend at the tip of the wire serves as a barb to keep the electrodes in place. (Reproduced with permission from Caldwell and Reswick [57])

The winding reduces the bending stresses on the wire and enhances the longevity of the electrodes [57, 42]. The use of multistranded wires also mitigates the effects of wire breakage.

Intramuscular electrodes are used in most current clinical FES systems. The second generation of the FreeHand system uses a combination of epimysial and intramuscular electrodes to enable tetraplegic patients to control wrist and forearm motion as well as grasp [2]. A fully implantable system for walking in patients with paraplegia also used a combination of epimysial and intramuscular electrodes. After

one year, the system was still functioning and the patient reported increased health and fitness due to its use [56]. In recent studies by Dutta et al., stimulation via IM electrodes supplemented the volitional control of walking by patients with incomplete spinal cord injury [58, 59]. Current levels reported for intramuscular stimulation are up to 20 mA [56, 60, 61]—slightly lower than those used for empirical electrodes.

Peripheral Nerve Electrodes

The muscle-based electrodes described above have been proven effective at reliably activating muscles for FES applications. They are simple in design and easy to employ; however, they suffer from several limitations. Because the electrodes are relatively far from the nerve tissue they are activating, large stimulus currents must be used, reducing the battery life of an implanted system. The distance between electrode and activated tissue also reduces the ability to maximally activate the targeted muscle without excitation spillover to neighboring muscles. Further, lead wire failures are common due to their location in or on contracting muscles.

To mitigate these problems, peripheral nerve electrodes have been developed. Instead of residing in or on the muscles, these electrodes are placed in or on the nerves that innervate the muscles. Because the electrodes are so much closer to the tissue they activate, stimulus currents are considerably lower and stimulation is more localized, even to the point that only small portions of the nerve can be selectively activated. This proximity also allows peripheral nerve electrodes to fully excite nerve tissue, which results in full muscle contractions because of the faithful distribution and transmission from nerve action potentials to muscle contraction. Peripheral nerve electrodes have the added benefit of being able to activate several muscles with a single implant, because most major nerve trunks innervate several muscles. As with muscle-based electrodes, there are several styles of peripheral nerve electrodes, each of which strikes a different balance between invasiveness and selectivity.

Epineural Electrodes

The most widely used peripheral nerve electrodes are those that reside on the outside of the nerve. The simplest form of epineural electrode is an insulated wire

secured on or near the nerve with a deinsulated portion at the tip [62]. This type of electrode can reliably activate the implanted nerve from threshold to saturation using stimulus currents up to 4 mA [62, 63, 11], but offers little selectivity within the nerve. Epineural electrodes have been used for many FES applications, including diaphragm pacing [64, 65], lower limb FES systems [66], and to evoke bladder contractions in patients with SCI [67].

In order to prevent migration of the electrode over time, epineural electrodes are commonly formed into a helix [68] or spiral [69] that encircles the nerve trunk and exerts a gentle compression that keeps the electrode in place (Figure 1.4(a)). Because of the circumferential nature of these electrodes, they are called cuff electrodes. In attempt to selectively activate portions of the nerve, more sophisticated cuff electrodes have been made that have multiple electrode contacts imbedded in silicone where the side of the electrodes towards the nerve is exposed [63, 70, 11] (Figure 1.4(b)). This prevents current from spreading away from the nerve and creates more focal stimulation under each electrode contact.

A study by Fisher and colleagues [71] directly compared the functionality of epimysial electrodes to epineural cuff electrodes in an FES system for standing in a patient with motor-complete SCI. They found that when the epimysial electrode on the knee extensor vastus lateralis was replaced with a cuff electrode on the femoral nerve—which innervates vastus lateralis—the patient was able to generate significantly more knee extension torque and was able to stand for longer durations. The cuff electrode not only could recruit vastus lateralis force more completely than the epimysial electrode, it could also recruit other knee extensor muscles to aid in standing.

The proximity of epineural electrode contacts to the nerve not only allows for more complete activation of the nerve, it also provides the potential for selective activation of subpopulations of fibers within the nerve. The ability of multicontact cuff electrodes to selectively stimulate portions of a nerve has been extensively studied in animal models [63, 11, 72], and recently in humans [73, 74]. These studies suggest that multicontact cuffs are often able to selectively excite individual fascicles within

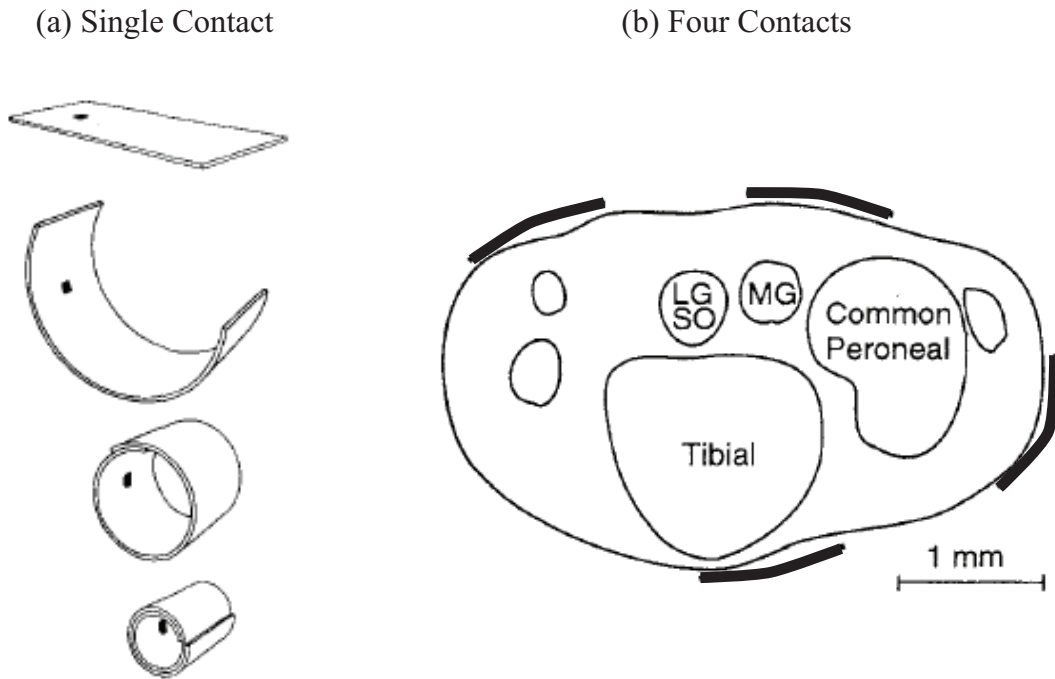


Figure 1.4: Spiral Cuff Electrodes

(a) Spiral cuff electrodes encircle the nerve. They have active electrode contacts embedded into the inside surface of the cuff so that the electrodes rest on the surface of the nerve. (b) Cuffs with multiple contacts can allow the electrode contacts (thick lines) to be positioned near different fascicles in the nerve. Reproduced with permission (a) from Naples and colleagues [69], (b) from Grill and colleagues [12].

small nerves such as the cat sciatic nerve. In the cases where individual fascicles innervate a single muscle, near branch points for example, multi-contact cuffs can selectively activate single muscles.

In the cases of larger nerves with more fascicles, the selectivity of spiral nerve cuffs is limited [75, 73]. This is due, in part, to the fact that large nerves have fascicles in the middle of the nerve that are not close to any electrode contact and thus cannot be stimulated without stimulating other fascicles as well. To mitigate this problem, a cuff electrode with a rectangular cross section was developed [8]. This electrode, called a flat interface nerve electrode (FINE), slowly reshapes the nerve from a round cross section to a rectangular cross section (Figure 1.5). This forces the nerve fascicles into a row, positioning them close to the cuff surface and the electrode contacts. The

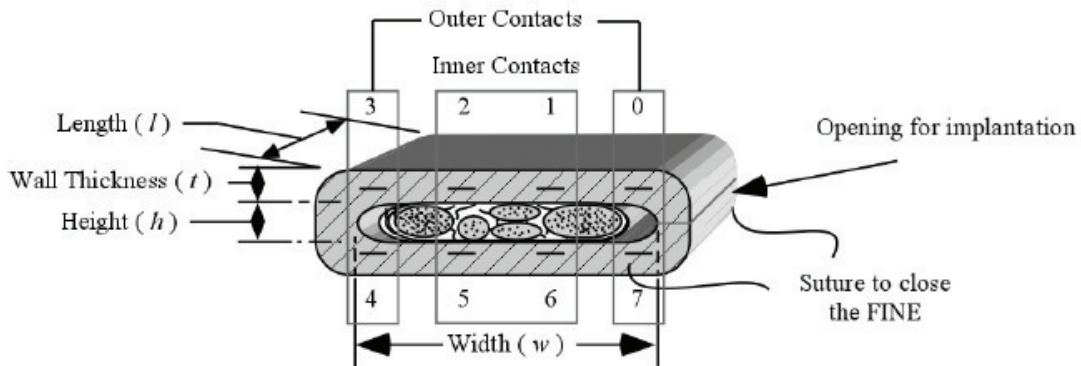


Figure 1.5: Flat Interface Nerve Electrode

The FINE exerts pressure on the nerve to reshape it into a rectangular cross section. This positions more electrode contacts on the surface of the cuff in close proximity to nerve fascicles, allowing for greater selectivity over spiral cuff electrodes. (Reproduced with permission from Tyler and colleagues [8])

FINE has been shown to selectively excite fascicles in the cat sciatic nerve [76, 77], and has recently been used in humans to selectively activate muscles innervated by the femoral nerve [74]. The typical FINE has eight electrode contacts allowing for a maximum of eight independent populations of axons within a nerve to be activated, doubling that of the traditional spiral cuff electrodes.

In summary, epineural electrodes allow for graded activation of a nerve from threshold to saturation. By including multiple contacts on the surface of the electrode and by reshaping the nerve geometry, epineural electrodes can selectively activate a handful of independent groups of fibers within the nerve. This degree of selectivity allows for activation of different fascicles in small nerves but only allows for a small degree of subfascicular selectivity [78, 76].

Intrafascicular Electrodes

Although multicontact extraneural electrodes allow for several independent sets of fibers within a nerve to be activated, the selectivity of these types of electrodes is

poor compared to that of natural neuromuscular function—where hundreds of motor units per muscle act to produce movement. To further improve the selectivity of peripheral nerve electrodes, the active electrode contacts must be located inside the nerve. Microelectrodes that penetrate into nerve fascicles have been used to stimulate and record from single nerve axons since the late 1960s [79, 80]. Previous studies of single nerve fibers required extensive dissection of nerve rootlets, and thus prevented investigations in intact animal preparations and human subjects [81, 82]. Because penetrating microelectrodes can be inserted without extensive dissection of the nerve, they allow for studies in intact animal preparations and human subjects, and have been used extensively to study the physiology of the sensory and motor systems [80, 83, 84, 85, 86, 87].

Researchers in the field of FES saw the potential performance improvements that might be gained from such fine access to the nervous system, and began to develop intrafascicular electrodes that would be well suited for use in FES systems. Schoenberg and colleagues at the University of Utah developed an electrode that could be threaded into nerve fascicles for short distances, thus placing a small active electrode contact within the nerve fascicle [88, 89, 90] (Figure 1.6(a)). These longitudinal intrafascicular electrodes (LIFEs) were used to stimulate motor fibers, and allowed for finely graded control of muscle force using 10–150 μA current amplitudes [91]. Yoshida and Horch demonstrated that LIFEs were able to excite independent groups of motor units within a single fascicle [92]. By alternating activation of two independent groups of motor units, they were able to evoke contractions that were slower to fatigue than contractions evoked using concurrent activation of both groups of motor units [93]. Yoshida and Horch continued to demonstrate the potential of LIFE electrodes for FES applications by creating a closed-loop system in cat that controlled ankle position by stimulation of medial gastrocnemius based on muscle spindle activity recorded from the tibialis anterior and lateral gastrocnemius muscles [94].

The construction of LIFEs has continued to evolve from the initial platinum-iridium wires [88] to polymer-based [95] and polyimide-based thin-film versions [96]. Along with advanced signal processing techniques [97, 98], LIFEs are now being

used to develop neurally-integrated prosthetic limbs [99, 100]. In an effort to access more independent axon populations with a single implant, a transverse intrafascicular multichannel electrode (TIME) has been developed [101] (Figure 1.6(b)). The TIME is similar to the LIFE, but currently has five contacts and is inserted transversely to span the cross section of the nerve instead of being inserted longitudinally. Stimulation via the different contacts of the TIME is being investigated as a means to relieve phantom limb pain in amputees [102]. After loss of a limb, there is often a reorganization of the somatosensory cortex where regions serving the amputated limb are overtaken by surrounding regions. It is thought that this reorganization leads to phantom limb pain [103]. Restoration of afferent signals to the appropriate cortical areas by means of electrical stimulation of the nerve stump may be able to mitigate cortical reorganization and alleviate phantom limb pain.

The early intrafascicular electrode studies demonstrated their focal stimulation and recording abilities; however, to approach the specificity of the intact neuromuscular system, many independent electrode contacts must be placed within a single nerve to provide both focal and complete access to the entire axon pool. In the 1990s,

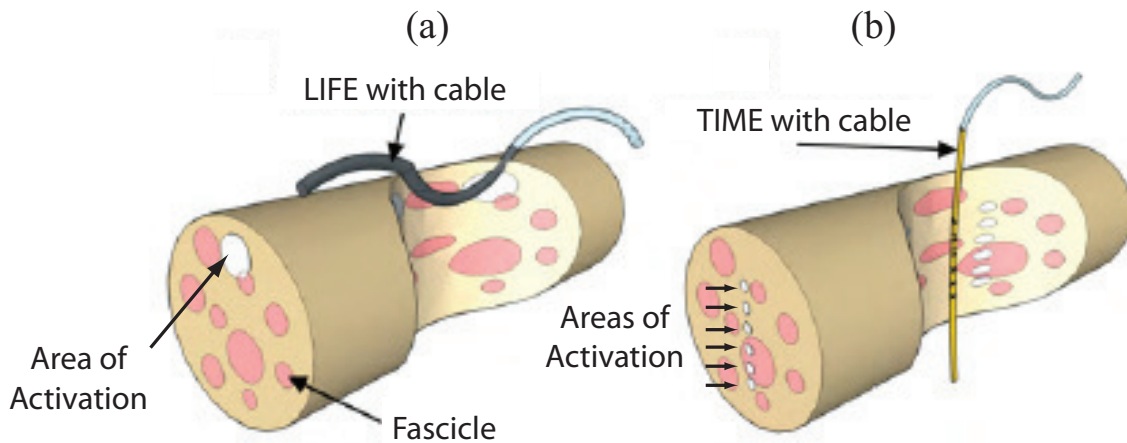


Figure 1.6: Longitudinal and Transverse Intrafascicular Electrodes

(a) LIFE electrodes are threaded longitudinally through a fascicle and place the electrode contact in close proximity to nerve fibers. (b) The TIME electrode passes transversely through the nerve, placing several electrode contacts throughout the cross section of the nerve. (From Boretius and colleagues [101])

while the initial studies using LIFEs in peripheral nerves were being conducted, many research teams were developing high-density microelectrode arrays for stimulation and recording in the cortex [104, 105, 106, 107, 108, 109, 110]. One such array was adapted to the dimensions of the cat sciatic nerve and used to stimulate groups of peripheral nerve axons [111, 112]. Termed the Utah Slanted Electrode Array (USEA), it consists of a 10-by-10 grid of needle-like electrodes fabricated from a silicon substrate (Figure 1.7). Earlier versions of the array that were developed for use in the cortex had electrodes of uniform length [113], but the USEA has electrodes that vary in length from 0.5–1.5 mm to adequately cover the full cross section of the nerve.

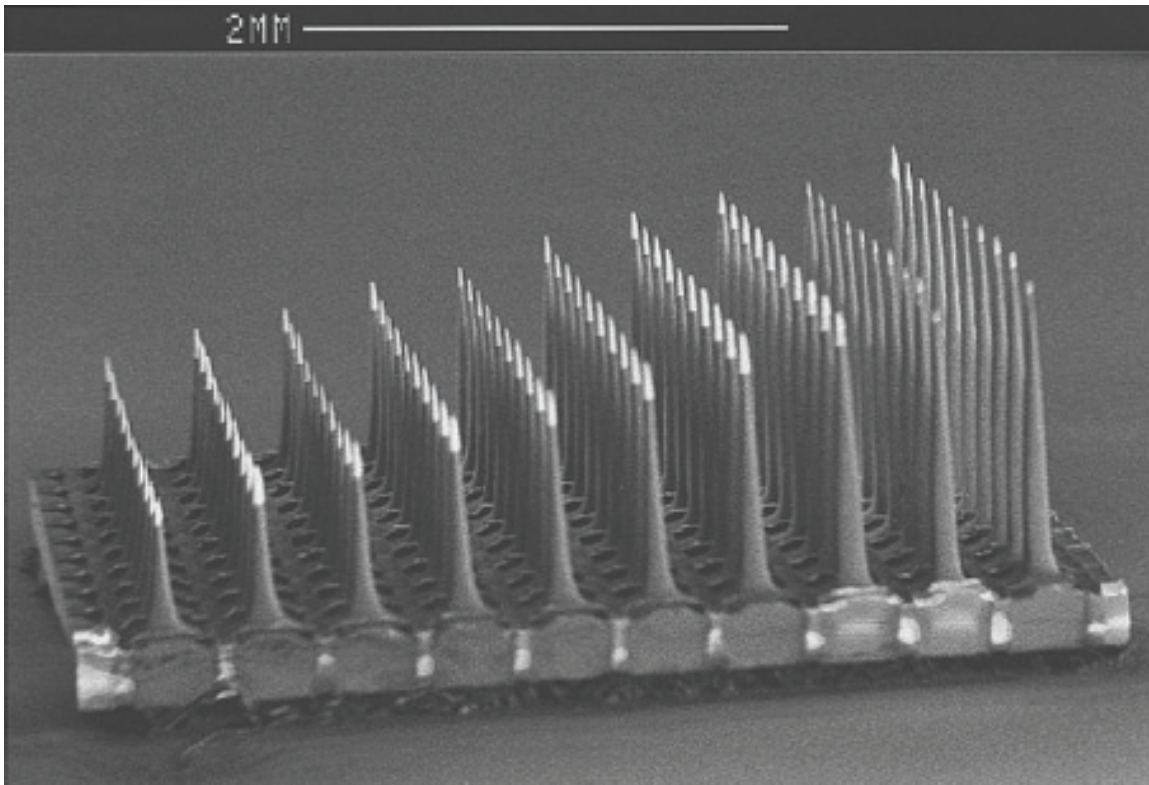


Figure 1.7: Utah Slanted Electrode Array

The USEA is a 10-by-10 grid of microelectrodes. The varied length of electrodes allows for comprehensive coverage of the cross section of the nerve. (Reproduced with permission from Branner and colleagues [111])

Initial studies with the USEA in cat sciatic nerve by Branner and colleagues showed that the presence of 100 individual microelectrodes throughout the nerve enabled threshold stimulation of 9 different muscles, and that different electrodes could excite different groups of motor units within a muscle [111]. The ability of several different electrodes to excite independent groups of synergist fibers was leveraged by McDonnall and colleagues to produce muscle contractions that were much slower to fatigue than those generated with a single stimulation channel [114]. By demonstrating that the USEA could selectively excite multiple muscles to maximum force and produce fatigue-resistant muscle contractions, all with a single implant, Branner and McDonnall illustrated the performance gains that intrafascicular electrode arrays could lend to FES systems [111, 112, 114, 115]. The work presented in this dissertation aims to further explore the capabilities of the USEA to selectively control peripheral nerve activity, and to make its use more practical in FES systems.

Research Outline

The research presented in this dissertation explores the selectivity afforded by the intrafascicular electrodes of the Utah Slanted Electrode Array. Although there are many possible avenues for improvement upon current neuroprosthetic systems and many open questions regarding the nature of intrafascicular stimulation, the work presented here addresses three specific topics.

Selective Activation of Hamstring Muscles

Previous work with the USEA by Branner and McDonnall documented its ability to selectively excite the muscles innervated by the sciatic nerve [111, 115]. They also demonstrated that individual electrodes could excite independent populations of fibers innervating a single muscle, and McDonnall used interleaved stimulation via these independent electrodes to evoke fatigue-resistant muscle contractions [111, 114]. To extend the use of the USEA to evoke hind limb movements such as sit-to-stand or gait in a fatigue-resistant manner, it is necessary to go beyond activation of muscles acting around the ankle and activate muscles acting around the hip and knee. An as-of-yet unpublished study by Nicholas Brown and colleagues demonstrated that a

USEA implanted in the femoral nerve could evoke knee extension torques of sufficient strength for stance. However, generation of hip extension torques using a USEA remained unexplored.

Hip extension can be generated by the hamstring muscles semimembranosus (SM) and the anterior and middle compartments of biceps femoris (BFa and BFm, respectively) [116, 117]. In the cat, these muscles are innervated by the muscular branch of the sciatic nerve. The muscular branch innervates other hamstring muscles—semitendinosus (ST) and the posterior compartment of biceps femoris (BFp)—which act to flex the knee [116, 117]. Independent activation of these different hamstring muscles serves to extend the limb during sit-to-stand and the stance phase of gait, and to flex the limb during the swing phase of gait. A stance or gait neuroprosthesis would be required to selectively control these two different actions. Chapter 2 documents the ability of the USEA to selectively recruit the different muscles of the hamstring muscle group using a single implant in the muscular branch of the sciatic nerve. Different electrodes on the array were able to selectively recruit each hamstring muscle, thus allowing for a single implant and single surgical exposure to generate hip extension torques as well as knee flexion torques.

Selective Block of Muscle Activation

Electrical stimulation of nerves is most often used to evoke neural activity, as in the case of paralysis; however, some neurological disorders are characterized by too much activity rather than too little. Previous studies have shown that high-frequency alternating current (HFAC) delivered to nerves can block action potential conduction [81, 41]—this effect is termed high-frequency block. These studies primarily use extraneural electrodes to deliver the HFAC, and typically this results in block of conduction throughout the entire nerve. Adjustment of the HFAC amplitude can result in partial blockade of the nerve; however, no control over which parts of the nerve are blocked has been demonstrated [118, 119, 120, 121]. For certain therapeutic applications of high-frequency block, it may be desirable to block a subset of fibers in a nerve without disrupting normal activity in the remaining fibers.

Because the intrafascicular electrodes of the USEA are capable of selectively activating subpopulations of fibers within a nerve, it may be possible to selectively block subpopulations of fibers by delivering HFAC through USEA electrodes. A study by Ackermann and colleagues demonstrated that block could be achieved using intrafascicular electrodes; however, no effort was made to determine if portions of the nerve could be blocked selectively [122]. Chapter 3 demonstrates, for the first time, that high-frequency alternating currents delivered through intrafascicular electrodes can block action potential conduction through a portion of a nerve while leaving the remaining portion to function normally. This approach could expand the options for therapeutic applications of high-frequency block.

Noninvasive Selection of Stimulus Parameters

A complete USEA-based neuroprosthetic system capable of producing stance and gait in a paralyzed individual would require implantation of several intrafascicular arrays into the nerves of both lower limbs. The ability to selectively activate several hundred independent groups of motor units would enable enhanced performance over current systems, but would introduce the sizable challenge of characterizing the stimulation properties of each electrode.

Most studies investigating the use of electrical stimulation of peripheral nerves to evoke muscular output have used muscle tendon force [115, 11, 123, 91, 92], electromyography [124, 63, 73, 74], or joint torque [72, 13, 125, 77] to quantify the effects of nerve stimulation. Tendon force provides a direct metric of muscle output; however, this technique requires a tenotomy, which is unacceptable for chronic animal studies or clinical applications. EMG is minimally invasive, but requires instrumentation of each muscle separately and provides only relative information about contraction strength. Joint torque, although noninvasive and simple to instrument, is poorly suited for instrumentation of several joints simultaneously and for characterizing activation of biarticular muscles. In the case of a sit-to-stand prosthesis, characterization of muscle activation acting around 3 joints will be required for each limb. A single

system capable of characterizing all implanted electrodes in such a prosthesis would be highly desirable.

Chapter 4 presents a technique to perform this characterization using simple noninvasive instrumentation. By measuring endpoint forces produced by USEA stimulation, electrodes and stimulus parameters can be chosen that produce either flexion or extension in a graded manner. Further, sets of electrodes that excite mutually independent sets of motor units can be identified, which allows for fatigue-resistant activation via interleaved stimulation.

References

- [1] P H Peckham, M W Keith, K L Kilgore, J H Grill, K S Wuolle, G B Thrope, P Gorman, J Hobby, M J Mulcahey, S Carroll, V R Hentz, A Wiegner, and Implantable Neuroprosthesis Research Group. Efficacy of an implanted neuroprosthesis for restoring hand grasp in tetraplegia: a multicenter study. *Arch Phys Med Rehabil*, 82(10):1380–8, Oct 2001.
- [2] P Hunter Peckham, Kevin L Kilgore, Michael W Keith, Anne M Bryden, Niloy Bhadra, and Fred W Montague. An advanced neuroprosthesis for restoration of hand and upper arm control using an implantable controller. *J Hand Surg Am*, 27(2):265–76, Mar 2002.
- [3] R Brissot, P Gallien, M P Le Bot, A Beaubras, D Laisné, J Beillot, and J Dassonville. Clinical experience with functional electrical stimulation-assisted gait with parastep in spinal cord-injured patients. *Spine*, 25(4):501–8, Feb 2000.
- [4] G S Brindley, C E Polkey, and D N Rushton. Sacral anterior root stimulators for bladder control in paraplegia. *Paraplegia*, 20(6):365–81, Dec 1982.
- [5] Daniel Graupe, Humberto Cerrel-Bazo, Helmut Kern, and Ugo Carraro. Walking performance, medical outcomes and patient training in fes of innervated muscles for ambulation by thoracic-level complete paraplegics. *Neurol Res*, 30(2):123–30, Mar 2008.
- [6] J C Eccles and Charles S Sherrington. Numbers and contraction-values of individual motor-units examined in some muscles of the limb. *Proceedings of the Royal Society of London. Series B*, 106(745):326–357, Jan 1930.
- [7] J D Sweeney, D A Ksienski, and J T Mortimer. A nerve cuff technique for selective excitation of peripheral nerve trunk regions. *IEEE Trans Biomed Eng*, 37(7):706–15, Jul 1990.
- [8] Dustin J Tyler and Dominique M Durand. Functionally selective peripheral nerve stimulation with a flat interface nerve electrode. *IEEE Trans Neural Syst Rehabil Eng*, 10(4):294–303, Dec 2002.
- [9] Kenneth J Gustafson, Gilles C J Pinault, Jennifer J Neville, Ishaq Syed, John A Davis, Jesse Jean-Claude, and Ronald J Triolo. Fascicular anatomy of human femoral nerve: implications for neural prostheses using nerve cuff electrodes. *J Rehabil Res Dev*, 46(7):973–84, Jan 2009. Lots of good Case references.
- [10] Kenneth J Gustafson, Paul F Zelkovic, Adrian H Feng, Christine E Draper, Donald R Bodner, and Warren M Grill. Fascicular anatomy and surgical access of the human pudendal nerve. *World J Urol*, 23(6):411–8, Dec 2005.
- [11] C Veraart, W M Grill, and J T Mortimer. Selective control of muscle activation with a multipolar nerve cuff electrode. *IEEE Trans Biomed Eng*, 40(7):640–53, Jul 1993.

- [12] W M Grill and J T Mortimer. Quantification of recruitment properties of multiple contact cuff electrodes. *IEEE Trans Rehabil Eng*, 4(2):49–62, Jun 1996.
- [13] W M Grill and J T Mortimer. Non-invasive measurement of the input-output properties of peripheral nerve stimulating electrodes. *J Neurosci Methods*, 65(1):43–50, Mar 1996.
- [14] W A Catterall. Interactions of presynaptic ca^{2+} channels and snare proteins in neurotransmitter release. *Ann N Y Acad Sci*, 868:144–59, Apr 1999.
- [15] Yoshi Kidokoro. Roles of snare proteins and synaptotagmin i in synaptic transmission: studies at the drosophila neuromuscular synapse. *Neurosignals*, 12(1):13–30, Jan 2003.
- [16] Silvio O Rizzoli and William J Betz. Synaptic vesicle pools. *Nat Rev Neurosci*, 6(1):57–69, Jan 2005.
- [17] Charles S Sherrington. Remarks on some aspects of reflex inhibition. *Proceedings of the Royal Society of London. Series B*, 97(686):519–545, Jan 1925. First paper to use the term motor-unit.
- [18] George Ralph Mines. On the summation of contractions. *The Journal of Physiology*, 46(1):1–27, Mar 1913.
- [19] E.L Porter and V.W Hart. Reflex contractions of an all-or-none character in the spinal cat. *American Journal of Physiology*, 66(2):391, 1923. motor-units.
- [20] A M McPhedran, R B Wuerker, and E Henneman. Properties of motor units in a homogeneous red muscle (soleus) of the cat. *J Neurophysiol*, 28:71–84, Jan 1965.
- [21] R B Wuerker, A M McPhedran, and E Henneman. Properties of motor units in a heterogeneous pale muscle (m. gastrocnemius) of the cat. *J Neurophysiol*, 28:85–99, Jan 1965.
- [22] E Henneman, G Somjen, and D O Carpenter. Functional significance of cell size in spinal motoneurons. *J Neurophysiol*, 28:560–80, May 1965.
- [23] D Denny-Brown and JB Pennybacker. Fibrillation and fasciculation in voluntary muscle. *Brain*, 61(3):311, 1938.
- [24] S Schiaffino, S Ausoni, L Gorza, L Saggin, K Gundersen, and T Lomo. Myosin heavy chain isoforms and velocity of shortening of type 2 skeletal muscle fibres. *Acta Physiol Scand*, 134(4):575–6, Dec 1988.
- [25] R E Burke, D N Levine, P Tsairis, and F E Zajac. Physiological types and histochemical profiles in motor units of the cat gastrocnemius. *The Journal of Physiology*, 234(3):723–48, Nov 1973.

- [26] F Buchthal and H Schmalbruch. Motor unit of mammalian muscle. *Physiol Rev*, 60(1):90–142, Jan 1980.
- [27] A W Monster and H Chan. Isometric force production by motor units of extensor digitorum communis muscle in man. *Journal of Neurophys*, 40(6):1432–43, Nov 1977.
- [28] B L Hicken, J D Putzke, and J S Richards. Bladder management and quality of life after spinal cord injury. *Am J Phys Med Rehabil*, 80(12):916–22, Dec 2001.
- [29] G J Snoek, M J IJzerman, H J Hermens, D Maxwell, and F Biering-Sorensen. Survey of the needs of patients with spinal cord injury: impact and priority for improvement in hand function in tetraplegics. *Spinal Cord*, 42(9):526–32, Sep 2004.
- [30] Kim D Anderson. Consideration of user priorities when developing neural prosthetics. *J Neural Eng*, 6(5):055003, Oct 2009.
- [31] National Spinal Cord Injury Statistical Center. Spinal cord injury facts at a glance. <https://www.nscisc.uab.edu>, February 2011.
- [32] The Dana and Christopher Reeve Foundation. One degree of separation: Paralysis and spinal cord injury in the united states. http://www.christopherreeve.org/site/c.mtKZKgMWKwG/b.5184255/k.6D74/Prevalence_of_Paralysis.htm.
- [33] R A Cripps, B B Lee, P Wing, E Weerts, J Mackay, and D Brown. A global map for traumatic spinal cord injury epidemiology: towards a living data repository for injury prevention. *Spinal Cord*, 49(4):493–501, Apr 2011.
- [34] V. L Roger, A. S Go, D. M Lloyd-Jones, R. J Adams, J. D Berry, T. M Brown, M. R Carnethon, S Dai, G De Simone, E. S Ford, C. S Fox, H. J Fullerton, C Gillespie, K. J Greenlund, S. M Hailpern, J. A Heit, P. M Ho, V. J Howard, B. M Kissela, S. J Kittner, D. T Lackland, J. H Lichtman, L. D Lisabeth, D. M Makuc, G. M Marcus, A Marelli, D. B Matchar, M. M Mcdermott, J. B Meigs, C. S Moy, D Mozaffarian, M. E Mussolino, G Nichol, N. P Paynter, W. D Rosamond, P. D Sorlie, R. S Stafford, T. N Turan, M. B Turner, N. D Wong, J Wylie-Rosett, V. L Roger, and M. B Turner. Heart disease and stroke statistics–2011 update: A report from the american heart association. *Circulation*, 123(4):e18–e209, Feb 2011.
- [35] Margaret Kelly-Hayes, Alexa Beiser, Carlos S Kase, Amy Scaramucci, Ralph B D’Agostino, and Philip A Wolf. The influence of gender and age on disability following ischemic stroke: the framingham study. *J Stroke Cerebrovasc Dis*, 12(3):119–26, Jan 2003.
- [36] T Rekan. Clinical assessment and management of spasticity: a review. *Acta Neurol Scand, Suppl*, 122(190):62–6, Jan 2010.

- [37] Sherif M Elbasiouny, Daniel Moroz, Mohamed M Bakr, and Vivian K Mushahwar. Management of spasticity after spinal cord injury: current techniques and future directions. *Neurorehabil Neural Repair*, 24(1):23–33, Jan 2010.
- [38] Volker Dietz and Thomas Sinkjaer. Spastic movement disorder: impaired reflex function and altered muscle mechanics. *Lancet Neurol*, 6(8):725–33, Aug 2007.
- [39] Allison Brashear and Elie Elovic, editors. *Spasticity Diagnosis and Management*, chapter Epidemiology of Spasticity in the Adult and Child. Demos Medical Publishing, New York, 2011.
- [40] Eleanor L Olvey, Edward P Armstrong, and Amy J Grizzle. Contemporary pharmacologic treatments for spasticity of the upper limb after stroke: a systematic review. *Clin Ther*, 32(14):2282–303, Dec 2010.
- [41] K L Kilgore and N Bhadra. Nerve conduction block utilising high-frequency alternating current. *Med Biol Eng Comput*, 42(3):394–406, May 2004.
- [42] J Thomas Mortimer and Narendra Bhadra. Peripheral nerve and muscle stimulation. *Neuroprosthetics: Theory and Practice*. World Scientific Pub Co Inc, Nov 2004.
- [43] J H Burridge, P N Taylor, S A Hagan, D E Wood, and I D Swain. The effects of common peroneal stimulation on the effort and speed of walking: a randomized controlled trial with chronic hemiplegic patients. *Clin Rehabil*, 11(3):201–10, Aug 1997.
- [44] J Burridge, P Taylor, S Hagan, and I Swain. Experience of clinical use of the odstock dropped foot stimulator. *Artif Organs*, 21(3):254–60, Mar 1997.
- [45] P N Taylor, J H Burridge, A L Dunkerley, D E Wood, J A Norton, C Singleton, and I D Swain. Clinical use of the odstock dropped foot stimulator: its effect on the speed and effort of walking. *Arch Phys Med Rehabil*, 80(12):1577–83, Dec 1999.
- [46] A Kralj, T Bajd, R Turk, J Krajinik, and H Benko. Gait restoration in paraplegic patients: a feasibility demonstration using multichannel surface electrode fes. *J Rehabil R D*, 20(1):3–20, Jul 1983.
- [47] D Popovic, R Tomović, and L Schwirtlich. Hybrid assistive system—the motor neuroprosthesis. *IEEE Trans Biomed Eng*, 36(7):729–37, Jul 1989.
- [48] M Solomonow, E Aguilar, E Reisin, R V Baratta, R Best, T Coetzee, and R D’Ambrosia. Reciprocating gait orthosis powered with electrical muscle stimulation (rgo ii). part i: Performance evaluation of 70 paraplegic patients. *Orthopedics*, 20(4):315–24, Apr 1997.
- [49] R Spadone, G Merati, E Bertocchi, E Mevio, A Veicsteinas, A Pedotti, and M Ferrarin. Energy consumption of locomotion with orthosis versus parastep-assisted gait: a single case study. *Spinal Cord*, 41(2):97–104, Feb 2003.

- [50] S Saxena, S Nikolić, and D Popović. An emg-controlled grasping system for tetraplegics. *J Rehabil Res Dev*, 32(1):17–24, Feb 1995.
- [51] A Prochazka, M Gauthier, M Wieler, and Z Kenwell. The bionic glove: an electrical stimulator garment that provides controlled grasp and hand opening in quadriplegia. *Arch Phys Med Rehabil*, 78(6):608–14, Jun 1997.
- [52] D Popović, A Stojanović, A Pjanović, S Radosavljević, M Popović, S Jović, and D Vulović. Clinical evaluation of the bionic glove. *Arch Phys Med Rehabil*, 80(3):299–304, Mar 1999.
- [53] G J Snoek, M J IJzerman, F A in 't Groen, T S Stoffers, and G Zilvold. Use of the ness handmaster to restore handfunction in tetraplegia: clinical experiences in ten patients. *Spinal Cord*, 38(4):244–9, Apr 2000.
- [54] James P Uhler, Ronald J Triolo, John A Davis, and Carol Bieri. Performance of epimysial stimulating electrodes in the lower extremities of individuals with spinal cord injury. *IEEE Trans Neural Syst Rehabil Eng*, 12(2):279–87, Jun 2004.
- [55] P A Grandjean and J T Mortimer. Recruitment properties of monopolar and bipolar epimysial electrodes. *Ann Biomed Eng*, 14(1):53–66, Jan 1986.
- [56] R Kobetic, R J Triolo, J P Uhler, C Bieri, M Wibowo, G Polando, E B Marsolais, J A Davis, and K A Ferguson. Implanted functional electrical stimulation system for mobility in paraplegia: a follow-up case report. *IEEE Trans Rehabil Eng*, 7(4):390–8, Dec 1999.
- [57] C W Caldwell and J B Reswick. A percutaneous wire electrode for chronic research use. *IEEE Trans Biomed Eng*, 22(5):429–32, Sep 1975.
- [58] Anirban Dutta, Rudi Kobetic, and Ronald J Triolo. Ambulation after incomplete spinal cord injury with emg-triggered functional electrical stimulation. *IEEE Trans Biomed Eng*, 55(2 Pt 1):791–4, Feb 2008.
- [59] Anirban Dutta, Rudi Kobetic, and Ronald J Triolo. Gait initiation with electromyographically triggered electrical stimulation in people with partial paralysis. *J Biomech Eng*, 131(8):081002, Aug 2009.
- [60] Lisa Guevremont, Jonathan A Norton, and Vivian K Mushahwar. Physiologically based controller for generating overground locomotion using functional electrical stimulation. *J Neurophysiol*, 97(3):2499–510, Mar 2007.
- [61] Bernice Lau, Lisa Guevremont, and Vivian K Mushahwar. Strategies for generating prolonged functional standing using intramuscular stimulation or intraspinal microstimulation. *IEEE Trans Neural Syst Rehabil Eng*, 15(2):273–85, Jun 2007.

- [62] M Bijak, W Mayr, W Girsch, H Lanmüller, E Unger, H Stöhr, H Thoma, and H Plenk. Functional and biological test of a 20 channel implantable stimulator in sheep in view of functional electrical stimulation walking for spinal cord injured persons. *Artif Organs*, 25(6):467–74, Jun 2001.
- [63] D R McNeal and B R Bowman. Selective activation of muscles using peripheral nerve electrodes. *Med Biol Eng Comput*, 23(3):249–53, May 1985.
- [64] H Thoma, W Girsch, J Holle, and W Mayr. Technology and long-term application of an epineural electrode. *ASAIO Trans*, 35(3):490–4, Jan 1989.
- [65] Peter Khong, Amanda Lazzaro, and Ralph Mobbs. Phrenic nerve stimulation: the australian experience. *J Clin Neurosci*, 17(2):205–8, Feb 2010.
- [66] T E Johnston, R R Betz, B T Smith, B J Benda, M J Mulcahey, R Davis, T P Houdayer, M A Pontari, A Barriskill, and G H Creasey. Implantable fes system for upright mobility and bladder and bowel function for individuals with spinal cord injury. *Spinal Cord*, 43(12):713–23, Dec 2005.
- [67] Paul B Yoo, Stephen M Klein, Neil H Grafstein, Eric E Horvath, Cindy L Amundsen, George D Webster, and Warren M Grill. Pudendal nerve stimulation evokes reflex bladder contractions in persons with chronic spinal cord injury. *Neurol Urodyn*, 26(7):1020–3, Jan 2007.
- [68] W F Agnew, D B McCreery, T G Yuen, and L A Bullara. Histologic and physiologic evaluation of electrically stimulated peripheral nerve: considerations for the selection of parameters. *Ann Biomed Eng*, 17(1):39–60, Jan 1989.
- [69] G G Naples, J T Mortimer, A Scheiner, and J D Sweeney. A spiral nerve cuff electrode for peripheral nerve stimulation. *IEEE Trans Biomed Eng*, 35(11):905–16, Nov 1988.
- [70] J Rozman and M Trlep. Multielectrode spiral cuff for selective stimulation of nerve fibres. *J Med Eng Technol*, 16(5):194–203, Jan 1992.
- [71] Lee E Fisher, Michael E Miller, Stephanie N Bailey, John A Davis, James S Anderson, Lori Rhode, Dustin J Tyler, and Ronald J Triolo. Standing after spinal cord injury with four-contact nerve-cuff electrodes for quadriceps stimulation. *IEEE Trans Neural Syst Rehabil Eng*, 16(5):473–8, Oct 2008.
- [72] Matthew D Tarler and J Thomas Mortimer. Selective and independent activation of four motor fascicles using a four contact nerve-cuff electrode. *IEEE Trans Neural Syst Rehabil Eng*, 12(2):251–7, Jun 2004.
- [73] Katharine H Polasek, Harry A Hoyen, Michael W Keith, and Dustin J Tyler. Human nerve stimulation thresholds and selectivity using a multi-contact nerve cuff electrode. *IEEE Trans Neural Syst Rehabil Eng*, 15(1):76–82, Mar 2007.
- [74] M A Schiefer, K H Polasek, R J Triolo, G C J Pinault, and D J Tyler. Selective stimulation of the human femoral nerve with a flat interface nerve electrode. *J. Neural Eng.*, 7(2):26006, Apr 2010.

- [75] P H Veltink, B K van Veen, J J Struijk, J Holsheimer, and H B Boom. A modeling study of nerve fascicle stimulation. *IEEE Trans Biomed Eng*, 36(7):683–92, Jul 1989.
- [76] Daniel K Leventhal and Dominique M Durand. Chronic measurement of the stimulation selectivity of the flat interface nerve electrode. *IEEE Trans Biomed Eng*, 51(9):1649–58, Sep 2004.
- [77] Matthew D Tarler and J Thomas Mortimer. Linear summation of torque produced by selective activation of two motor fascicles. *IEEE Trans Neural Syst Rehabil Eng*, 15(1):104–10, Mar 2007.
- [78] Daniel K Leventhal and Dominique M Durand. Subfascicle stimulation selectivity with the flat interface nerve electrode. *Ann Biomed Eng*, 31(6):643–52, Jun 2003.
- [79] A B Vallbo and K E Hagbarth. Impulses recorded with micro-electrodes in human muscle nerves during stimulation of mechanoreceptors and voluntary contractions. *Electroencephalogr Clin Neurophysiol*, 23(4):392, Oct 1967.
- [80] A B Vallbo, K E Hagbarth, H E Torebjörk, and B G Wallin. Somatosensory, proprioceptive, and sympathetic activity in human peripheral nerves. *Physiol Rev*, 59(4):919–57, Oct 1979.
- [81] B R Bowman and D R McNeal. Response of single alpha motoneurons to high-frequency pulse trains. firing behavior and conduction block phenomenon. *Appl Neurophysiol*, 49(3):121–38, Jan 1986.
- [82] L Larsson, L Edström, B Lindgren, L Gorza, and S Schiaffino. Mhc composition and enzyme-histochemical and physiological properties of a novel fast-twitch motor unit type. *Am J Physiol*, 261(1 Pt 1):C93–101, Jul 1991.
- [83] B McKeon and D Burke. Muscle spindle discharge in response to contraction of single motor units. *Journal of neurophysiology*, 49(2):291–302, Feb 1983.
- [84] G Westling, R S Johansson, C K Thomas, and B Bigland-Ritchie. Measurement of contractile and electrical properties of single human thenar motor units in response to intraneural motor-axon stimulation. *Journal of Neurophys*, 64(4):1331–8, Oct 1990.
- [85] C K Thomas, R S Johansson, G Westling, and B Bigland-Ritchie. Twitch properties of human thenar motor units measured in response to intraneural motor-axon stimulation. *Journal of neurophysiology*, 64(4):1339–46, Oct 1990.
- [86] V G Macefield, A J Fuglevand, and B Bigland-Ritchie. Contractile properties of single motor units in human toe extensors assessed by intraneural motor axon stimulation. *Journal of neurophysiology*, 75(6):2509–19, Jun 1996.
- [87] Penelope A McNulty and Vaughan G Macefield. Intraneural microstimulation of motor axons in the study of human single motor units. *Muscle Nerve*, 32(2):119–39, Aug 2005.

- [88] M S Malagodi, K W Horch, and A A Schoenberg. An intrafascicular electrode for recording of action potentials in peripheral nerves. *Ann Biomed Eng*, 17(4):397–410, Jan 1989.
- [89] T Lefurge, E Goodall, K Horch, L Stensaas, and A Schoenberg. Chronically implanted intrafascicular recording electrodes. *Ann Biomed Eng*, 19(2):197–207, Jan 1991.
- [90] E V Goodall, T M Lefurge, and K W Horch. Information contained in sensory nerve recordings made with intrafascicular electrodes. *IEEE Trans Biomed Eng*, 38(9):846–50, Sep 1991.
- [91] N Nannini and K Horch. Muscle recruitment with intrafascicular electrodes. *IEEE Trans Biomed Eng*, 38(8):769–76, Aug 1991.
- [92] K Yoshida and K Horch. Selective stimulation of peripheral nerve fibers using dual intrafascicular electrodes. *IEEE Trans Biomed Eng*, 40(5):492–4, May 1993.
- [93] K Yoshida and K Horch. Reduced fatigue in electrically stimulated muscle using dual channel intrafascicular electrodes with interleaved stimulation. *Ann Biomed Eng*, 21(6):709–14, Jan 1993.
- [94] K Yoshida and K Horch. Closed-loop control of ankle position using muscle afferent feedback with functional neuromuscular stimulation. *IEEE Trans Biomed Eng*, 43(2):167–76, Feb 1996.
- [95] Steve M Lawrence, G S Dhillon, W Jensen, K Yoshida, and Ken W Horch. Acute peripheral nerve recording characteristics of polymer-based longitudinal intrafascicular electrodes. *IEEE Trans Neural Syst Rehabil Eng*, 12(3):345–8, Sep 2004.
- [96] Natalia Lago, Ken Yoshida, Klaus P Koch, and Xavier Navarro. Assessment of biocompatibility of chronically implanted polyimide and platinum intrafascicular electrodes. *IEEE Trans Biomed Eng*, 54(2):281–90, Feb 2007.
- [97] Milan Djilas, Christine Azevedo-Coste, David Guiraud, and Ken Yoshida. Spike sorting of muscle spindle afferent nerve activity recorded with thin-film intrafascicular electrodes. *Computational Intelligence and Neuroscience*, page 836346, Jan 2010.
- [98] Luca Citi, Jacopo Carpaneto, Ken Yoshida, Klaus-Peter Hoffmann, Klaus Peter Koch, Paolo Dario, and Silvestro Micera. On the use of wavelet denoising and spike sorting techniques to process electroneurographic signals recorded using intraneural electrodes. *Journal of Neuroscience Methods*, 172(2):294–302, Jul 2008.
- [99] Silvestro Micera, Xavier Navarro, Jacopo Carpaneto, Luca Citi, Oliver Tonet, Paolo Maria Rossini, Maria Chiara Carrozza, Klaus Peter Hoffmann, Meritxell

- Vivó, Ken Yoshida, and Paolo Dario. On the use of longitudinal intrafascicular peripheral interfaces for the control of cybernetic hand prostheses in amputees. *IEEE Trans Neural Syst Rehabil Eng*, 16(5):453–72, Oct 2008.
- [100] Silvestro Micera, Luca Citi, Jacopo Rigosa, Jacopo Carpaneto, Stanisa Raspopovic, Giovanni Di Pino, Luca Rossini, Ken Yoshida, Luca Denaro, Paolo Dario, and Paolo Maria Rossini. Decoding information from neural signals recorded using intraneural electrodes: Toward the development of a neurocontrolled hand prosthesis. *Proceedings of the IEEE*, 98(3):407 – 417, 2010.
- [101] Tim Boretius, Jordi Badia, Aran Pascual-Font, Martin Schuettler, Xavier Navarro, Ken Yoshida, and Thomas Stieglitz. A transverse intrafascicular multichannel electrode (time) to interface with the peripheral nerve. *Biosens Bioelectron*, 26(1):62–9, Sep 2010.
- [102] W Jensen, S Micera, X Navarro, T Stieglitz, D Guiraud, J Divoux, and P Rossini. Development of an implantable transverse intrafascicular multichannel electrode (time) system for relieving phantom limb pain. *Engineering in Medicine and Biology Society (EMBC), 2010 Annual International Conference of the IEEE*, pages 6214 – 6217, 2010.
- [103] X Navarro, Meritxell Vivó, and Antoni Valero-Cabré. Neural plasticity after peripheral nerve injury and regeneration. *Prog Neurobiol*, 82(4):163–201, Jul 2007.
- [104] P K Campbell, R A Normann, K W Horch, and S S Stensaas. A chronic intracortical electrode array: preliminary results. *J Biomed Mater Res*, 23(A2 Suppl):245–59, Aug 1989.
- [105] M A Wilson and B L McNaughton. Dynamics of the hippocampal ensemble code for space. *Science*, 261(5124):1055–8, Aug 1993.
- [106] M A Nicolelis, R C Lin, D J Woodward, and J K Chapin. Dynamic and distributed properties of many-neuron ensembles in the ventral posterior medial thalamus of awake rats. *Proc Natl Acad Sci USA*, 90(6):2212–6, Mar 1993.
- [107] M A Nicolelis, L A Baccala, R C Lin, and J K Chapin. Sensorimotor encoding by synchronous neural ensemble activity at multiple levels of the somatosensory system. *Science*, 268(5215):1353–8, Jun 1995.
- [108] J P Welsh, E J Lang, I Sugihara, and R Llinás. Dynamic organization of motor control within the olivocerebellar system. *Nature*, 374(6521):453–7, Mar 1995.
- [109] C T Nordhausen, E M Maynard, and R A Normann. Single unit recording capabilities of a 100 microelectrode array. *Brain Res*, 726(1-2):129–40, Jul 1996.

- [110] N G Hatsopoulos, C L Ojakangas, L Paninski, and J P Donoghue. Information about movement direction obtained from synchronous activity of motor cortical neurons. *Proc Natl Acad Sci USA*, 95(26):15706–11, Dec 1998.
- [111] A Branner, R B Stein, and R A Normann. Selective stimulation of cat sciatic nerve using an array of varying-length microelectrodes. *J Neurophysiol*, 85(4):1585–94, Apr 2001.
- [112] Almut Branner, Richard B Stein, Eduardo Fernandez, Yoichiro Aoyagi, and Richard A Normann. Long-term stimulation and recording with a penetrating microelectrode array in cat sciatic nerve. *IEEE Trans Biomed Eng*, 51(1):146–57, Jan 2004.
- [113] K E Jones, P K Campbell, and R A Normann. A glass/silicon composite intracortical electrode array. *Annals of Biomedical Engineering*, 20(4):423–37, Jan 1992.
- [114] Daniel McDonnall, Gregory A Clark, and Richard A Normann. Interleaved, multisite electrical stimulation of cat sciatic nerve produces fatigue-resistant, ripple-free motor responses. *IEEE Trans Neural Syst Rehabil Eng*, 12(2):208–15, Jun 2004.
- [115] Daniel McDonnall, Gregory A Clark, and Richard A Normann. Selective motor unit recruitment via intrafascicular multielectrode stimulation. *Can J Physiol Pharmacol*, 82(8-9):599–609, Jan 2004.
- [116] D I Carrasco and A W English. Mechanical actions of compartments of the cat hamstring muscle, biceps femoris. *Prog Brain Res*, 123:397–403, Jan 1999.
- [117] S E Peters and C Rick. The actions of three hamstring muscles of the cat: a mechanical analysis. *J Morphol*, 152(3):315–28, Jun 1977.
- [118] Narendra Bhadra, Niloy Bhadra, Kevin Kilgore, and Kenneth J Gustafson. High frequency electrical conduction block of the pudendal nerve. *J. Neural Eng.*, 3(2):180–7, Jun 2006.
- [119] D Michael Ackermann, Christian Ethier, Emily L Foldes, Emily R Oby, Dustin Tyler, Matt Bauman, Niloy Bhadra, Lee Miller, and Kevin L Kilgore. Electrical conduction block in large nerves: High-frequency current delivery in the nonhuman primate. *Muscle Nerve*, 43(6):897–9, Jun 2011.
- [120] Niloy Bhadra and Kevin L Kilgore. High-frequency electrical conduction block of mammalian peripheral motor nerve. *Muscle Nerve*, 32(6):782–90, Dec 2005.
- [121] Changfeng Tai, James R Roppolo, and William C de Groat. Block of external urethral sphincter contraction by high frequency electrical stimulation of pudendal nerve. *J Urol*, 172(5 Pt 1):2069–72, Nov 2004.

- [122] D Michael Ackermann, Emily L Foldes, Niloy Bhadra, and Kevin L Kilgore. Conduction block of peripheral nerve using high-frequency alternating currents delivered through an intrafascicular electrode. *Muscle Nerve*, 41(1):117–9, Jan 2010.
- [123] Z P Fang and J T Mortimer. A method to effect physiological recruitment order in electrically activated muscle. *IEEE Trans Biomed Eng*, 38(2):175–9, Feb 1991.
- [124] Brett R Dowden, Andrew M Wilder, Scott D Hiatt, Richard A Normann, Nicholas A T Brown, and Gregory A Clark. Selective and graded recruitment of cat hamstring muscles with intrafascicular stimulation. *IEEE Trans Neural Syst Rehabil Eng*, 17(6):545–52, Dec 2009.
- [125] W M Grill and J T Mortimer. Stability of the input-output properties of chronically implanted multiple contact nerve cuff stimulating electrodes. *IEEE Trans Rehabil Eng*, 6(4):364–73, Dec 1998.

CHAPTER 2

**SELECTIVE AND GRADED RECRUITMENT OF
FELINE HAMSTRING MUSCLES WITH
INTRAFASCICULAR STIMULATION**

Abstract

The muscles of the hamstring group can produce different combinations of hip and knee torque. Thus, the ability to activate the different hamstring muscles selectively is of particular importance in eliciting functional movements such as stance and gait in a person with spinal cord injury. We investigated the ability of intrafascicular stimulation of the muscular branch of the sciatic nerve to recruit the feline hamstring muscles in a selective and graded fashion. A Utah Slanted Electrode Array, consisting of 100 penetrating microelectrodes, was implanted into the muscular branch of the sciatic nerve in 6 cats. Muscle twitches were evoked in the three compartments of biceps femoris (anterior, middle, and posterior), as well as semitendinosus and semimembranosus, using pulse-width modulated constant-voltage pulses. The resultant compound muscle action potentials were recorded using intramuscular fine-wire electrodes. Seventy-four percent of the electrodes per implant were able to evoke a threshold response in these muscles, and these electrodes were evenly distributed among the instrumented muscles. Of the five muscles instrumented, on average, 2.5 could be selectively activated to 90% of maximum EMG, and 3.5 could be selectively activated to 50% of maximum EMG. The muscles were recruited selectively with a mean stimulus dynamic range of 4.14 ± 5.05 dB between threshold and either spillover to another muscle or a plateau in the response. This selective and graded activation afforded by intrafascicular stimulation of the muscular branch of the sciatic nerve suggests that it is a potentially useful stimulation paradigm for eliciting distinct forces in the hamstring muscle group in motor neuroprosthetic applications

Introduction

The past two decades have seen major advances in the use of functional electrical stimulation (FES) to restore movements such as basic stance and gait to persons with spinal cord injury (SCI) [1, 2, 3, 4, 5, 6]. This technique has improved the quality of life for some SCI patients by providing them a means to exercise and by enhancing their ability to navigate and interact with their environment. However, factors that limit the performance of many current FES systems are 1) the rapid onset of muscle fatigue resulting from overstimulation due to poor control of muscle force and 2) insufficient hip extension during stance and gait, which requires the arms to be used for stability and to pull the body forward [7]. Because the different hamstring muscles evoke various amounts of knee flexion or hip extension torque [8, 9], the ability to activate each muscle selectively is of particular importance for effecting functional movements.

Current clinical prostheses achieve selective muscle activation with bipolar electrodes implanted in or on the surface of the targeted muscle or on the skin [4, 7]. Because each electrode has a dedicated lead and must be implanted separately, these systems are limited in the number of muscles that can be practically accessed, which limits the grace of the movement and the joint torques that can be generated [6, 7]. Selective activation of multiple muscles using a single implant has been achieved in cat sciatic nerve using multicontact extraneural cuff electrodes [10, 11, 12]. These cuff electrodes are capable of between-fascicle selectivity, and when each fascicle innervates a single muscle, individual muscle activation can be achieved [13, 14, 15]. However, similar selectivity in humans has yet to be demonstrated, and may be confounded by a higher fascicle count in human nerves [16]. Further, selectivity within a given fascicle is not well controlled. Another approach to selective activation of multiple muscles with a single implant is the use of microelectrode arrays that penetrate the epineurium of implanted motor nerves. The intrafascicular stimulation (IFS) that can be achieved with such arrays has provided highly selective access to the ankle dorsi- and plantar-flexors innervated by the sciatic nerve of cat [17, 18, 19].

To restore graceful movements, nerve stimulation must not only be muscle-selective, but must also activate the muscles in a graded fashion. To command fine control of muscle force and limb movement, there should be a broad range of achievable stimulus intensities that evoke a broad range of muscle forces. In previous experiments using Utah Slanted Electrode Arrays (USEAs) in sciatic nerve, IFS not only mediated muscle-selective activation, it also provided fine control of muscle force from submaximal to maximal levels [17, 18, 19].

In the present study, we investigated the ability of IFS via a 100-electrode USEA to provide selective and graded activation of the feline hamstring muscles: biceps femoris (BF), semimembranosus (SM), and semitendinosus (ST). Fine-wire electromyograms (EMGs) were used to validate muscle-selective activation as well as to quantify the range of stimulus intensities that produced selective muscle responses. It was found that a simple surgical access allowed implantation of a USEA into the muscular branch of the sciatic nerve and that IFS of this nerve mediated graded, selective activation of each of the hamstring muscles. This stimulation paradigm thus holds promise for future generations of motor prostheses for stance and gait.

Methods

Animal Preparation and Surgery

Six adult cats were used in this study. All experimental procedures were approved by the University of Utah Institutional Animal Care and Use Committee. Anesthesia was induced with an intramuscular injection of 10 mg/kg Telazol (Fort Dodge Animal Health, Fort Dodge, IA) and maintained throughout the remainder of the procedure with mechanical ventilation using isoflurane (1.5–2.5%). Breath rate and tidal volume were adjusted to maintain appropriate blood oxygen saturation and levels of inspired and expired CO₂. Vital signs (rectal temperature, ECG, CO₂, blood oxygen saturation) were monitored and recorded every 15 minutes. Data were collected only when the animals were deemed to be in good condition on the basis of these vital signs. The animals were placed in a prone position in a supporting trough that was rigidly fixed to the experimental table. The pelvis was fixed to the support using 2

bone screws into the iliac crests, and the hindlimbs hung freely from the end of the trough.

To monitor muscle activity, pairs of fine-wire EMG electrodes (Medwire, Mt. Vernon, NY) were inserted into the bellies of 3 hamstring muscles: semimembranosus, semitendinosus, and each of the compartments of biceps femoris (anterior, middle, and posterior) [20]. Each EMG electrode had 2–3 mm of deinsulated wire at the tip, and the 2 electrodes in each muscle were separated by about 1 cm. In 1 animal, EMG wires were implanted through the skin and placement was verified by postmortem dissection. In the 5 other animals, the hamstring muscles were visualized via an incision at the posterior thigh, and EMG wire placements were confirmed visually. The incision was closed after EMG electrode placement.

The muscular branch of the sciatic nerve of the left hindlimb was exposed via an incision 1 cm distal to and 1–2 cm caudal to the greater trochanter of the left femur. Blunt dissection between biceps femoris and caudofemoralis exposed the sciatic nerve and its muscular branch. Caudofemoralis was either reflected or, in some cases, removed to ease access. A 100-electrode USEA in a 10-by-10 configuration was implanted into the muscular branch of the sciatic nerve distal to its branch from the main sciatic using high-speed insertion [21] (Figure 2.1). The USEA consists of 100 electrically-isolated silicon microelectrodes ranging in length from 0.5 mm to 1.5 mm, so that the tips are in contact with nerve fibers at different depths from the nerve surface. The electrodes are insulated with parylene C, and the surface of the exposed tips are iridium oxide; an earlier version is described in detail elsewhere [18]. Several different USEAs were used across the six preparations.

Stimulation and Recording Setup

All stimuli to the nerve were delivered through single electrodes of the USEA. All animals received voltage-controlled stimuli consisting of a cathodic rectangular voltage pulse followed by a 50- μ s delay, then a comparable anodic voltage pulse. Pulse amplitude was held constant throughout each experiment, and charge was modulated by varying the cathodic and anodic phase widths symmetrically between 1 and 1000 μ s. Voltage-pulse amplitudes ranged between ± 1.14 V and ± 3.5 V to adjust for

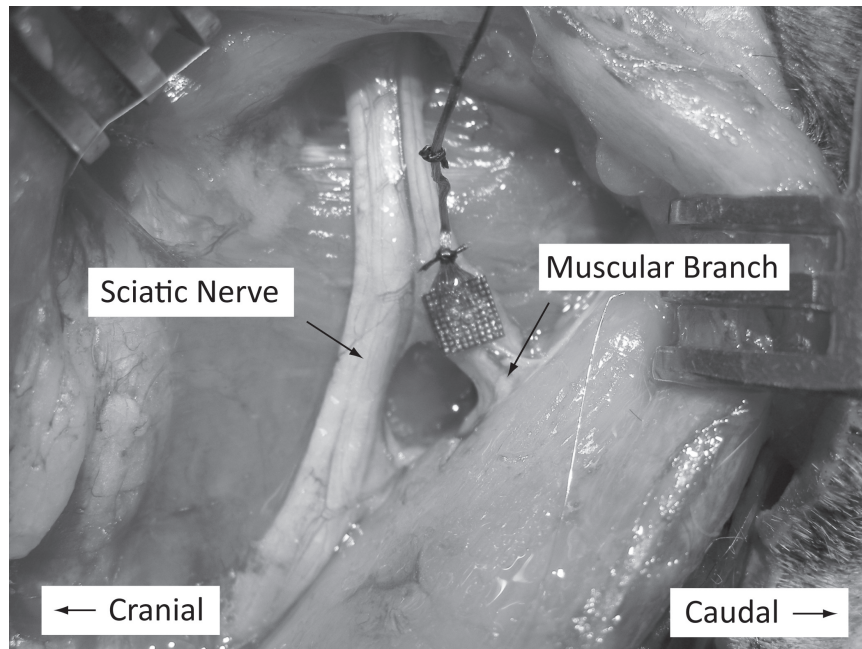


Figure 2.1: Muscular Branch Implantation.

A 10-by-10 USEA implanted into the muscular branch of the sciatic nerve of the left hindlimb. The size of the array (4 mm x 4 mm) is well matched to the nerve. This spatial coverage provided access to all hamstring muscles innervated by the muscular branch.

variations in USEA electrode impedances but were constant for each preparation. All stimuli were single biphasic pulses delivered using custom hardware and software described elsewhere [22, 23].

Compound muscle action potentials (CMAPs) resulting from IFS were monitored via implanted EMG electrodes using a Cerebus data acquisition system (Cyberkinetics, Foxborough, MA). All EMG data were bandpass filtered to 10–250 Hz using built-in Cerebus analog and digital filters. Data for the first cat were digitized at 2 ksamples/s and data for the last five cats were digitized at 10 ksamples/s.

Experimental Design

1) Array Mapping: Perithreshold stimulus intensities were determined for each USEA electrode (600 electrodes, 6 cats) using a binary search algorithm [23]. The minimum stimulus intensity required to evoke a 50- μ V peak rectified CMAP on at least one muscle was deemed the perithreshold stimulus for that electrode.

2) Stimulus-Response Curves: For a subset of electrodes, EMG recruitment curves were generated by monotonically increasing stimulus intensity from below threshold to either a plateau in the activation curve, or a predetermined maximum stimulus intensity (a 1000- μ s pulse width), whichever came first. Stimuli were separated by at least 1 second to minimize muscle fatigue. EMG recruitment curves were generated for a total of 333 electrodes.

Data Analysis

The spatial arrangement of the electrodes in the array was used to assess the spatial arrangement of the motoneurons in the implanted nerve. For each electrode that was able to evoke a muscle twitch at perithreshold ($n = 447$), the muscle activated by that electrode was compared with those activated by the surrounding electrodes that also evoked a muscle twitch. The number of these surrounding electrodes that activated the same muscle as the center electrode was compared with the number that would be expected by chance alone. If a greater number of electrodes than predicted by chance activate the same muscle, there would be evidence for a musculotopic arrangement of motor axons in the nerve.

In each preparation, peak rectified CMAP signals from each muscle were normalized to the maximum peak rectified CMAP recorded for that muscle in response to single USEA electrode stimulation. This normalized EMG (nEMG) was used for all analyses. To validate the use of this normalization technique, the maximum peak rectified CMAP recorded in each muscle in response to single USEA electrode stimulation was compared with the maximum evoked CMAP from whole-nerve stimulation. Data from 11 USEA implants in either the sciatic nerve (8 implants), its muscular branch (2 implants), or the femoral nerve (1 implant) were used for this analysis. Whole-nerve stimulation was evoked using either extraneural cuff stimulation (3 sciatic implants) or simultaneous activation of all 100 USEA electrodes. Data from the 2 USEA implants in the muscular branch were from 2 animals included in the present study, whereas the data from USEAs at other implant sites were from animals used for other

investigations, and are included here only with respect to the validation of our EMG normalization technique.

For each electrode for which a recruitment curve was generated, the ability of the electrode to recruit a single muscle selectively was quantified using a Selectivity Index (SI) (2.1) at three target nEMG levels: 0.1, 0.5, and 0.9. The SI was computed by first finding the lowest stimulus intensity where one muscle reached the target nEMG value. The difference between the target nEMG value and the largest nEMG response evoked on another muscle at this stimulus intensity was normalized to the target nEMG value. This quantity was defined as the Selectivity Index. In the cases where the target nEMG was not achieved exactly, the points recorded above and below were linearly interpolated. With the use of this equation, muscles that were exclusively excited had an SI of 1, whereas those that were simultaneously and equally excited with one or more other muscles had an SI of 0.

$$SI = \frac{\text{Target nEMG} - \text{2nd Largest nEMG}}{\text{Target nEMG}} \quad (2.1)$$

Accurate assessment of muscle-selective activation requires EMG recordings with little or no cross-talk between EMG pairs in different muscles. Cross-talk was evaluated in each preparation by comparing the EMG waveforms recorded from each muscle using cross-correlation analysis. Low correlation coefficients between EMG channels would suggest independent signals and thus accurate EMG and selectivity measurements.

The dynamic range of each electrode that reached a plateau response at or above 0.5 nEMG was calculated. The dynamic range was defined to be the range of stimuli for an electrode that evoked a selective muscle response [24]. To calculate dynamic range, the first muscle to reach 0.1 nEMG was found. The pulse width required to evoke this threshold response was found by linearly interpolating between the points above and below 0.1 nEMG. The upper functional limit of the dynamic range was defined as the point where another muscle reached 0.1 nEMG (spillover), or the primary muscle reached a plateau before another muscle became active. Plateau was

defined when the nEMG evoked from four consecutive stimuli of increasing pulse widths varied by less than 5% of their mean. In the case where the plateau was used as the upper limit for the dynamic range, the plateau response with the lowest pulse width was used. Dynamic range is the difference between the spillover or plateau pulse width and the threshold pulse width. Over this stimulus range, a single muscle was activated. Along with dynamic range, the width of each recruitment curve was also calculated for the first muscle to reach 0.1 nEMG. This width was defined as the pulse width range between 0.1 and 0.9 nEMG. Both dynamic range and recruitment width are expressed as a difference in microseconds and as a ratio in decibels.

Results

Surgical Access

We observed the muscular branch to be a relatively flat nerve that further flattens and increases in width as it leaves the common sciatic nerve. The width of the nerve immediately distal to the branch from the sciatic approximately matched the 4-mm-square size of a 10-by-10 USEA (Figure 2.1).

Hamstring Activation at Perithreshold

Across all six implanted animals, we found that 74 ± 13 (mean \pm SD) electrodes per implant were able to evoke a perithreshold twitch in one of the hamstring muscles. In each of the six preparations, we were able to evoke twitches in SM, ST, and all three compartments of BF. The mean number of electrodes activating each muscle or compartment at perithreshold was not statistically different (Repeated Measures ANOVA, $F_{4,20} = 0.44$, $p = 0.78$) (Figure 2.2). These data indicate that for any given 10-by-10 USEA implanted in the muscular branch, approximately 15 electrodes will excite each muscle or compartment at perithreshold.

Musculotopic Organization

Histology from previous studies has shown that USEA electrodes penetrate nerve fascicles and closely abut nerve axons [25]. Thus, at perithreshold levels of activation, the excited nerve fibers are presumably very close to the charge-carrying electrode

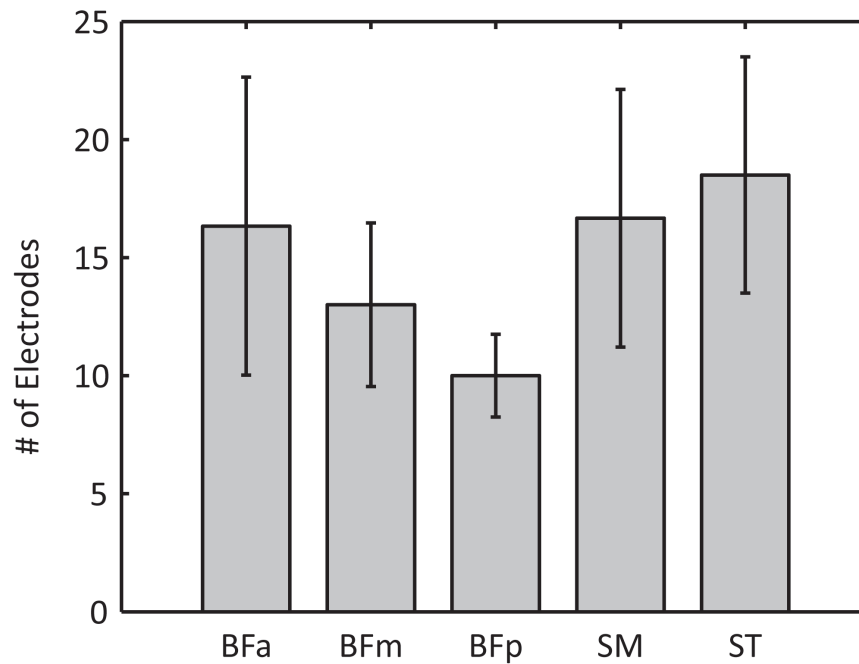


Figure 2.2: Perithreshold Activation of Hamstring Muscles.

The number of electrodes (mean \pm SEM) activating each muscle are shown for 6 cats. There was no statistical difference in the number of electrodes activating each muscle at perithreshold.

tip. As described in Methods, we assessed the musculotopic organization of the nerve by comparing the muscle activated by each electrode to those activated by the neighboring electrodes. Electrodes activating a particular muscle or compartment were often in close proximity to one another. An example from one implant shows the spatial arrangement of the muscles activated by each electrode (Figure 2.3). For each electrode able to activate some muscle at perithreshold, the mean number of neighboring electrodes that activated the same muscle (2.95) was significantly greater than the number of electrodes that would be expected by chance alone (1.59) (mean difference per preparation = 1.37 electrodes, $t_5 = 4.97$, $p < 0.01$). These data suggest that there is musculotopic organization of the motor axons in the nerve at the location of the USEA implants.

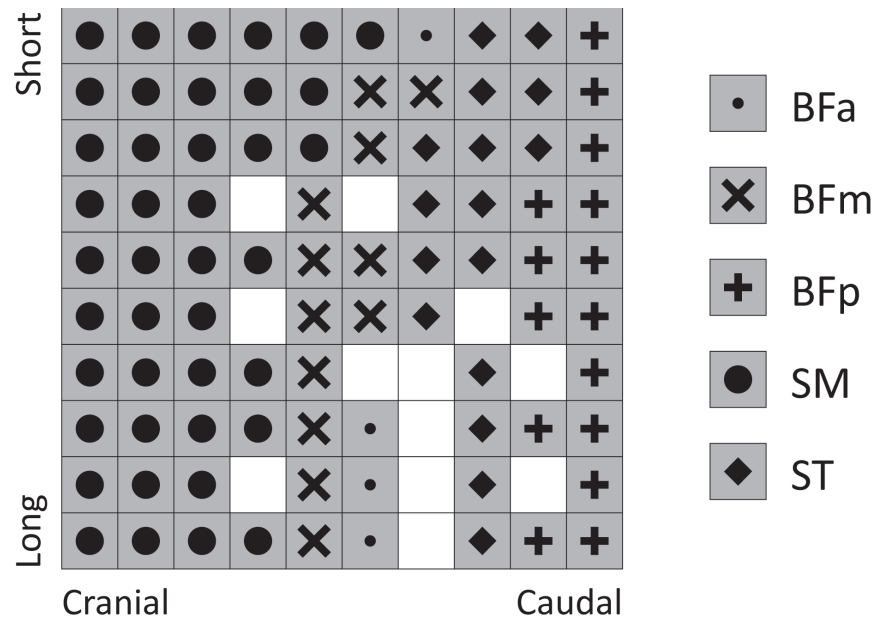


Figure 2.3: Threshold Map From 1 Animal.

Each tile in the 10-by-10 grid represents 1 electrode, and the symbols depict the muscle that it activated at perithreshold. The grid is oriented to match the orientation of the array shown in Figure 2.1. Short and Long refer to the lengths of the electrodes at these positions (0.5 and 1.5 mm, respectively). In this animal, ± 3 V pulses were used, and the number of electrodes activating BFa, BFm, BFp, SM, and ST were 4, 12, 15, 41, and 16, respectively; 12 electrodes failed to activate any muscle (white tiles). For each active electrode, on average 2.56 more neighboring electrodes activated the same muscle than would be expected in a random distribution.

Validation of EMG Normalization

To validate the use of maximum CMAPs evoked from individual USEA electrodes for EMG normalization, we compared the maximum CMAP evoked from whole-nerve stimulation to CMAPs evoked from single USEA electrodes in 48 muscles from 11 animals. In 8 of these preparations, simultaneous activation of all 100 USEA electrodes was used as whole-nerve stimulation; in the remaining 3 preparations, extraneural cuff stimulation was used. Two of these animals were used for the present study, whereas the others were used primarily for other investigations. The maximum CMAP values were $5047 \pm 2978 \mu\text{V}$ (mean \pm SD) for whole-nerve stimulation and $5101 \pm 2681 \mu\text{V}$ (mean \pm SD) for single-electrode stimulation recruitment curves, with a mean difference of $54 \pm 255 \mu\text{V}$ (mean \pm SEM). There was no statistical difference between

the two forms of maximum values for each muscle (paired t-test, $p = 0.83$). These data suggest that the maximum CMAP evoked in each muscle from individual USEA electrodes is a valid maximum for EMG normalization.

Selective Muscle Activation

EMG recruitment curves were collected for a total of 333 electrodes. The USEAs ability to activate each muscle selectively was assessed by comparing the relative sizes of the CMAPs generated in each muscle (Figure 2.4). Across all 6 preparations, selective activation to near-maximal activity was achieved in SM, ST, and in each compartment of BF (Figure 2.5).

The mean number of highly selectively activated (nominally $SI \geq 0.8$) muscles at 0.9 nEMG was 2.5 (range: 1–4). No single preparation manifested highly selective

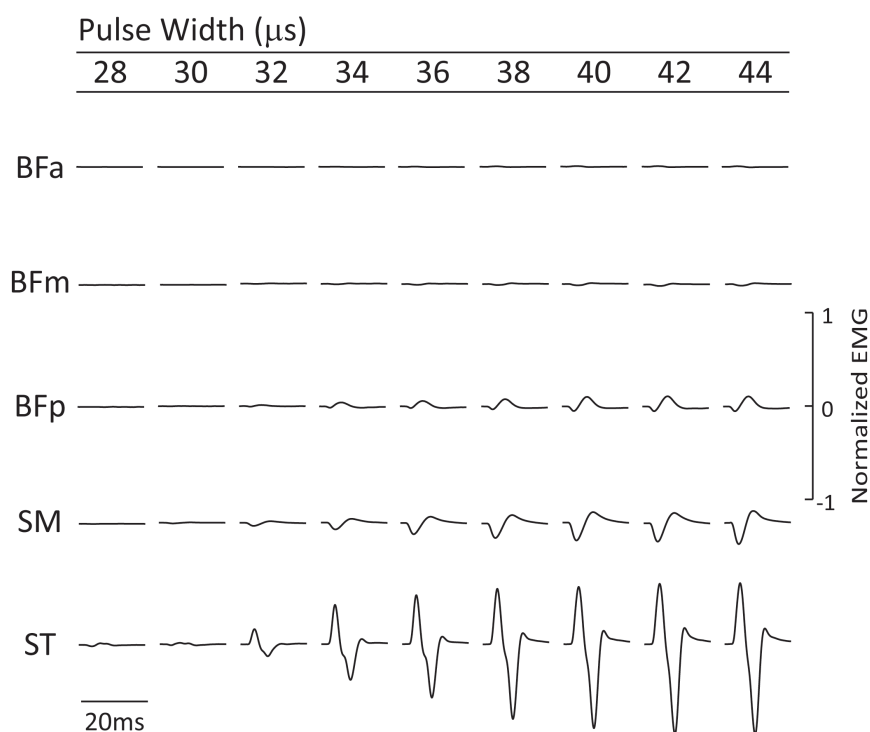


Figure 2.4: EMG Recruitment Curve.

Stimuli of increasing pulse width were delivered through a single USEA electrode, and the CMAP in each muscle was recorded. The peak of the rectified CMAP in each muscle for each stimulus was used to construct recruitment curves. This electrode primarily activated semitendinosus.

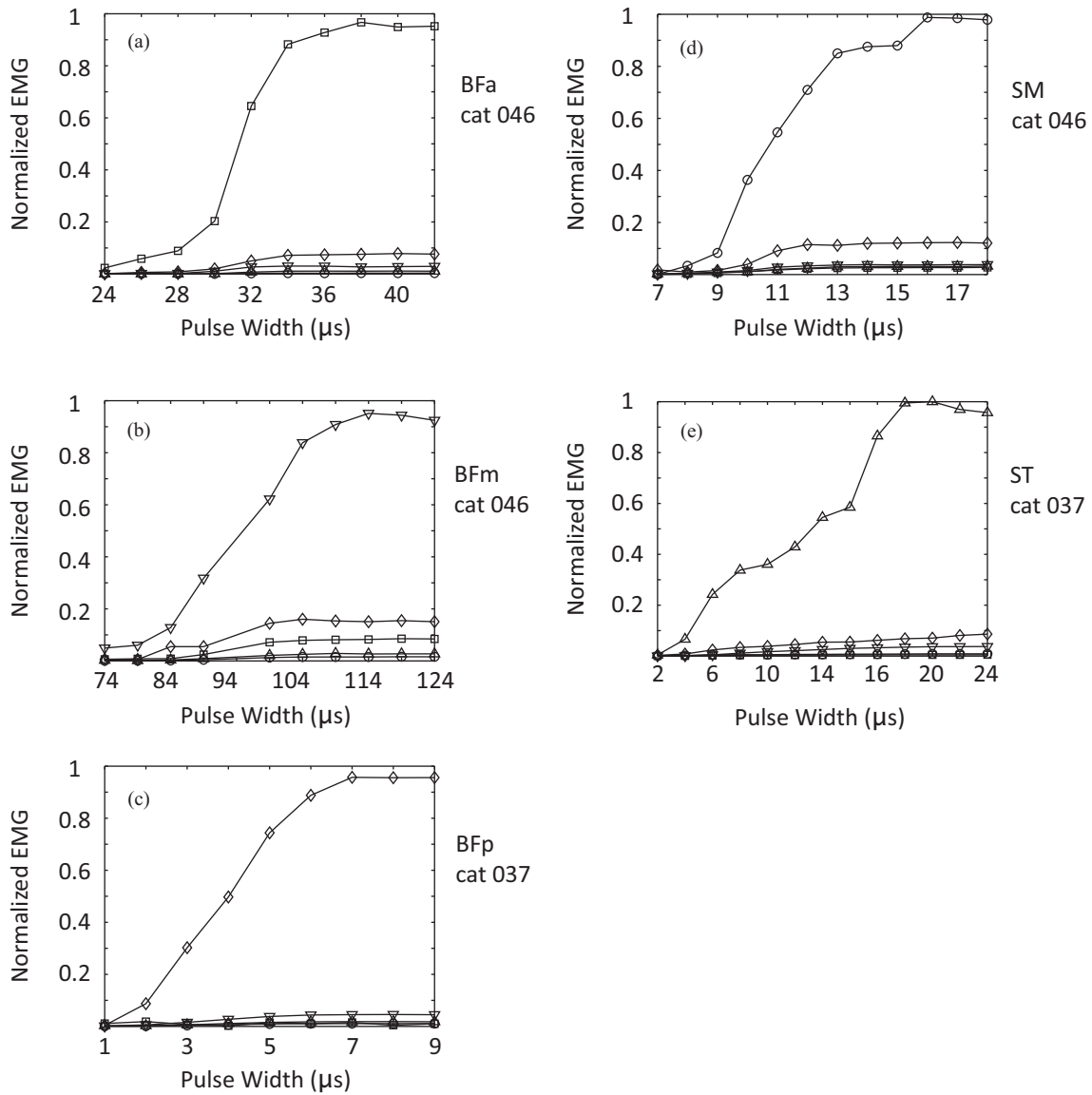


Figure 2.5: Selective Activation of Each Muscle.

Recruitment curves demonstrating selective activation of BFa (\square), BFm (∇), BFp (\diamond), SM (\circ), and ST (\triangle), are shown in panels (a)–(e), respectively. Examples are from 2 different animals.

activation of all muscles at this nEMG level. At 0.5 nEMG, the mean number of muscles activated selectively was 3.5 (range: 2–5) with one preparation activating all muscles selectively. Cross-correlation analysis showed minimal cross-talk between EMG recordings in different muscles. Across all 6 animals, the mean cross-correlation coefficient magnitude was 0.08.

The degree to which an electrode could activate a single muscle was quantified at three different levels of activation using the selectivity index (SI) described in Methods and illustrated in Figure 2.6(a).

At least 33% of electrodes were highly selective (nominally $SI \geq 0.8$) at each level of activation (Figure 2.6(b–d)). Fewer electrodes were able to achieve the higher levels of activation (279, 239, and 92 electrodes at 0.1, 0.5, and 0.9 nEMG respectively). Of the electrodes able to achieve each target nEMG (86 electrodes), there was significantly greater selectivity at 0.1 nEMG and 0.5 nEMG than at 0.9 nEMG (Repeated Measures ANOVA, $F_{2,170} = 5.26$, $p < 0.01$). Although statistically significant, this difference was relatively small; on average, each electrode had 0.07 and 0.09 greater selectivity at 0.1 nEMG and 0.5 nEMG, respectively, than at 0.9 nEMG. The selectivity index presented here could overestimate selectivity if several muscles are activated together, because this index compares only the two most active muscles. To assist interpretation of the selectivity data above, the number of muscles activated above 0.1 nEMG, excluding from the dominant muscle, were calculated. At 0.5 nEMG, 0.8 ± 0.8 (mean \pm SD) other muscles were active, whereas at 0.9 nEMG, 1.4 ± 1.3 (mean \pm SD) other muscles were active.

To assess the USEAs ability to recruit the two major actions of the hamstring muscles, hip extension and knee flexion, the muscles were grouped into extensors (BFa, BFm, and SM) and flexors (BFp and ST) and the selectivity index was recalculated. For this case, activation of a secondary muscle was ignored if it belonged to the same functional group as the primary muscle. The mean SIs at 0.1, 0.5, and 0.9 nEMG using this method were 0.76, 0.83, and 0.72, respectively, whereas the mean SIs for single muscle selectivity were 0.60, 0.65, and 0.57, respectively. There was significantly

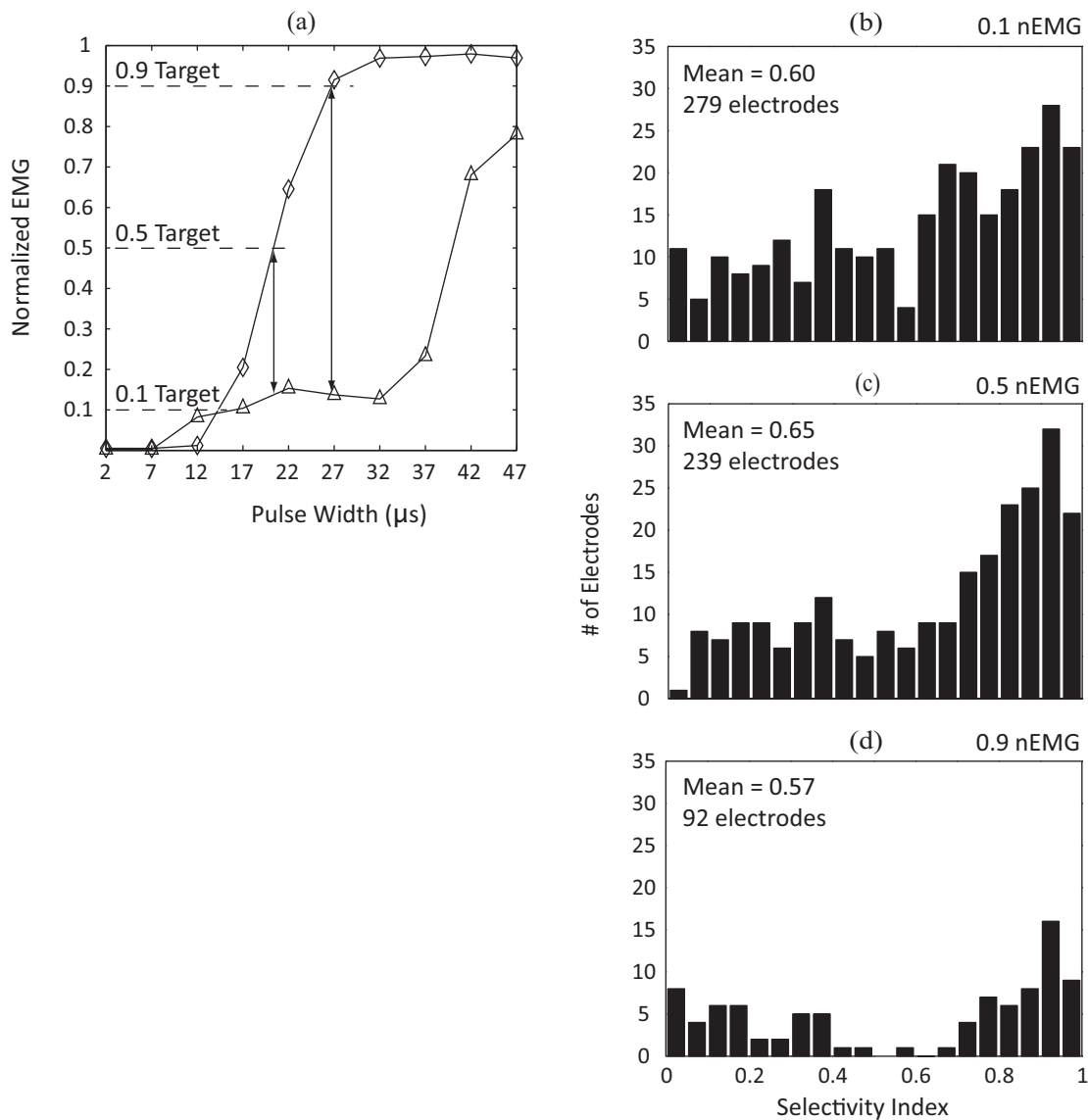


Figure 2.6: Selectivity Indices at Three Levels of Muscle Activation.

(a) The SI was calculated by subtracting the next largest nEMG value from the target nEMG, and dividing by the target nEMG. (b)–(d) Group data for all electrodes tested are shown for 0.1, 0.5, and 0.9 nEMG, respectively.

greater selectivity between functional groups than between single muscles at each nEMG level (paired t-tests, $p < 0.001$ for each 0.1, 0.5, and 0.9 nEMG).

Stimulus Dynamic Range and Recruitment Width

We calculated the dynamic range and recruitment width of all electrodes that evoked a plateau response on a muscle (188 electrodes). Dynamic range was defined as the range of stimulus pulse widths between threshold and either the intensity above which a plateau in the response was observed or another muscle reached threshold. The dynamic range was $13.6 \pm 29.3 \mu\text{s}$ (mean \pm SD) and ranged from 0 to 165.1 μs . Expressed as the ratio of plateau or spillover pulse width to threshold pulse width, the dynamic range was $4.14 \pm 5.05 \text{ dB}$ (mean \pm SD) and ranged from 0 to 25.0 dB. At the point of plateau or spillover, the nEMG of the dominant muscle was 0.42 ± 0.25 (mean \pm SD) and ranged from 0.1 to 0.95. EMG recruitment width compared the threshold pulse width to the pulse width required to reach plateau regardless of spillover. The recruitment width was $33.3 \pm 55.1 \mu\text{s}$ (mean \pm SD) and ranged from 0 to 417 μs . Expressed as a ratio, the recruitment width was $7.99 \pm 6.18 \text{ dB}$ (mean \pm SD) and ranged from 0.72 to 31.72 dB. Thus, on average, the pulse width required to achieve 90% of maximum for a given electrode was 2.51 times larger than the threshold pulse width.

Discussion

By passing charge through individual electrodes in USEAs implanted in the muscular branch of the sciatic nerve, we were able to selectively activate each feline hamstring muscle to near-maximum as measured by implanted fine-wire EMGs. In many cases, multiple electrodes manifested such selective activation. As in humans, the cat hamstring muscles have been shown to produce complex torques around the hip and knee [8, 26], and have specific roles during gait [20, 26]. The IFS approach explored here would allow for independent control of these muscles for functional movements in a motor neuroprosthesis.

Although we were able to selectively activate each of the hamstring muscles to near-maximum evoked EMG, we were not able to do so in a single preparation.

In 1 preparation, we were able to excite all muscles selectively to 0.5 nEMG. In most preparations, BFa and BFm were recruited simultaneously, often with minimal activity in other muscles. It is possible that the close proximity of the BFa and BFm EMG recording electrodes, without a distinct fascial boundary between them, resulted in crosstalk between the EMG pairs. This is unlikely, however, because the average cross-correlation magnitude between these two EMG channels was only 0.16 across all 6 animals. BFa and BFm are individual neuromuscular compartments in the same muscle head [20], and thus it is possible that their innervating motoneurons are in the same nerve fascicle at the location of our implant. Subfascicular selectivity using USEAs has been demonstrated to maximum force in individual muscles innervated by the sciatic nerve [19], so it is unclear why we were unable to achieve this consistently in the muscular branch.

By comparing the muscles activated by neighboring electrodes at perithreshold, we found a musculotopic arrangement of motor axons in the nerve. Because the independence of motor fibers activated by different electrodes was not measured, it is possible that neighboring electrodes were activating the same fibers. This is unlikely, however, because musculotopy was assessed at perithreshold-stimulus pulse widths when the activated axons are very close to the electrode tip [27], and the tips of neighboring electrodes are up to over 400 μm apart. Further, the musculotopic segregation was evident across multiple adjacent electrodes (Figure 2.3).

The musculotopy we observed in the nerve as assayed by perithreshold activation corresponds well to previously reported anatomy where the fibers innervating the hip extensors BFa, BFm, and SM were located in the cranial portion of the nerve and the knee flexors BFp and ST were located in the caudal portion [20]. This orderly arrangement seemed to affect which secondary muscles were recruited as charge injection increased beyond single-muscle activation. If the first muscle activated was predominantly a hip extensor, the second muscle excited was usually a hip extensor also. The same trend was observed for the knee flexors. The increase in the selectivity index when muscles were grouped into extensors and flexors supports

this observation and suggests that generation of a specific movement may not require purely muscle-selective activation.

To assess the ability of this stimulation approach to achieve fine control of muscle activation, we measured the dynamic range of 188 electrodes across 6 cats. Because our stimulation system is capable of $0.5\text{-}\mu\text{s}$ pulse-width resolution, the stimulus dynamic range of $13.6\ \mu\text{s}$ that we observed translates to 27 points of graded access along the recruitment curve. Because muscle output is subject to time-varying processes such as potentiation and fatigue, this graded level of access along the recruitment curve should allow us to maintain target force levels despite ongoing changes in muscle responses.

Of the 333 electrodes used to generate recruitment curves, only 92 were able to evoke 90% of maximum EMG or greater in one muscle. If sufficient charge was passed through a single electrode, it should, in principle, be able to excite the entire nerve, yet we sometimes observed a plateau in muscle activation before either maximum activation or maximum stimulus intensity was reached. Because constant-voltage stimuli have a decaying exponential current waveform whose charge delivery capacity is dependent on electrode impedance [22, 28], it is possible that the pulse-width modulated constant-voltage stimuli used to generate the recruitment curves were limited by electrode impedance. Therefore, increasing pulse width may not have sufficiently increased charge injection to evoke full muscle activation. However, aside from the experimental demands to normalize activation to maximal responses, our infrequent ability to evoke near-maximal responses is not of major consequence, because most functional movements involve submaximal muscle activations.

Conclusion

This study has demonstrated that the hamstring muscles of the cat can be activated selectively over a broad range of stimulus intensities using a simple surgical implantation of a USEA into the muscular branch of the sciatic nerve. These findings suggest that the specific limb movements evoked by the hamstring muscles could be independently generated to effect coordinated limb movements such as a sit-to-stand maneuver. Eventually, such selective and graded access to the hamstring muscles

using a single intrafascicular implant could be an important component in a system designed to produce stance and gait for paraplegic patients.

References

- [1] R Kobetic, R J Triolo, J P Uhler, C Bieri, M Wibowo, G Polando, E B Marsolais, J A Davis, and K A Ferguson. Implanted functional electrical stimulation system for mobility in paraplegia: a follow-up case report. *IEEE Trans Rehabil Eng*, 7(4):390–8, Dec 1999.
- [2] P Hunter Peckham and Jayme S Knutson. Functional electrical stimulation for neuromuscular applications. *Annu Rev Biomed Eng*, 7:327–60, Jan 2005.
- [3] J A Davis, R J Triolo, J Uhler, C Bieri, L Rohde, D Lissy, and S Kukke. Preliminary performance of a surgically implanted neuroprosthesis for standing and transfers—where do we stand? *J Rehabil Res Dev*, 38(6):609–17, Jan 2001.
- [4] Vivian K Mushahwar, Patrick L Jacobs, Richard A Normann, Ronald J Triolo, and Naomi Kleitman. New functional electrical stimulation approaches to standing and walking. *J. Neural Eng.*, 4(3):S181–97, Sep 2007.
- [5] R Brissot, P Gallien, M P Le Bot, A Beaubras, D Laisné, J Beillot, and J Dassonville. Clinical experience with functional electrical stimulation-assisted gait with parastep in spinal cord-injured patients. *Spine*, 25(4):501–8, Feb 2000.
- [6] R Kobetic, R J Triolo, and E B Marsolais. Muscle selection and walking performance of multichannel fes systems for ambulation in paraplegia. *IEEE Trans Rehabil Eng*, 5(1):23–9, Mar 1997.
- [7] Manfred Bijak, Monika Rakos, Christian Hofer, Winfried Mayr, Maria Strohhöfer, Doris Raschka, and Helmut Kern. Stimulation parameter optimization for fes supported standing up and walking in sci patients. *Artif Organs*, 29(3):220–3, Mar 2005.
- [8] D I Carrasco and A W English. Mechanical actions of compartments of the cat hamstring muscle, biceps femoris. *Prog Brain Res*, 123:397–403, Jan 1999.
- [9] Lisa N MacFadden and Nicholas A T Brown. Biarticular hip extensor and knee flexor muscle moment arms of the feline hindlimb. *Journal of biomechanics*, 40(15):3448–57, Jan 2007.
- [10] Matthew D Tarler and J Thomas Mortimer. Linear summation of torque produced by selective activation of two motor fascicles. *IEEE Trans Neural Syst Rehabil Eng*, 15(1):104–10, Mar 2007.
- [11] D R McNeal and B R Bowman. Selective activation of muscles using peripheral nerve electrodes. *Med Biol Eng Comput*, 23(3):249–53, May 1985.
- [12] J Rozman and M Trlep. Multielectrode spiral cuff for selective stimulation of nerve fibres. *J Med Eng Technol*, 16(5):194–203, Jan 1992.
- [13] Dustin J Tyler and Dominique M Durand. Functionally selective peripheral nerve stimulation with a flat interface nerve electrode. *IEEE Trans Neural Syst Rehabil Eng*, 10(4):294–303, Dec 2002.

- [14] J D Sweeney, D A Ksienski, and J T Mortimer. A nerve cuff technique for selective excitation of peripheral nerve trunk regions. *IEEE Trans Biomed Eng*, 37(7):706–15, Jul 1990.
- [15] C Veraart, W M Grill, and J T Mortimer. Selective control of muscle activation with a multipolar nerve cuff electrode. *IEEE Trans Biomed Eng*, 40(7):640–53, Jul 1993.
- [16] Katharine H Polasek, Harry A Hoyen, Michael W Keith, and Dustin J Tyler. Human nerve stimulation thresholds and selectivity using a multi-contact nerve cuff electrode. *IEEE Trans Neural Syst Rehabil Eng*, 15(1):76–82, Mar 2007.
- [17] K Yoshida and K Horch. Selective stimulation of peripheral nerve fibers using dual intrafascicular electrodes. *IEEE Trans Biomed Eng*, 40(5):492–4, May 1993.
- [18] A Branner, R B Stein, and R A Normann. Selective stimulation of cat sciatic nerve using an array of varying-length microelectrodes. *J Neurophysiol*, 85(4):1585–94, Apr 2001.
- [19] Daniel McDonnall, Gregory A Clark, and Richard A Normann. Selective motor unit recruitment via intrafascicular multielectrode stimulation. *Can J Physiol Pharmacol*, 82(8-9):599–609, Jan 2004.
- [20] A W English and O I Weeks. An anatomical and functional analysis of cat biceps femoris and semitendinosus muscles. *J Morphol*, 191(2):161–75, Feb 1987.
- [21] PJ Rousche and RA Normann. Chronic intracortical microstimulation (icms) of cat sensory cortex using the utah intracortical electrode array. *Rehabilitation Engineering, IEEE Transactions on*, 7(1):56–68, 1999.
- [22] Scott D Hiatt, Andrew M Wilder, K Shane Guillory, Brett R Dowden, Richard A Normann, and Gregory A Clark. 1100-channel neural stimulator for functional electrical stimulation using high-electrode-count neural interfaces. *IFESS Abstract*, pages 1–3, Jul 2010.
- [23] Andrew M Wilder, Scott D Hiatt, Brett R Dowden, Nicholas A T Brown, Richard A Normann, and Gregory A Clark. Automated stimulus-response mapping of high-electrode-count neural implants. *IEEE Trans Neural Syst Rehabil Eng*, 17(5):504–11, Oct 2009.
- [24] W M Grill and J T Mortimer. Quantification of recruitment properties of multiple contact cuff electrodes. *IEEE Trans Rehabil Eng*, 4(2):49–62, Jun 1996.
- [25] A Branner and R A Normann. A multielectrode array for intrafascicular recording and stimulation in sciatic nerve of cats. *Brain Res Bull*, 51(4):293–306, Mar 2000.
- [26] S E Peters and C Rick. The actions of three hamstring muscles of the cat: a mechanical analysis. *J Morphol*, 152(3):315–28, Jun 1977.

- [27] W M Grill and J T Mortimer. The effect of stimulus pulse duration on selectivity of neural stimulation. *IEEE Trans Biomed Eng*, 43(2):161–6, Feb 1996.
- [28] Daniel R Merrill, Marom Bikson, and John G R Jefferys. Electrical stimulation of excitable tissue: design of efficacious and safe protocols. *J Neurosci Methods*, 141(2):171–98, Feb 2005.

CHAPTER 3

MUSCLE-SELECTIVE BLOCK USING INTRAFASCICULAR HIGH-FREQUENCY ALTERNATING CURRENT

Abstract

High-frequency alternating current (HFAC) applied to a peripheral nerve can reversibly block skeletal muscle contractions. We evaluated the ability of HFAC delivered via intrafascicular electrodes to selectively block activation of targeted muscles without affecting activation of other muscles. Utah Slanted Electrode Arrays (USEAs) were implanted into the sciatic nerves of 5 cats, and HFAC was delivered to individual USEA electrodes. The effects of HFAC block were monitored by recording evoked electromyograms (EMGs) and three-dimensional endpoint forces. In each animal, activity evoked in targeted muscles by nerve cuff stimulation could be selectively abolished by HFAC delivered via individual USEA electrodes. Two mechanisms of blockade were evoked: selective neuromuscular blocks were achieved with 500–8000-Hz HFAC, and selective nerve conduction block was achieved in 1 animal using 16-kHz HFAC. These results show that intrafascicular HFAC can be used to block selected muscles independent of activation of other muscles.

Introduction

Many neuropathological conditions are characterized by an increase in neuronal activity resulting in chronic pain or abnormal muscular activity, such as dystonia, spasticity, or tremor. Although current surgical or pharmacological treatments can mitigate some negative impacts of these conditions, a safe, effective, and reversible method for selectively abolishing undesired peripheral nerve activity could improve treatment outcomes.

Prior research has demonstrated that high-frequency alternating current (HFAC) in the 1–30 kHz range, delivered to a peripheral nerve via extraneural electrodes, can block neural activity [1, 2, 3, 4, 5, 6, 7, 8]. This extraneural HFAC blockade has usually been studied using sets of electrodes that encircle the nerve with the degree of block measured with forces generated by the distal musculature. These studies have shown that contractions evoked by stimulation of the cuff electrode closest to the spinal cord can be blocked by HFAC delivered to the more distally positioned cuff electrode. The onset of HFAC transiently excites the distal muscles and a large force is produced that quickly decays, after which the muscles remain unresponsive to electrical stimulation at locations proximal to the blocking electrode. Almost immediately upon termination of the HFAC block, muscle twitches return with amplitudes and kinetics very similar to those evoked prior to the block.

Although extraneural electrodes can block activation of distal musculature, they do so nonselectively [1, 2, 4]. In cases where only certain muscles innervated by a single nerve manifest pathological activity, it may be desirable to selectively block activation of those muscles while leaving the other muscles unaffected. It has been shown that stimulation of selected muscles can be achieved by the use of electrodes that penetrate individual nerve fascicles where the tips of the electrodes are in close proximity to small groups of fibers [9, 10, 11, 12]. We hypothesize that the highly selective peripheral nerve fiber access that can be obtained with intrafascicular penetrating microelectrodes can be exploited to provide selective HFAC blockade of individual muscles. We further hypothesize that other fibers in the nerve implanted with intrafascicular penetrating microelectrodes may remain unaffected by this blockade and would therefore be responsive to either intrinsic or extrinsic neural stimulation.

To test these hypotheses, we implanted arrays of penetrating intrafascicular microelectrodes into feline sciatic nerves and evaluated the effects of HFAC on the blockade of activation of targeted muscles. Fast and reversible block of individual muscles or muscle subsets was achieved in each animal tested. Moreover, we were also able to selectively activate other target muscles innervated by the implanted peripheral nerve during this localized HFAC block. The results presented herein

show that HFAC delivered via intrafascicular microelectrodes can achieve selective and reversible blockade of muscle activation. We suggest that this selective muscle blockade can be used for the basis for new neuroprosthetic clinical applications.

Methods

Surgical Preparation

Five adult cats were studied using procedures approved by the University Utah Institutional Animal Care and Use Committee. Anesthesia was induced with an intramuscular injection of Telezol (Fort Dodge Animal Health, Fort Dodge, IA) and maintained with isoflurane via mechanical ventilation. Vital signs (heart rate, blood oxygen saturation, expired CO₂, and rectal temperature) were monitored and recorded to assess the condition of the animal as well as depth of anesthesia.

The animal was placed in a prone position in a rigid trough with its hindlimbs suspended from the end of the trough. The left limb was fixed at approximately 90 degree joint angles at the hip, knee, and ankle by placing two bone screws in the left iliac crest and two bone screws in the left tibia. The foot was secured to the recording surface of a six-axis load cell (AMTI MC3A6-500, Advanced Mechanical Technology, Inc., Newton, MA) for monitoring of evoked endpoint forces.

The sciatic nerve of the left hind limb was exposed at midhigh by separating biceps femoris and vastus lateralis. In each animal, a 100-microelectrode Utah Slanted Electrode Array (USEA) was implanted at midhigh [9]. A cuff electrode was implanted approximately 2 cm proximal to the USEA and a second cuff electrode was implanted 2 cm distal to the USEA (Figure 3.1). Before USEA implantation in 1 animal, three cuff electrodes were implanted and the middle cuff was used to deliver HFAC blocking sinusoids. After several trials, the middle cuff electrode was removed and the USEA was implanted in its place. Each extraneural cuff electrode was custom made from silicone tubing and had two stainless steel wires inside the cuff that encircled the circumference of the nerve. The two wire electrodes had a longitudinal spacing of about 3 mm. The USEA is a 10-by-10 array of silicon microelectrodes that vary in length from 0.5 mm to 1.5 mm. Each electrode is tipped with sputtered iridium oxide and the remainder of the array is insulated with Parylene

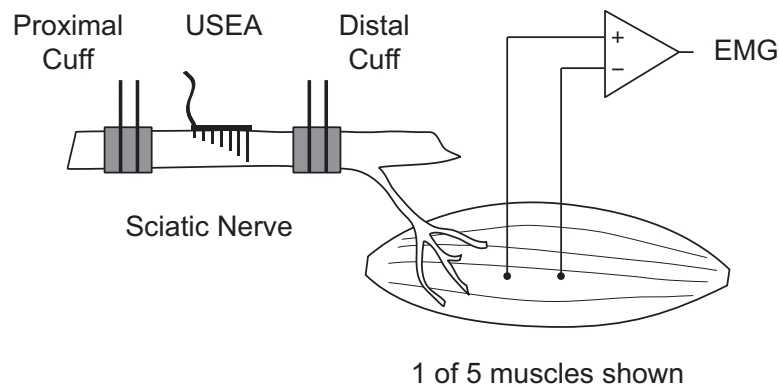


Figure 3.1: Experimental Setup

Schematic showing the orientation of implanted cuff electrodes and USEA. The two cuff electrodes were used to deliver 0.8–1.0-Hz pulsatile stimulation, and the USEA was used to deliver high-frequency sinusoidal stimuli. EMGs were recorded from MG, PLAN, LG, SOL, and TA using pairs of fine-wire electrodes inserted into each muscle belly (only one muscle is shown). Any generated forces were measured as endpoint forces at the foot using a 6-axis load cell.

C. The counter electrode for all stimulation and block with USEA electrodes was a platinum wire placed outside the nerve near the location of the implanted USEA. The electrodes impedances were $170 \pm 135 \text{ k}\Omega$ at 1 kHz (mean \pm SD). The exposure was closed after implantation of the USEA and cuff electrodes.

Five muscles innervated by the sciatic nerve were each instrumented with a pair of intramuscular fine-wire EMG electrodes, including: tibialis anterior (TA), medial and lateral gastrocnemius (MG and LG, respectively), plantaris (PLAN), and soleus (SOL). EMG electrodes were separated by approximately 7 mm with approximately 2 mm of insulation removed from each tip. A differential recording was made between the two wires in each muscle to minimize cross-talk from other muscles. All muscles except TA were visualized for EMG electrode insertion by an incision in the posterior calf; the TA electrodes were inserted through the skin. All EMG electrode placements were verified by stimulation through the EMG electrodes.

Stimulation and Recording Setup

Three types of stimulators were used in this study. Single-pulse stimuli delivered to the cuff electrodes were voltage-controlled stimuli generated using a commercial

stimulator (Grass SD9, Grass Technologies, West Warwick, RI) set to biphasic mode. HFAC waveforms were generated with a PC running either a custom LabView (National Instruments, Austin, TX) program or a custom Matlab (The MathWorks, Natick, MA) program and delivered to the electrodes by a National Instruments DAQ card (NI6711). The NI6711 card generates analog signals using a 12-bit D/A converter at an output rate of 1 MSamples/s. Its output range is ± 10 V with currents up to ± 5 mA. Floating outputs were used for the Grass stimulators and the NI6711. Force and EMG recruitment curves were automatically generated for each USEA microelectrode using custom software and hardware described in detail elsewhere [13]. Stimuli were voltage-controlled, pulse-width-modulated cathodic pulses. A range of pulse widths were selected by the software to evoke graded force magnitudes that ranged from threshold to plateau. The evoked EMG peaks were used to evaluate which muscle or muscle combinations were excited by stimulation via each USEA electrode.

All force and EMG data were recorded with a Cerebus data acquisition system (Blackrock Microsystems, Inc., Salt Lake City, UT) and digitized at 10 kSamples/s. EMG data were band-pass filtered at 10–250 Hz (2nd-order Butterworth filters) using the built-in Cerebus analog and digital filters, and all force measurements were low-pass filtered at 50 Hz using Matlab. The animal was grounded using a 22-gauge needle placed under the skin and connected to Earth ground.

Block Using HFAC

In each animal, the proximal cuff electrode was used to deliver supramaximal single-pulse stimuli at a rate of 0.8–1 Hz before, during, and after HFAC block. Typical supramaximal stimulus parameters were 5–7 V in amplitude and 200–400 μ s in duration. After 5–7 stimuli were delivered to the proximal cuff, an HFAC sinusoid was delivered to a single USEA electrode for 5 seconds. The USEA electrodes used to deliver the blocking waveform were chosen based on their ability to selectively stimulate a single muscle or a small subset of muscles as evaluated from the force and EMG recruitment curves. The peak-to-peak voltage and frequency of the HFAC sinusoid were varied to evaluate and optimize muscular block. Because the HFAC

parameters shown to produce block with extraneural electrodes vary widely, and because no attempts to block using intrafascicular electrodes have been reported, a variety of frequency and amplitude combinations were used to evaluate and optimize muscular block. HFAC frequencies between 250 Hz and 30 kHz with peak-to-peak amplitudes up to 20 V were tested.

In 2 of 5 animals studied, supramaximal stimulation via a distal cuff electrode was alternated with proximal cuff stimulation to identify the location of block. Force and/or EMG reduction was considered to be a result of a conduction block at or near the blocking electrode if responses evoked by the proximal cuff were diminished but responses evoked by the distal cuff were unaffected. If distal stimulation also produced attenuated responses, then the block occurred distal to all implanted electrodes and was termed neuromuscular block.

A third animal was used to evaluate the possibility of using two intrafascicular electrodes to produce a simultaneous block and activation of different muscles. Pairs of USEA electrodes that selectively and independently activated separate groups of muscles were chosen for this study. One electrode was used to deliver HFAC sinusoids while the other electrode delivered 0.8 Hz stimulation alternated with 0.8 Hz stimulation of the proximal cuff electrode. HFAC was delivered for 5 s durations after 5–7 s of low-frequency stimulation.

Classification of Responses to HFAC

To quantify the ability of the USEA to produce selective muscle blockade using HFAC, each trial was categorized as producing muscle-selective block, nonselective block, sustained firing, or no effect. Further discrimination was made between partial and complete blocks. Classification of the results of each trial into one of these categories was made using two quantities calculated from the EMG recordings of each muscle in each trial. The first metric quantified the degree to which the HFAC waveform decreased the muscle response evoked by the supramaximal cuff stimulation proximal to the site of HFAC delivery. This metric, termed the block ratio, was calculated for each muscle and compared the average peak EMG response before HFAC to the average peak EMG response during HFAC (3.1). Using this equation,

complete block of EMG responses evoked by cuff stimuli would have a block ratio of 1, whereas a block ratio of 0 would indicate no changes in EMG responses during HFAC. The second metric used to categorize each trial quantifies the amount of tonic activation evoked in each muscle by HFAC by dividing the time-averaged integral of the rectified EMG signal during block by the integral before HFAC. This integrated EMG ratio represents the increase or decrease of overall EMG activity for each muscle before and during HFAC.

$$\text{Block Ratio} = 1 - \frac{\text{Mean EMG peak during HFAC}}{\text{Mean EMG peak before HFAC}} \quad (3.1)$$

Categorization of the results of each trial was made based on these two metrics for each muscle in each trial as described in Table 3.1. A trial was categorized as evoking sustained firing if any muscle had an integrated EMG ratio of greater than 2. The results of all trials without sustained firing were categorized as: no effect, selective, or nonselective block. A further distinction was made between complete (block ratio ≥ 0.8) and partial blocks (block ratio between 0.2 and 0.8). HFAC was deemed to produce muscle-selective block if only one muscle exceeded a block ratio of 0.2. If two or more muscles exceeded block ratios of 0.2, the block was deemed nonselective.

Table 3.1: Classification of HFAC Trials

Classification	EMG block ratio
No effect	All muscles < 0.2
Selective block	
Complete	1 muscle > 0.8
Partial	1 muscle between 0.2 and 0.8
Nonselective	
Complete	1 muscle > 0.8 AND 1 ⁺ muscle > 0.2 OR 2 ⁺ muscles > 0.8
Partial	2 ⁺ muscles between 0.2 and 0.8

Results

Nonselective Neuromuscular Block Using a Cuff Electrode

HFAC block with a cuff electrode resulted in cessation of force generation and EMG activity across all five instrumented muscles (Figure 3.2a). Before HFAC onset, the two cuff electrodes—proximal and distal to the cuff electrode that was used to deliver HFAC—evoked robust force and EMG responses. The net muscle forces evoked by proximal and distal cuff electrode stimulation generally consisted of two components; a fast-twitch component peaking at about 30 ms, and a slow-twitch component peaking at about 85–95 ms (Figure 3.2b). In this example, 2 kHz HFAC delivered to the middle cuff electrode resulted in a large, transient onset force followed by complete elimination of evoked forces and EMGs from both proximal and distal cuff electrode stimulation. It is unclear why the large force evoked by HFAC onset was not accompanied by comparably large EMG responses. It is possible that the large onset response briefly saturated the Cerebus amplifiers. After termination of HFAC, the responses evoked by proximal and distal cuff electrode stimuli rapidly returned to preblock amplitudes. The lack of forces evoked by both proximal and distal cuff stimulation indicates that the HFAC caused either a widespread conduction block that extended to the distal cuff electrode, or interrupted a downstream neuromuscular process.

The response kinetics shown in the force twitches evoked by distal and proximal cuff electrode stimulation (and in more detail in Figure 3.2b) illustrate differences in the speed of recovery of the muscle forces following HFAC. The slow-twitch component of the response typically recovered to its preblock levels within 300 ms. However, the fast-twitch component of the response recovered with a more complex time course, often manifesting a transient augmentation of amplitude above pre-HFAC levels (Figure 3.2b). This complex recovery process for the fast-twitch component only allowed for an approximate estimate of from 2–60 s for its full recovery to pre-HFAC levels, with the longer recoveries seen later in the experiments where the HFAC had been delivered many times. These data suggest that force recovery

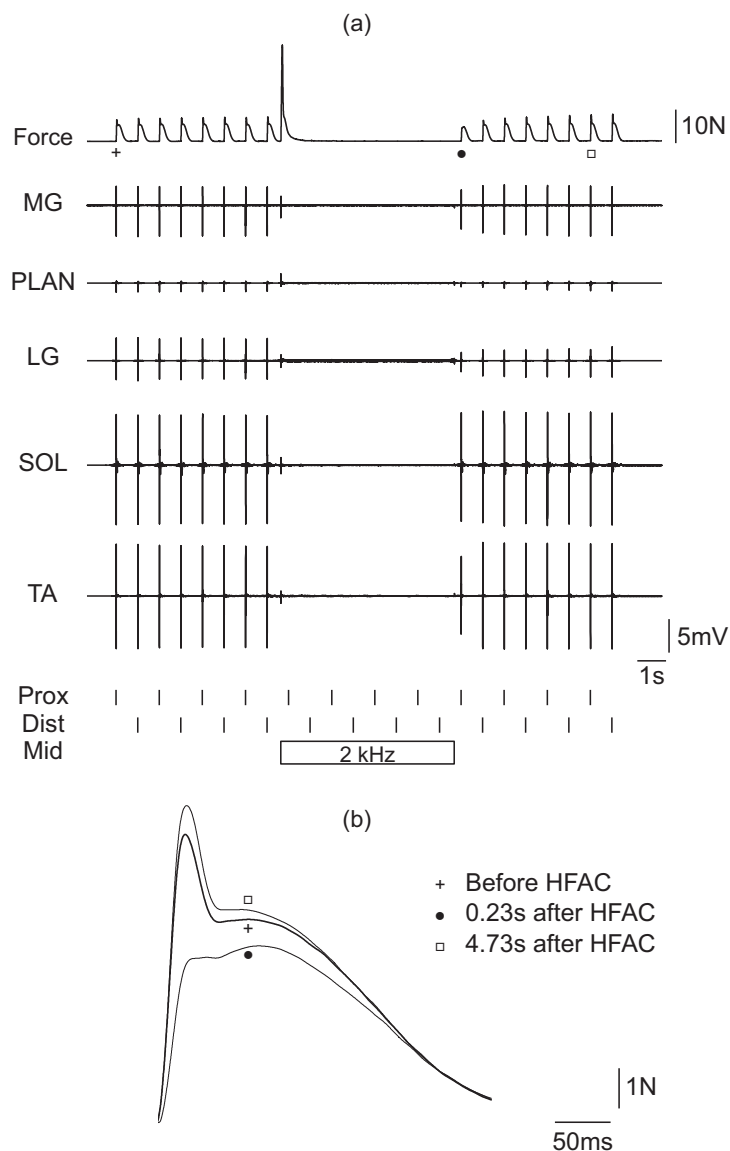


Figure 3.2: Nonselective Block Using a Cuff Electrode

(a) Complete nonselective block of hindlimb muscles produced by 2-kHZ, 2-V HFAC delivered via a cuff electrode around the sciatic nerve. Trains of alternating stimuli were delivered via the distal and proximal cuff electrodes throughout the record (bottom ticks). HFAC evoked a transient onset response and eliminated the EMG (middle traces) and force (top trace) responses evoked by distal and proximal stimulation. (b) Twitch amplitudes recovered rapidly following the termination of HFAC block. Recovery was first seen for the slow-twitch fibers; in this case, the fast-twitch fibers showed augmentation after block (Force = force magnitude at foot; MG = medial gastrocnemius; PLAN = plantaris; LG = lateral gastrocnemius; SOL = soleus; TA = tibialis anterior; Prox = proximal cuff stimulation; Dist = distal cuff stimulation; Mid = middle cuff block]

after neuromuscular block is stimulus-history dependent and warrants further, more rigorous investigation.

Selective Neuromuscular Block Using USEA Electrodes

In all 5 animals studied, HFAC delivered through individual USEA electrodes resulted in block (nominally, block ratio ≥ 0.2) of a subset of the instrumented muscles without evoking activation of other muscles (nominally, integrated EMG ratio < 2.00). See Materials and Methods for definitions of different categories of block. This nonselective block was achieved with 31 of the 55 electrodes tested (Table 3.2). In 4 of the 5 animals, a single muscle could be blocked without affecting the other muscles; however, only 4 electrodes in 2 of the animals could achieve complete muscle block (nominally, block ratio ≥ 0.8). Figure 3.3 shows an example of complete and nonselective block of medial gastrocnemius (MG) by application of a 3 V, 2 kHz sinusoid to a single USEA electrode. The HFAC block resulted in a block ratio of 0.92 for MG and block ratios of 0.22, 0.05, 0.01, and 0.00 for plantaris (PLAN), lateral gastrocnemius (LG), soleus (SOL), and tibialis anterior (TA), respectively. The block

Table 3.2: HFAC Block with USEA Electrodes

	Animal					Total
	1	2	3	4	5	
No. of electrodes tested	6	10	14	7	18	55
No activation of other muscles						
Selective						
Partial block	0	2	0	2	2	6
Complete block	0	3	1	0	0	4
Total	0	5	1	2	2	10
Nonselective						
Partial block	2	3	0	2	1	8
Complete block	0	6	11	3	8	28
Total	2	7	11	3	8	31
Activation of other muscles						
Partial block	4	6	3	4	9	26
Complete block	2	5	9	3	12	31

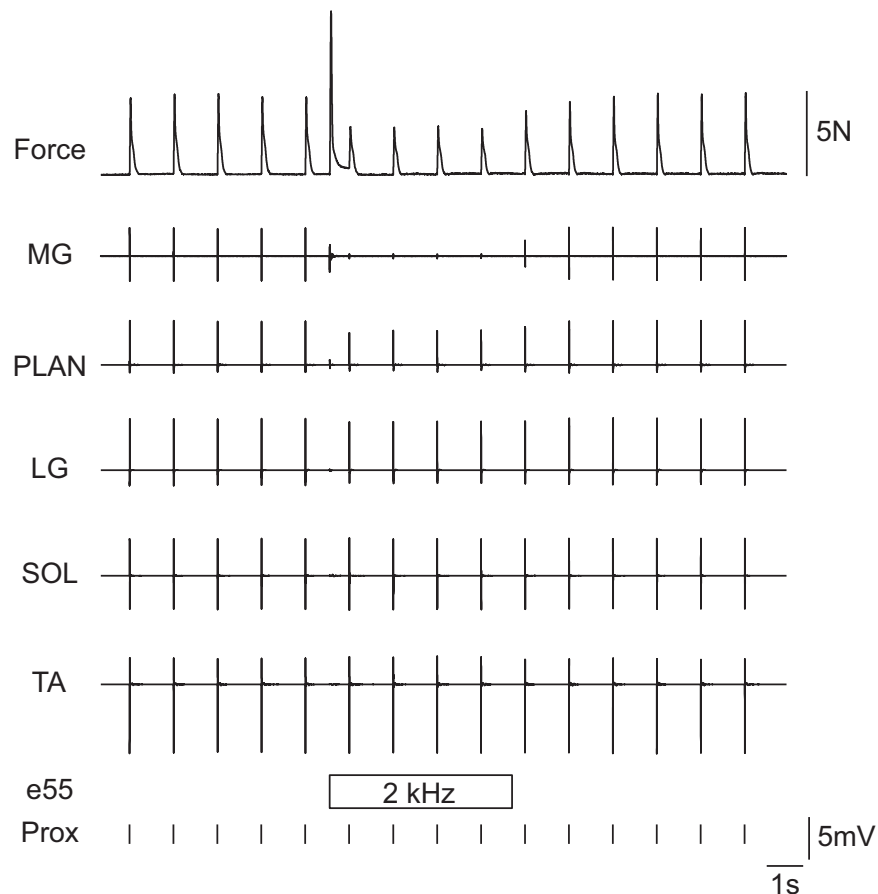


Figure 3.3: Block Using an Intrafascicular Electrode

A complete and nonselective neuromuscular block of MG using 2-kHz, 3-V HFAC delivered via a single USEA electrode (e55). Cuff stimulation proximal to the array evoked large EMG responses in all muscles. When HFAC block was delivered to electrode 55, EMG activity in MG was greatly reduced (block ratio of 0.92), whereas the other muscles showed slight or no decrease in EMG activity (block ratios of 0.22, 0.05, 0.01, and 0.00 for PLAN, LG, SOL, and TA, respectively). The block ratio of PLAN was just over the threshold (0.20) for a trial to be categorized as nonselective. All integrated EMG ratios were <1.10 . When the HFAC block was terminated, EMG and force responses returned to pre-HFAC levels. (See Figure 3.2 for abbreviations.)

ratio for PLAN was just above the threshold of 0.20 for the results of this trial to be categorized as nonselective.

Only 4 electrodes were found to produce complete and selective block. However, complete and nonselective block was achieved in 4 of 5 animals with 28 of the 55 electrodes tested (Table 3.2). The HFAC amplitude required to produce tonic activation and the amplitude to produce block varied across muscles for any given electrode. Because of this, the amplitude required to block one muscle was often above the threshold for activating another muscle. Figure 3.4 shows an example of complete block of MG (block ratio of 0.90) with tonic activation of PLAN (integrated EMG ratio of 4.42). The similar activation and block thresholds for different muscles greatly reduced the yield of electrodes that could produce block without activating other muscles.

The most effective HFAC frequency for generating neuromuscular block was 2 kHz. In order to minimize fatiguing contractions, the threshold voltage amplitude was not usually identified with high precision. The lowest voltages delivered that evoked activation and those that evoked block on each electrode were tabulated, and on average, muscle activation occurred at 2.5 ± 2.75 V (mean \pm SD, range: 0.5–9 V), partial block occurred at 6.35 ± 3.4 V (mean \pm SD, range: 0.5–10), and complete block occurred at 6.28 ± 3.91 V (mean \pm SD, range: 1.05–17 V). Most other HFAC frequencies tested did not produce neuromuscular block; however, those that did required voltages higher than those used at 2 kHz (Table 3.3).

Simultaneous Neuromuscular Block and Muscle Activation Using USEA Electrodes

One goal of this study was to demonstrate that a pair of electrodes from a single implanted USEA could be used to block one muscle while simultaneously activating another. In 1 animal, 4 electrodes were identified that could produce complete neuromuscular block: 2 electrodes produced complete selective block of MG and 2 electrodes produced complete nonselective block of LG, PLAN, and SOL. In all pairings of these electrodes, MG could be blocked with 2 kHz HFAC while stimulating

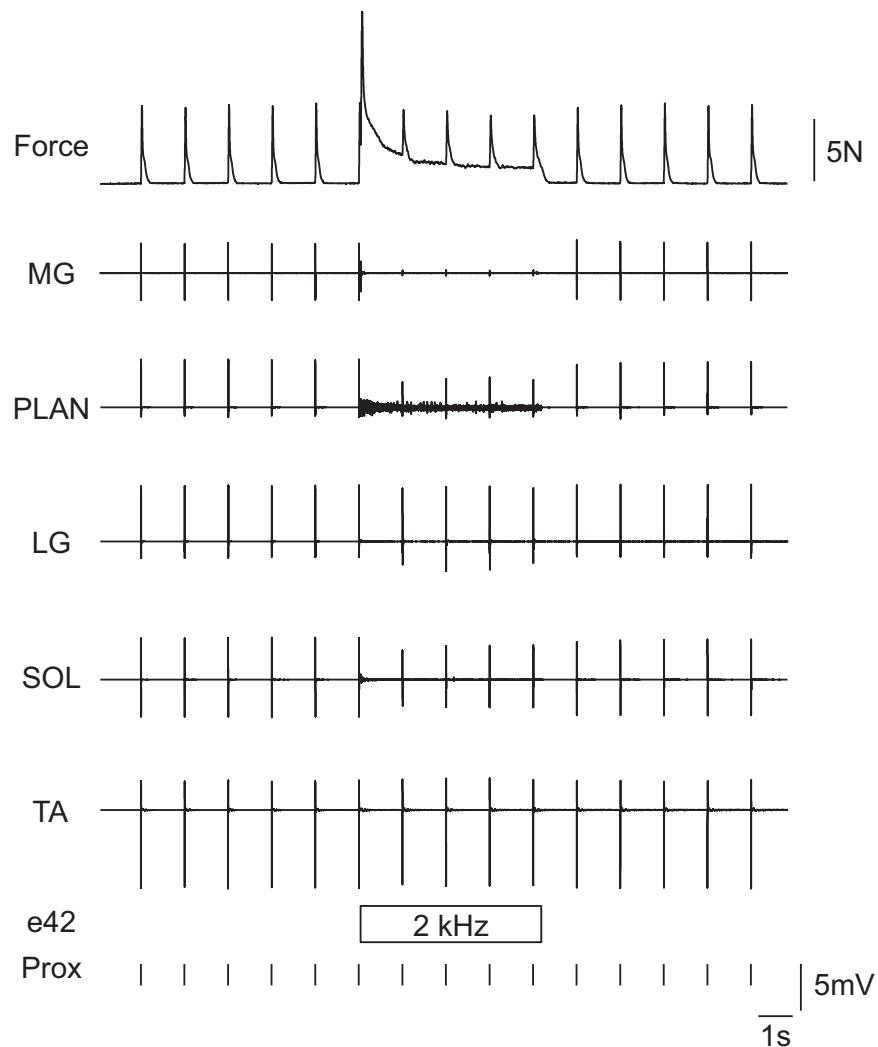


Figure 3.4: Sustained Activation and Block

Sustained activation and block in response to intrafascicular HFAC. A 4-V, 2-kHz sinusoidal stimulus delivered via 1 electrode (e42) blocked activation of MG (block ratio of 0.90), but evoked both sustained activity in PLAN (integrated EMG ratio of 4.42) and sustained force throughout HFAC delivery. There were no HFAC amplitudes tested for this electrode that could block MG without producing tetanus or block of PLAN. The other muscles were differentially affected by HFAC (block ratios of 0.42, 0.03, 0.21, and 0.03 for PLAN, LG, SOL, and TA, respectively). (See Figure 3.2 for abbreviations.)

Table 3.3: HFAC Parameters Tested Using USEA Electrodes and the Evoked Effects

HFAC Parameters Tested			Neuromuscular Block		Conduction Block		
Frequency	Voltage	# electrodes	Sustained Activation	partial	complete	partial	complete
0.25	0.25-2	1	-	-	-	-	-
0.5	0.5-2	1	-	-	-	-	-
1	0.5-10	9	4.75±1.5 (n=4)	-	8 (n=1)	-	-
2	0.5-17	54	2.5±2.75 (n=13)	6.35±3.4 (n=10)	6.28±3.91 (n=25)	-	-
4	0.5-15	3	0.75 (n=1)	9 (n=1)	15 (n=1)	-	-
6	15	1	-	-	-	-	-
8	0.5-20	8	1.5 (n=2)	-	20 (n=1)	-	-
10	20	1	-	-	-	-	-
16	2-20	13	14 (n=1)	-	-	11,15 (n=2)	17 (n=3)
18	20	1	-	-	-	-	-
20	9-20	2	-	-	-	-	-
32	8	1	8 (n=1)	-	-	-	-

LG/PLAN/SOL with 0.8 Hz pulsatile stimulation or vice-versa (Figure 3.5). The forces and EMGs evoked by the low-frequency stimuli on electrode 43 were nearly unaffected by the HFAC blocking waveform on electrode 42, suggesting a localized effect of the HFAC block (Figure 3.6).

Prolonged Muscle Block Using USEA Electrodes

In order for neuromuscular block using HFAC delivered via implanted USEA electrodes to have a relevant clinical impact for certain applications, it would be desirable to produce prolonged periods of muscular block. Therefore, we investigated the ability of HFAC to produce block for up to 30 minutes. Figure 3.7 shows selected time epochs of EMGs recorded for a 30-minute period of 2 kHz, 11.5 V HFAC delivered via a single USEA electrode. In this trial, MG was completely blocked (block ratio of 0.96) and the other plantar-flexors PLAN, LG, and SOL were partially blocked (block ratios of 0.60, 0.61, and 0.41, respectively) while the dorsi-flexor TA was mostly unaffected (block ratio of 0.11). This figure illustrates that prolonged muscular block of muscle subsets can be achieved and is reversible. The constant amplitude of the EMG evoked in TA indicates that the selectivity of muscle block can be maintained over long periods of HFAC delivery. However, such prolonged periods of HFAC muscle block appear to invoke processes that are not seen with the 5–7 s periods of HFAC block described above. In particular, the recovery of MG to pre-HFAC levels occurred over several minutes instead of over 1–2 seconds (compare to Figure 3.3).

Conduction Block Using USEA Electrodes

Although we found the use of 2 kHz HFAC to be the most robust and repeatable method to achieve neuromuscular block of muscle subsets, conduction block of fiber subsets was also achieved. We were unable to produce a conduction block using HFAC delivered via a cuff electrode, but we were able to achieve conduction block with three different USEA electrodes in 1 preparation. Conduction block on these electrodes required an HFAC peak-to-peak amplitude of at least 15 V (Table 3.3). Figure 3.8 shows an example of conduction block produced with 16 kHz HFAC delivered to a single USEA electrode for 60 s. As seen in this figure, HFAC onset produced a large

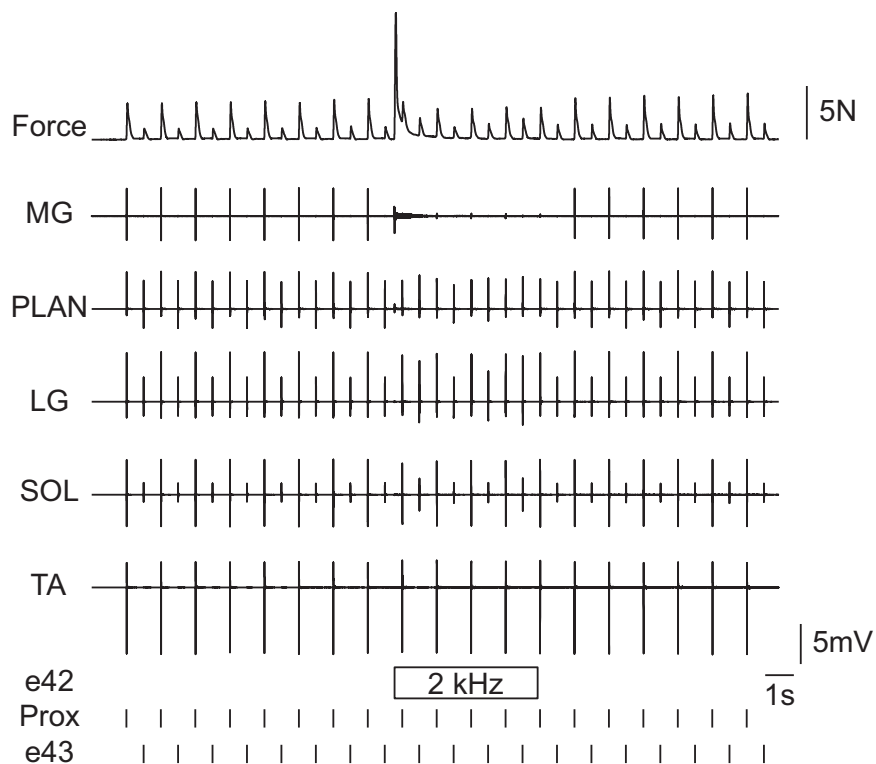


Figure 3.5: Block and Activation Using 2 USEA Electrodes

Simultaneous neuromuscular block and muscle activation using 2 USEA electrodes. Electrode 42 blocked activation of MG using 3.5-V, 2-kHZ HFAC, whereas electrode 43 activated LG, PLAN, and SOL using 0.75-V single-pulse stimulation. TA was unaffected by either USEA stimuli, but it was activated by the proximal cuff electrode. (See Figure 3.2 for abbreviations.)

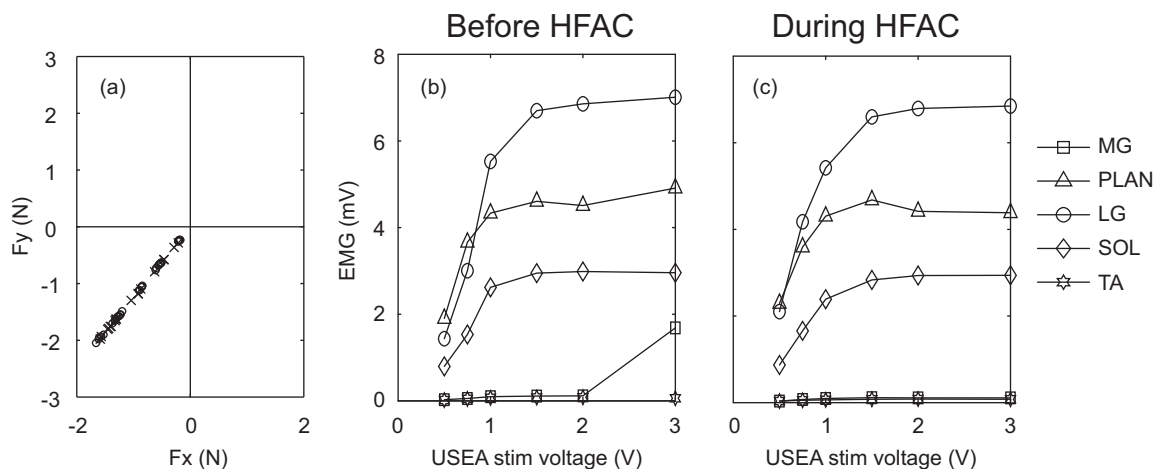


Figure 3.6: Activation was Unaffected by Block on Another Electrode

Muscle activation using single-pulse stimulation on USEA electrode 42 was unaffected by HFAC block on electrode 43. (a) The peak force trajectory produced with increasing stimulus intensities before block (o) was nearly identical to the force trajectory produced during block (x). The force trajectories are only shown for the transverse plane, but they were similar in all three orthogonal planes. Recruitment of EMG responses evoked in each muscle by electrode 43 before HFAC delivery (b) was nearly identical to that of the peak EMG responses evoked during HFAC on electrode 42 (c). Note that, without block, MG is recruited at 3 V (b); however, when MG is blocked using another electrode, 3-V stimulation fails to activate MG (c). (See Figure 3.2 for abbreviations.)

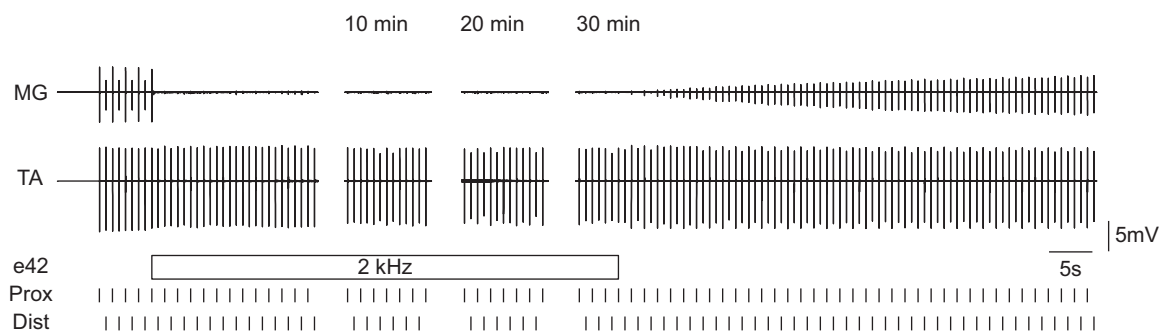


Figure 3.7: Block for 30 minutes

Complete nonselective muscular block produced by 30 minutes of 2-kHz, 11.5-V HFAC delivered via a single USEA electrode. Only selected time epochs are shown in this figure. MG activity is completely blocked (block ratio of 0.96) during the period of HFAC delivery, and the EMGs of PLAN, LG, and SOL showed somewhat reduced amplitude (block ratios of 0.60, 0.61, and 0.41, respectively; EMG traces not shown). EMG of TA was unaffected during HFAC delivery (block ratio of 0.11). The integrated EMG ratios for all muscles were <2 . All muscle responses recovered following HFAC termination, but over a longer time period than was observed with 5–7-s periods of HFAC. (See Figure 3.2 for abbreviations.)

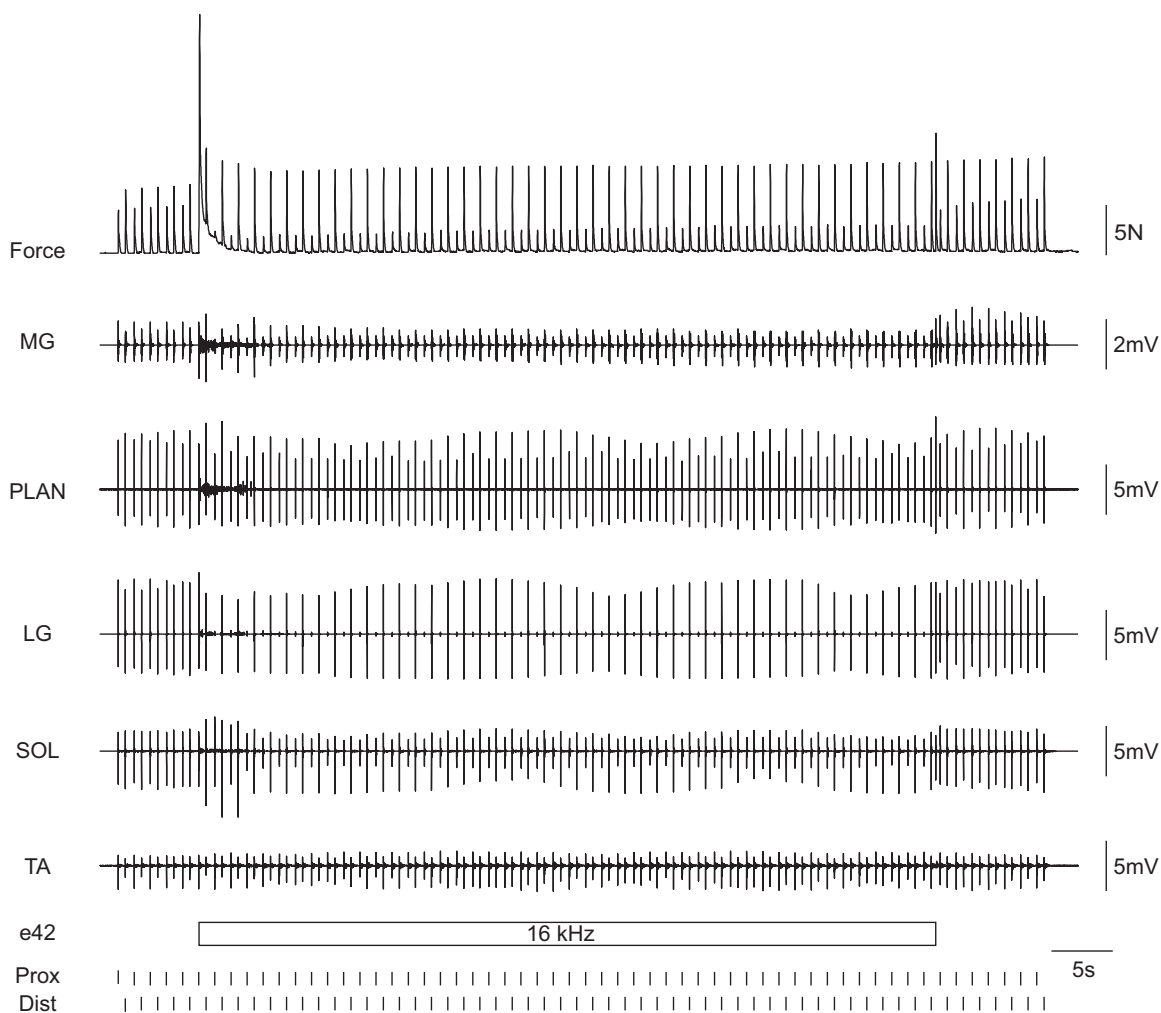


Figure 3.8: Conduction Block

Complete nonselective conduction block using a single USEA electrode for 60 s. Block of activation evoked by the proximal cuff electrode was achieved using 17-V, 16-kHz HFAC, resulting in complete block of LG (block ratio of 0.96) and partial block of the other plantar-flexors, MG, PLAN, and SOL (block ratios of 0.64, 0.35, and 0.50, respectively). The dorsi-flexor TA was unaffected (block ratio of 0.04). Activation of all muscles by stimulation via the distal cuff electrode persisted, and was slightly augmented, throughout HFAC delivery (all block ratios between 0.20 and 0.00). Block of activation by the proximal cuff electrode and the persistence of activation by the distal cuff electrode suggests block of action potential conduction at the location of the USEA. (See Figure 3.2 for abbreviations.)

onset response followed by about 4 s of asynchronous activation in several muscles. After this initial burst of activity, the EMG responses evoked by stimulation of the proximal cuff electrode were greatly reduced in the plantar-flexor muscles MG, PLAN, LG, and SOL (block ratios of 0.64, 0.35, 0.96, and 0.50, respectively) with complete block of LG, but were unaffected in the dorsi-flexor TA (block ratio of -0.04). However, the distal cuff produced EMG responses that were the same size, or slightly larger, than those evoked before HFAC. The force response showed a similar effect with a 50% decrease in response to proximal cuff stimulation during HFAC, and a 32% increase in response to distal cuff stimulation. The force augmentation persisted for at least 8 s after HFAC cessation (end of trial). Two electrodes were tested up to 60 s and a third electrode was tested for 10 minutes. All extended HFAC trials on these electrodes produced block throughout HFAC delivery with immediate force and EMG recovery after HFAC cessation.

Discussion

In this study, we have demonstrated that intrafascicular microelectrodes can be used to selectively block specific muscles and muscle subsets using HFAC, and that the blockade is fast, sustainable, and reversible. Further, it leaves the nonblocked motor units responsive to selective excitation by other intrafascicular electrodes. Consistent with studies that used extraneural electrodes to deliver HFAC, two types of muscle block were observed using intrafascicular electrodes [1, 4]. At HFAC frequencies below 8 kHz, a neuromuscular block occurred that left the muscles unresponsive to nerve stimulation distal to the site of HFAC delivery. At 16 kHz, a localized conduction block was achieved. Muscle responses returned to preblock amplitudes immediately after conduction block, whereas recovery after neuromuscular block was dependent on the duration of block. Despite the different mechanisms of block, and the HFAC parameters required to produce them, both block types abolished proximally-evoked muscle twitches in a subset of the muscles innervated by the sciatic nerve, suggesting that either block mechanism could be useful for abolishing undesired muscle activity.

Although we achieved our primary goal of producing a selective block of a subset of muscles innervated by a single nerve, there remain several challenges that must be addressed before intrafascicular block could become a viable clinical technique. The yield of electrodes that were able to produce selective block of a single muscle was lower than expected. Only 4 of the 55 electrodes tested (7%) were able to completely block a single muscle without blocking or activating the other muscles, and each of these electrodes blocked MG. SOL and TA were each partially blocked selectively in 2 animals. The inability to block the other muscles selectively could be due to the small fraction (11%) of implanted electrodes that were used to deliver HFAC, or it could be due to the intrafascicular location of the electrode tips. For either conduction block or neuromuscular block, HFAC amplitudes just below the block threshold activate axons [2, 14]. For an intrafascicular electrode, this would suggest that it is unlikely that HFAC could block some fibers within a fascicle without activating others. Fascicular boundaries could provide a sufficient barrier to current flow such that HFAC block delivered inside a fascicle might fail to excite fibers in neighboring fascicles. Histological examinations of the feline sciatic nerve by others have shown that fibers innervating MG reside in a single fascicle well before reaching the muscle, whereas other fascicles contain fibers that innervate multiple muscles until they are much closer to their muscle targets [15, 16]. If the selectivity of block using HFAC is indeed limited to within fascicles, then muscle selectivity and clinical utility could be increased by implanting the blocking electrodes as near to the muscles or nerve branches as possible.

Another factor that will impact the clinical use of this technique is the safety of long-term intrafascicular electrode implantation and HFAC charge delivery. Conduction block required 16 kHz sinusoids with peak-to-peak amplitudes between 15 and 20 V; neuromuscular blocks were achieved at an average of 6.3 V at 2 kHz. Although the currents used in each individual experiment were not measured, the currents generated through 15 of the USEA electrodes used in this study were measured in 0.9% sodium chloride solution for frequencies of 2–30 kHz and peak-to-peak voltages of 1–20 V. These 15 electrodes had impedances of 156 ± 154 k Ω (mean \pm SD) when

tested with 1 nA at 1 kHz. For a typical neuromuscular block trial (2 kHz, 5 V), the mean peak-to-peak current amplitude was 163 μA . With an average surface area of 12400 μm^2 , the mean charge per phase and charge density per phase were 13 nC and 105 $\mu\text{C}/\text{cm}^2$, respectively. For a typical conduction block trial (16 kHz, 15 V), the mean current amplitude was 2.6 mA and the mean charge per phase and charge density per phase were 26 nC and 210 $\mu\text{C}/\text{cm}^2$, respectively. These charges per phase and charge densities per phase appear to be within safe limits [17, 18, 19]; however, the electrode geometries and stimulation frequencies used by McCreery et al. [17] to create the empirical relationship for safe charge delivery were substantially different from those used in this study. A recent study has shown that the block threshold can be reduced by optimizing the distance between the two contacts of a cuff electrode delivering HFAC [20]. It is possible that the charge injection required to produce block using intrafascicular electrodes could be reduced by delivering the HFAC between two appropriately spaced electrodes in the nerve. Clearly, a rigorous study of the effects on surrounding tissue of charge injection during HFAC blocks is needed before these techniques could be applied clinically.

One motivation for the study described herein was the development of a new targeted therapy for a variety of neuromuscular pathological conditions. Detrusor-sphincter dyssynergia, resulting from spinal cord injury or other neurodegenerative diseases can leave patients unable to void urine [21]. The pudendal nerve contains efferent fibers innervating the external urethral sphincter and an afferent pathway that can trigger detrusor contraction [22, 23, 24]. Selective block of these efferent fibers combined with activation of the afferent pathway may be able to produce coordinated voiding in these patients. Intrafascicularly delivered HFAC block could also be useful in cases of chronic pain and of spasticity where only certain muscles exhibit excess tone, but these muscles render a joint or limb nonfunctional. Selective intrafascicular block of these hyperactive reflex circuits could enable the nonspastic muscles to restore some level of functionality. Our results suggest that selected muscle blocking via high-frequency alternating current delivered through intrafascicular electrodes could be a valuable addition to the repertoire of neuromuscular electrical stimulation techniques.

Copyright

This chapter has been published as Muscle-Selective Block Using Intrafascicular High-Frequency Alternating Current, Dowden BR, Wark HAC, Normann RA, *Muscle and Nerve*, vol. 42, Copyright © 2010, and is reproduced in accordance with the Wiley-Blackwell copyright transfer agreement.

References

- [1] K L Kilgore and N Bhadra. Nerve conduction block utilising high-frequency alternating current. *Med Biol Eng Comput*, 42(3):394–406, May 2004.
- [2] Niloy Bhadra and Kevin L Kilgore. High-frequency electrical conduction block of mammalian peripheral motor nerve. *Muscle Nerve*, 32(6):782–90, Dec 2005.
- [3] JA Tanner. Reversible blocking of nerve conduction by alternating-current excitation. *Nature*, 195:712–3, Aug 1962.
- [4] Richard P Williamson and Brian J Andrews. Localized electrical nerve blocking. *IEEE Trans Biomed Eng*, 52(3):362–70, Mar 2005.
- [5] MY Woo and B Campbell. Asynchronous firing and block of peripheral nerve conduction by 20 kc alternating current. *Bull Los Angel Neuro Soc*, 29:87–94, Jun 1964.
- [6] Narendra Bhadra, Niloy Bhadra, Kevin Kilgore, and Kenneth J Gustafson. High frequency electrical conduction block of the pudendal nerve. *J. Neural Eng.*, 3(2):180–7, Jun 2006.
- [7] Changfeng Tai, James R Roppolo, and William C de Groat. Block of external urethral sphincter contraction by high frequency electrical stimulation of pudendal nerve. *J Urol*, 172(5 Pt 1):2069–72, Nov 2004.
- [8] Robert A Gaunt and Arthur Prochazka. Transcutaneously coupled, high-frequency electrical stimulation of the pudendal nerve blocks external urethral sphincter contractions. *Neurorehabil Neural Repair*, 23(6):615–26, Jan 2009.
- [9] A Branner, R B Stein, and R A Normann. Selective stimulation of cat sciatic nerve using an array of varying-length microelectrodes. *J Neurophysiol*, 85(4):1585–94, Apr 2001.
- [10] Daniel McDonnall, Gregory A Clark, and Richard A Normann. Selective motor unit recruitment via intrafascicular multielectrode stimulation. *Can J Physiol Pharmacol*, 82(8-9):599–609, Jan 2004.
- [11] Brett R Dowden, Andrew M Wilder, Scott D Hiatt, Richard A Normann, Nicholas A T Brown, and Gregory A Clark. Selective and graded recruitment of cat hamstring muscles with intrafascicular stimulation. *IEEE Trans Neural Syst Rehabil Eng*, 17(6):545–52, Dec 2009.
- [12] K Yoshida and K Horch. Selective stimulation of peripheral nerve fibers using dual intrafascicular electrodes. *IEEE Trans Biomed Eng*, 40(5):492–4, May 1993.
- [13] Andrew M Wilder, Scott D Hiatt, Brett R Dowden, Nicholas A T Brown, Richard A Normann, and Gregory A Clark. Automated stimulus-response mapping of high-electrode-count neural implants. *IEEE Trans Neural Syst Rehabil Eng*, 17(5):504–11, Oct 2009.

- [14] B R Bowman and D R McNeal. Response of single alpha motoneurons to high-frequency pulse trains. firing behavior and conduction block phenomenon. *Appl Neurophysiol*, 49(3):121–38, Jan 1986.
- [15] C Veraart, W M Grill, and J T Mortimer. Selective control of muscle activation with a multipolar nerve cuff electrode. *IEEE Trans Biomed Eng*, 40(7):640–53, Jul 1993.
- [16] W M Grill and J T Mortimer. Quantification of recruitment properties of multiple contact cuff electrodes. *IEEE Trans Rehabil Eng*, 4(2):49–62, Jun 1996.
- [17] D B McCreery, W F Agnew, T G Yuen, and L Bullara. Charge density and charge per phase as cofactors in neural injury induced by electrical stimulation. *IEEE Trans Biomed Eng*, 37(10):996–1001, Oct 1990.
- [18] Daniel R Merrill, Marom Bikson, and John G R Jefferys. Electrical stimulation of excitable tissue: design of efficacious and safe protocols. *J Neurosci Methods*, 141(2):171–98, Feb 2005.
- [19] R V Shannon. A model of safe levels for electrical stimulation. *IEEE Trans Biomed Eng*, 39(4):424–6, Apr 1992.
- [20] D Michael Ackermann, Emily L Foldes, Niloy Bhadra, and Kevin L Kilgore. Effect of bipolar cuff electrode design on block thresholds in high-frequency electrical neural conduction block. *IEEE Trans Neural Syst Rehabil Eng*, 17(5):469–77, Oct 2009.
- [21] D Castro-Diaz and J M Taracena Lafuente. Detrusor-sphincter dyssynergia. *Int J Clin Pract Suppl*, 60(151):17–21, Dec 2006.
- [22] Joseph W Boggs, Brian J Wenzel, Kenneth J Gustafson, and Warren M Grill. Spinal micturition reflex mediated by afferents in the deep perineal nerve. *J Neurophysiol*, 93(5):2688–97, May 2005.
- [23] Margaret M Roberts. Neurophysiology in neurourology. *Muscle Nerve*, 38(1):815–836, Jul 2008.
- [24] Changfeng Tai, Stanley E Smerin, William C de Groat, and James R Roppolo. Pudendal-to-bladder reflex in chronic spinal-cord-injured cats. *Exp Neurol*, 197(1):225–34, Jan 2006.

CHAPTER 4

**NONINVASIVE METHOD FOR SELECTION OF
ELECTRODES AND STIMULUS PARAMETERS
FOR FES APPLICATIONS WITH
INTRAFASCICULAR ARRAYS**

Abstract

High-channel-count intrafascicular electrode arrays provide comprehensive and selective access to the peripheral nervous system. One practical difficulty in using several electrode arrays to evoke coordinated movements in paralyzed limbs is the identification of the appropriate stimulation channels and stimulus parameters to evoke desired movements. Here we present the use of a six degree-of-freedom load cell placed under the foot of a feline to characterize the muscle activation produced by three 100-electrode Utah Slanted Electrode Arrays (USEAs) implanted into the femoral nerves, sciatic nerves, and muscular branches of the sciatic nerves of 3 cats. Intramuscular stimulation was used to identify the endpoint force directions produced by 15 muscles of the hind limb, and these directions were used to classify the forces produced by each intrafascicular USEA electrode as flexion or extension. For 440 USEA electrodes, stimulus intensities for threshold and saturation muscle forces were identified, and the 3-D direction and linearity of the force recruitment curves were determined. Further, motor unit excitation independence for 198 electrode pairs was measured using the refractory technique. This study demonstrates the utility of 3-D endpoint force monitoring as a simple and noninvasive metric for characterizing the muscle-activation properties of hundreds of implanted peripheral nerve electrodes, allowing for electrode and parameter selection for neuroprosthetic applications.

Introduction

Functional electrical stimulation (FES) of the neuromuscular system offers a means to restore mobility to spinal-cord-injured (SCI) patients (for reviews see [1, 2, 3, 4, 5]). Intrafascicularly implanted high-channel-count peripheral nerve interfaces such as the Utah Slanted Electrode Array (USEA) have the potential to improve current FES systems by providing comprehensive and selective access to many small populations of motor axons. Although these nerve interfaces hold promise for both the restoration of fatigue-resistant multijoint movements and the need for fewer implant sites, they also pose new challenges for clinical implementation. A single implanted nerve can innervate multiple muscles, and these muscles may produce a variety of joint moments, but there is no *a priori* knowledge of precisely where each electrode tip will lie after array implantation, or which muscle or muscles it will activate. Therefore, the limb motion evoked by stimulation via each electrode on the array and the range of stimulus parameters that evoke desired motions must be individually determined for each electrode.

The electrodes in an intrafascicularly implanted electrode array that are selected to generate desired fatigue-resistant limb motions ideally should satisfy the following performance criteria: the range of stimulus strengths that evoke graded forces should be known and be monotonic; they should exclusively excite either extension or flexion forces; and the stimuli that are delivered via each electrode should excite an independent group of motor fibers. Thus, the first step in choosing such a subset of electrodes is to determine a range of stimulus intensities for each electrode (between threshold activation and saturation or excitation spillover to an antagonist muscle) that produces graded force production. Next, the primary action evoked by each electrode (i.e., flexion or extension) must be determined. On the basis of these observations, a subset of electrodes can be chosen that evokes the desired muscle actions. This subset of selected electrodes must be further refined by discarding one of any pair of electrodes that excites the same population (or largely overlapping populations) of motor units. Studies using intrafascicular stimulation of the cat sciatic nerve have shown that muscle fatigue can be delayed by interleaving activation

across several groups of fibers innervating independent motor units in the same muscle [6, 7]. Such a stimulation protocol activates individual motor units at a relatively low frequency while producing a high composite frequency that generates a ripple-free tetanus. Muscle fatigue is minimized when the overlap of these groups of fibers is small, so that most motor units are not activated by more than one electrode.

The process of choosing electrodes and stimulus parameters as described above requires the measurement of muscle responses evoked by each of the electrodes in an implanted array, seemingly a large and time-consuming task. Many studies have characterized the responses evoked by peripheral nerve electrodes; however, most have used metrics of muscle activation that are poorly suited for clinical FES systems. The most common are muscle tendon force [8, 9, 10, 11, 12], electromyography (EMG) [13, 14, 15, 16], and joint torque [17, 18, 19, 20]. Tendon force provides a direct metric of muscle output, but requires a tenotomy. EMG is minimally invasive, but requires instrumentation of each muscle separately and does not provide direct information about contraction strength. Joint torque, although noninvasive and simple to instrument, is poorly suited for instrumentation of several joints simultaneously and for characterizing activation of biarticular muscles. This study investigates the use of 3-D limb endpoint force as a single metric to noninvasively characterize the muscular responses evoked by each of hundreds of electrodes intrafascicularly implanted into the three major feline hind limb nerves. The data presented herein demonstrate the utility of measuring evoked endpoint forces as a means for selecting electrodes and stimulus ranges that would be best suited for use in an FES system. This technique will make the use of high-channel-count peripheral nerve interfaces more practicable in clinical FES applications.

Methods

Surgical Preparation

Three adult cats (3.7, 4.2, and 5.0 kg) were used in this study. All experimental procedures were approved by the University Utah Institutional Animal Care and Use Committee. Anesthesia was induced with an intramuscular injection of Telezol (Fort Dodge Animal Health, Fort Dodge, IA) and maintained with isoflurane via mechanical

ventilation. Vital signs (heart rate, blood oxygen saturation, expired CO₂, and rectal temperature) were monitored and recorded to assess the depth of anesthesia and the condition of the animal.

The femoral nerve, sciatic nerve, and the muscular branch of the sciatic nerve were each implanted with a 100-microelectrode Utah Slanted Electrode Array [21]. Together, these three nerves innervate muscles that can flex and extend the hip, knee, and ankle (Table 4.1). The sciatic nerve also innervates several smaller muscles that can cause inversion and eversion of the ankle, as well as dorsi-flexion and plantar-flexion of the digits. The sciatic nerve was implanted at midhigh, approximately 3 cm proximal to the bifurcation into the tibial and peroneal nerves. The muscular branch was implanted approximately 1 cm distal to its bifurcation from the main trunk of the sciatic nerve near the hip joint. The femoral nerve was accessed from an incision in the inguinal crease, and the USEA was implanted in the nerve just distal to its exit from the iliopsoas muscle. In general, the 4-mm-by-4-mm size of the USEA was well matched to nerve dimensions at these three implant locations; however, the femoral nerve is typically narrower than 4 mm, resulting in 10–20 electrode tips located on the edges of the array lying outside the nerve.

Each electrode was tipped with sputtered iridium oxide, and the remainder of the array was insulated with Parylene C. Two 1.5 mm electrodes on each side of the array were wired as reference electrodes for an unrelated study, yielding 96 active electrodes per array. Electrode impedances were measured in 0.9% NaCl solution prior to implantation using a 1-kHz 10-mV sine wave delivered by a custom-built automated impedance measuring system using a Ag-AgCl reference electrode [22].

Table 4.1: Instrumented Muscles

Femoral n.	Muscular Branch of Sciatic n.	Sciatic n.
Rectus femoris (RF)	Biceps femoris anterior (BFa)	Medial gastrocnemius (MG)
Sartorius (SART)	Biceps femoris middle (BFm)	Lateral gastrocnemius (LG)
Vastus lateralis (VL)	Biceps femoris posterior (BFp)	Soleus (SOL)
Vastus intermedius (VI)	Semimembranosus (SM)	Plantaris (PLAN)
Vastus medialis (VM)	Semitendinosus (ST)	Tibialis anterior (TA)

Some electrodes had very high impedances; however, 90% of the electrodes had impedances at or below 250 k Ω , and the mean impedance of these electrodes was 98 ± 61 k Ω (mean \pm SD). The return electrode for all stimulation via USEA electrodes was a platinum wire placed outside the nerve near the location of each implanted USEA. After implantation, a cuff made from silicone tubing was sutured around the nerve at the location of the USEA. This containment system helped to secure the implant as well as protect it from movement of the surrounding muscles.

Each of the 15 muscles in Table 4.1 was surgically exposed and implanted near the nerve entry point with a pair of fine-wire electrodes (0.002 in. stainless steel, California Wire Company, Grover Beach, CA). The wire electrodes were spaced longitudinally along the muscle approximately 7 mm apart, and each electrode had 2 mm of insulation removed from the tip. These wires served as a means of intramuscular (IM) stimulation as well as for recording electromyographic (EMG) potentials resulting from nerve stimulation. The location of each fine-wire electrode pair was verified by visualization of the exposed muscle as well as by stimulation through the wires at the time of implantation.

The animal was placed in a prone position in a rigid trough with its hind limbs suspended from the end of the trough. A small tube extended from the bottom of the trough between the animal's legs to support its hindquarters. To prevent the animal from moving off the back of the trough during stimulation, a plate was placed behind the animal with a slot cut out for the tail. The left foot was secured to the recording surface of a six-axis load cell (Gamma US-15-50, ATI Industrial Automation, Apex, NC) at the metatarsal-phalangeal joint using plastic ties. The load cell can measure forces along, and moments about, three orthogonal axes. The height of the trough and position of the load cell were adjusted such that the angles at the hip, knee, and ankle were approximately 90 degrees, and the leg was aligned vertically in the sagittal plane. The position of the animal and orientation of the load cell axes are shown in Figure 4.1.

The leg was restrained during stimulation to enhance transmission of evoked muscle forces to the load cell under the foot. Two different leg immobilization

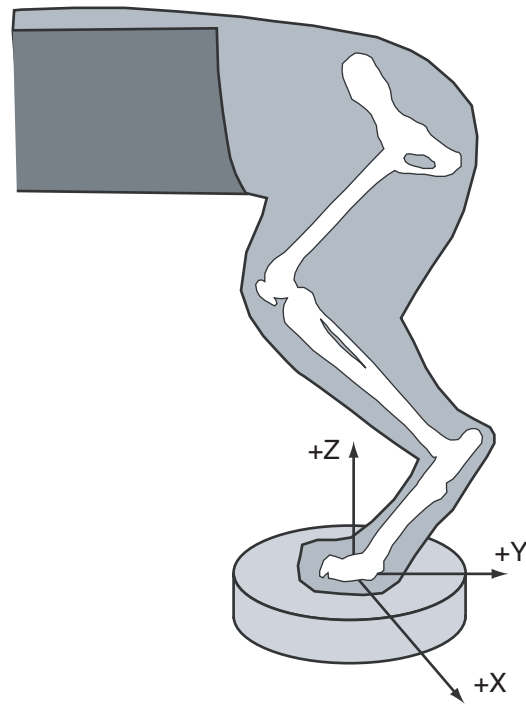


Figure 4.1: Limb Position and Load Cell Axes

The animal was placed in a supporting trough and its left paw was fastened to the recording surface of a 6-axis load cell. The trough and load cell positions were adjusted such that the leg was aligned in the sagittal plane, and the joint angles at the hip, knee, and ankle were approximately 90 degrees. The load cell axis directions are shown with respect to the position of the animal. X is in the medial/lateral direction, Y is in the anterior/posterior direction, and Z is in the dorsal/ventral direction. The load cell was capable of measuring forces and torques along and around each of these axes.

strategies were used depending on which muscles or nerves were being stimulated. For stimulation of the sciatic nerve via USEA electrodes or the muscles it innervates via implanted fine wires, a cupped support was placed on the anterior portion of the femur about 2 cm proximal to the knee. This support prevented forward motion of the leg during the strong plantar-flexion forces generated during activation of some muscles innervated by the sciatic nerve. For stimulation of the femoral nerve, the muscular branch, or the muscles they innervate, the cup in front of the knee was removed, and the ankle was immobilized at 90 degrees using a PVC elbow split into

two pieces and secured around the ankle with plastic ties. This immobilized the ankle joint at 90 degrees but did not otherwise constrain the limb. This immobilization was done to allow the forces generated by muscles acting around the hip and knee to be more directly translated to the load cell without inhibiting forces outside the sagittal plane.

Stimulation and Recording Hardware

All stimuli delivered to electrodes on the USEAs were voltage-controlled monophasic cathodic pulses. The voltage amplitude was held constant throughout each experiment at -2.4 V except for stimulation via one array in 1 animal where, because of an unusually poor yield of responsive electrodes, the stimulus intensity was increased to -4.0 V. Stimulus strength was modulated by varying the pulse width between 0.2 μs and 512 μs with 0.2- μs resolution. The maximum pulse width of the stimulator was set to 512 μs because, for most USEA electrodes, evoked responses increase only modestly beyond this pulse width (unpublished observations). These stimuli were delivered using custom-built hardware and software [23, 24], which is capable of automatically generating recruitment curves for all electrodes on each array. Intramuscular (IM) stimuli were generated using a commercial stimulator (SD9, Grass Technologies, West Warwick, RI) and were also voltage-controlled. All IM stimuli were 500 μs in duration, and stimulus strength was varied by adjusting the voltage amplitude. The SD9 stimulator was set to biphasic mode.

Evoked endpoint forces and EMGs were sampled at 10 kHz using a Cerebus data acquisition system (Blackrock Microsystems, Salt Lake City, UT). EMG data were band-pass filtered at 10–250 Hz using built-in Cerebus filters. Because the same electrodes were used for IM stimulation and EMG recording, no EMG data were recorded during IM stimulation. Force data were forward and backward low-pass filtered at 10 Hz using a 3rd-order Butterworth filter in MATLAB (The Mathworks, Natick, MA), which resulted in a 6th-order filter with no phase distortion. The cutoff frequency of 10 Hz was chosen to reduce the oscillations in endpoint forces of the partially restrained limb that occurred after muscle twitches were evoked. This

oscillation frequency was observed to be near 20 Hz for all 3 animals. The 10-Hz cutoff frequency had little effect on the force peak amplitudes.

Data Analyses

Twitch forces. All analyses of load cell data were performed using the peak force in each of the three force dimensions (F_x , F_y , F_z). Oscillations were sometimes still present after filtering, resulting in both positive and negative peaks. Therefore, the first peak to exceed 75% of the maximum absolute force value was used. Because the limb position for each animal may have been slightly different, an axis rotation was applied to all force peaks in each preparation to allow for grouping of data across animals. The rotation applied was such that the mean 3-D force vector for the soleus muscle was aligned along the negative z-axis. Before rotation, the mean soleus vectors for each animal were, on average, 6.2 degrees apart and 11.7 degrees from the negative z-axis.

The force peaks evoked at various stimuli by each IM fine-wire pair and each USEA electrode were fit with a 3-D line using singular value decomposition (SVD). The right singular vector with the largest singular value was the best-fit line unit vector. The ratio of the largest singular value to the sum of all singular values represented the fraction of the variance in the data captured by the fit line. This ratio is analogous to the r^2 coefficient and was termed the fit quality. A constant direction of the force recruitment vectors over a range of stimulus intensities suggests that current delivered to the nerve was not spreading to fibers innervating antagonist muscles.

Determining the usable stimulus range for each electrode. Before an electrode can be considered for use in an FES system, a range of stimulus intensities that evoke a graded muscle response must be determined. This range is bounded by the threshold pulse width at the lower end and the saturation or spillover pulse width at the upper end. To find these quantities, the custom stimulation hardware and software generated force recruitment curves for each electrode that evoked at least 0.1 N of force in response to a 256- μ s stimulus. This pulse width was half of the maximum stimulator pulse width, and the 0.1-N force threshold was chosen to ensure that electrodes were able to evoke at least a moderate amount of force before

collecting an entire recruitment curve. The 3-D peak force evoked from each stimulus was converted to force magnitude to create a 1-D relationship between stimulus pulse width and twitch force magnitude. This curve was then smoothed with a 5-element 3rd-order Savitzky-Golay filter [25] using MATLAB. This smoothing maintained the shape of the curve while removing small fluctuations; this made algorithmic detection of threshold and plateau more consistent. Threshold was found by identifying the largest pulse width that recruited less than 0.1 N of force; the next largest pulse width was deemed the threshold. The pulse width at which the recruitment slope dropped below $0.001 \text{ N}/\mu\text{s}$ was termed the plateau pulse width. A plateau in force magnitude occurs when excitation of a muscle or synergist group is saturated, and also occurs when an antagonist muscle begins to be recruited. Thus, a decrease in slope below $0.001 \text{ N}/\mu\text{s}$ was used to identify either saturation or antagonist activation. For each electrode, the pulse width range between threshold and plateau was termed the usable range.

EMG. The peak-to-peak EMG signal recorded for each stimulus was used in all analyses. The recorded EMG for each muscle in each animal was normalized using either the maximum EMG observed during the collection of all force recruitment curves, or the maximum EMG observed in response to a $512\text{-}\mu\text{s}$ pulse delivered simultaneously to each electrode on an array, whichever was largest [13]. This normalized EMG is referred to as nEMG. The primary muscle activated by each electrode was identified using the maximum nEMG at the plateau or saturation pulse width, as determined using the force magnitude curve described above.

Identifying the primary action evoked by USEA electrodes. The first step to identify a subset of electrodes for a specific motion is to classify each USEA electrode as able to activate either extensor or flexor muscles. To identify the forces produced by extension or flexion around each joint, each muscle was stimulated individually using the implanted fine-wire electrodes. Because each muscle can be classified as a flexor or extensor on the bases of its origin and insertion, these IM-evoked forces provided a means to identify flexion and extension endpoint force directions for the limb position and limb restraint used in this study.

For each muscle, IM stimulus intensities were varied to evoke forces between threshold and saturation or excitation of another muscle. The force peak in each dimension was identified, and these 3-D points were fit with a 3-D line using SVD as described above and normalized to unit length. We would expect the unit vectors for flexor muscles to be clearly distinguishable from the unit vectors for extensor muscles. To verify this, a multivariate analysis of variance (MANOVA) was performed in MATLAB on the collection of unit vectors from all 3 animals. The MANOVA performs a type of principal component analysis (PCA) on the collection of IM unit vectors. If the groups of flexor and extensor unit vectors are not statistically different, there will be no significant dimensions returned by the MANOVA; however, if there are 1–3 significant dimensions, then the flexor and extensor groups are statistically different.

The distributions of the flexor and extensor unit vectors in PCA space were then used to classify unit vectors evoked by each individual USEA electrode. Each USEA unit vector was transformed into the same PCA space used in the MANOVA of the IM unit vectors. If an electrode's principal component value fell within 95% probability range of the flexor or extensor distributions, it was classified as a flexor or extensor, respectively. If it fell outside of both distributions, it was classified as neither. If more electrodes fell into the flexor or extensor distributions than would be expected from a random uniform distribution of unit vectors, we determined that endpoint force measured from the partially restrained limb was sufficient to classify electrodes as evoking flexion or extension.

Excitation Overlap

The fatigue-reducing effects of interleaved stimulation are maximized when each interleaved electrode excites an independent population of motoneurons; otherwise, shared motoneurons are activated at higher frequencies. In 1 animal, 12 electrodes were chosen from each implant and the amount of excitation overlap was measured for each within-implant electrode pair combination using the refractory technique [9, 12, 18, 21, 26, 27, 28]. This resulted in a total of 198 pair-wise overlap measurements.

The refractory technique estimates excitation overlap by stimulating via one electrode, then stimulating via a second electrode during the refractory period of the response evoked by the first stimulus. If the force generated in this manner is equal to the sum of the forces generated by stimulation via each electrode alone, there is assumed to be no excitation overlap. This method relies on the superposition of muscle forces, and may not be valid if the limb is not rigidly immobilized and thus the muscles are allowed to change lengths [29].

To minimize limb motion during the refractory test, 40-Hz 500-ms pulse trains were used instead of single stimuli. Pulse trains of this duration were sufficiently long to allow most of the movement in the limb due to stimulation to reach a steady state after the onset of stimulation, but short enough to minimize fatigue resulting from repeated stimulation. The 40-Hz stimulation frequency was high enough to produce a nearly ripple-free tetanus but low enough to avoid fatigue produced by higher stimulus frequencies. The mean force between 100 and 500 ms after stimulus onset in each dimension was used in all overlap calculations.

For each pair-wise comparison, stimuli were delivered via each electrode alone for 500 ms at 40 Hz. A refractory test was made in which stimuli were delivered via both electrodes for 500 ms at 40 Hz, with stimuli on one electrode delayed by 750 μ s. A second refractory test was then made with the order of stimulation on the electrodes reversed. Because overlap tests were performed for each electrode against the other 11 electrodes chosen from that implant, each electrode was stimulated alone 11 times.

In an intact limb, stimulation via two electrodes may excite forces in different directions. Hence, the following approach was developed to calculate overlap in 3 dimensions. There are three possible groups of motor fibers activated by an electrode pair: those excited by stimuli delivered via electrode 1 only, a, those excited by stimuli via electrode 2 only, b, and those shared by stimulation via both electrodes, s. Let the 3-D force vectors produced by activation of each group of fibers be $\bar{\mathbf{F}}_a$, $\bar{\mathbf{F}}_b$, and $\bar{\mathbf{F}}_s$, respectively. Then, the forces produced by electrodes 1 and 2 are

$$\bar{\mathbf{F}}_1 = \bar{\mathbf{F}}_a + \bar{\mathbf{F}}_s \quad (4.1)$$

and

$$\bar{\mathbf{F}}_2 = \bar{\mathbf{F}}_b + \bar{\mathbf{F}}_s \quad (4.2)$$

During the refractory stimulation test, the shared population is activated only once and thus force, $\bar{\mathbf{F}}_R$, is given by

$$\bar{\mathbf{F}}_R = \bar{\mathbf{F}}_a + \bar{\mathbf{F}}_b + \bar{\mathbf{F}}_s \quad (4.3)$$

The percentage of force generated by the shared group of fibers compared with the total force of all groups is given by

$$\% \textit{ overlap} = 100 \times \frac{\|\bar{\mathbf{F}}_s\|}{\|\bar{\mathbf{F}}_a\| + \|\bar{\mathbf{F}}_b\| + \|\bar{\mathbf{F}}_s\|} \quad (4.4)$$

Because each electrode was stimulated alone 11 times, once for each pair-wise comparison, and each pair-wise refractory test was performed twice, a system of 24 vector equations was constructed to solve for $\bar{\mathbf{F}}_a$, $\bar{\mathbf{F}}_b$, and $\bar{\mathbf{F}}_s$. Creating separate equations for the x, y, and z components of each measurement yielded a total of 72 equations for each electrode pair. The linear least squares solution to this system of equations was solved in MATLAB, which solved for F_{ax} , F_{ay} , F_{az} , F_{bx} , F_{by} , F_{bz} , F_{sx} , F_{sy} , and F_{sz} . These values were then used to calculate the percentage of overlap using equation (4.4). An r^2 coefficient and p-value were calculated for each solution.

Results

This study successfully developed and validated a noninvasive approach to characterize aspects of evoked endpoint forces to allow for electrode and stimulus parameter selection for lower-limb FES applications. Stimulation via 440 of the 864 implanted electrodes (51%) resulted in muscle activation and corresponding endpoint forces. The following sections describe the specific characterization that was performed for

each of these electrodes, including 1) identification of a range of stimulus intensities between threshold and saturation/spillover; 2) the degree to which increasing stimulus intensities evoked forces in a constant direction; and 3) classification of each electrode as evoking limb flexion or extension. Further, the excitation overlap for 198 selected electrode pairs was determined. These data demonstrate the utility and simplicity of the use of endpoint force as a means to noninvasively characterize muscle responses evoked by intrafascicular microelectrodes that will allow for electrode and stimulus parameter selection for FES applications.

Determining the Stimulus Range for Each Electrode

For each USEA electrode, a range of stimulus intensities was identified that evoked a graded force response. Increasing stimulus pulse widths were correlated with increasing force magnitude, and across all 3 animals, more electrodes showed a significant correlation ($p < 0.05$) than would be expected from chance alone (t-test, $t_2 = 5.46$, $p < 0.05$). For the 440 electrodes tested, the threshold pulse width was $26.4 \pm 37.1 \mu\text{s}$ and the plateau pulse width was $120.5 \pm 114.8 \mu\text{s}$ (mean \pm SD). At plateau, $1.60 \pm 1.55 \text{ N}$ of twitch force magnitude was generated.

Figure 4.2 demonstrates this characterization for a single USEA electrode implanted in the muscular branch of the sciatic nerve (Figure 4.2a–c), and for an electrode implanted in the femoral nerve (Figure 4.2d–f). The usable pulse width range for each electrode was identified using endpoint force magnitude (Figure 4.2a, d), and the direction and straightness of force recruitment were identified using the 3-D force peaks (Figure 4.2b, e). For the electrode in the muscular branch, the consistent recruitment of extension force (Figure 4.2b, fit quality = 0.96) corresponded well to the selective recruitment of semimembranosus as shown by the EMG recorded from the muscles innervated by the muscular branch (Figure 4.2c).

The electrode implanted in the femoral nerve demonstrated a common outcome where an electrode started to recruit antagonist muscles at high stimulus intensities. Despite the eventual spillover to extensor muscles (Figure 4.2f), the usable stimulus range determined from the force magnitude (Figure 4.2d) identified a range of stimuli that evoked flexion forces in a constant direction (squares in Figure 4.2e, fit quality =

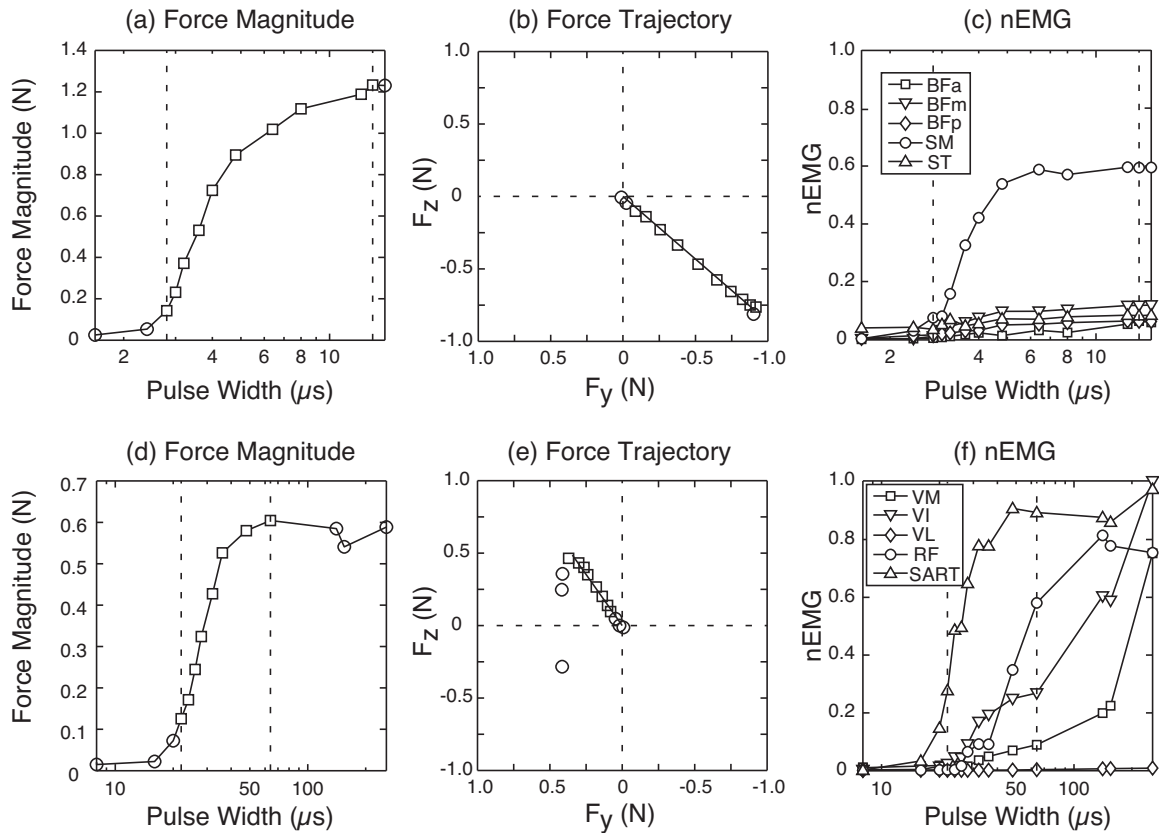


Figure 4.2: Characterization of Two USEA Electrodes

Characterization of muscle responses evoked by a USEA electrode in the muscular branch (a-c) and a USEA electrode in the femoral nerve (d-f). (a & d) Force magnitude, (b & e) sagittal plane view of the 3-D force peaks, and (c & f) EMG evoked by each electrode are shown. Threshold and plateau pulse widths were determined from the force magnitude vs. pulse width curve, and are shown with vertical dashed lines. Stimulus intensities between threshold and plateau were deemed the usable range and are shown as squares in (a), (b), (d), and (e). Responses outside of the usable range are shown as circles. (c) Stimuli delivered to the muscular branch electrode activated primarily SM, a hip extensor. This selective stimulation produced forces in a constant direction with increasing stimulus strength ((b), squares, fit quality = 0.96). (f) Stimuli delivered to the femoral nerve electrode activated the hip flexor SART at low stimulus intensities, but activation spread to extensor muscles at higher stimulus intensities. The plateau in force magnitude (d) enabled the detection of the recruitment of antagonist muscles, and thus the ability to identify a useful stimulus range that produced flexion forces in a constant direction ((e) squares, fit quality = 0.94).

0.94). For all electrodes tested, the fit quality of the usable range of forces was 0.94 ± 0.05 (mean \pm SD, 440 electrodes), indicating that this technique could reliably identify a stimulus range that evoked graded forces in a constant direction.

Classifying Flexor or Extensor Activation

After a usable stimulus range was identified for each electrode that evoked graded forces in a constant direction, each electrode was classified as evoking limb flexion, limb extension, or neither. This classification was made by comparing the forces evoked by each electrode with the forces evoked by intramuscular stimulation of each muscle. As expected, intramuscular stimulation vectors showed that the flexors acting around each joint typically generated upward (positive F_z) forces, and the extensor muscles generated downward (negative F_z) forces (Figure 4.3a–c). The biarticular rectus femoris is the one muscle that had a less clear distinction between upward and downward force (Figure 4.3b). In this limb position, the hip flexion and knee extension torques appeared to be somewhat balanced, resulting in a net force in the anterior direction. Because some intramuscular electrodes became dislodged in one preparation, data from only two preparations were used for SM, RF, and VM, resulting in a total of 42 IM stimulation vectors. Across preparations, the forces evoked by a given muscle varied by 19 ± 16 degrees (mean \pm SD, 36 pair-wise differences). The unit vectors produced by flexor muscles were statistically different from the unit vectors produced by extensor muscles, and this difference could be expressed with a single dimension (Multivariate Analysis of Variance, $p < 0.001$). As expected, this confirmed that twitch endpoint forces evoked in the partially restrained limb could be used to reliably differentiate activation of flexor muscles from activation of extensor muscles.

Stimulation via individual USEA electrodes produced forces in similar directions to those evoked by intramuscular stimulation (Figure 4.3d–f). After mapping the USEA unit vectors to the principal vector found by the MANOVA to differentiate between IM-evoked flexion and extension forces, 141 USEA electrodes were classified as evoking flexion forces, 271 electrodes were classified as evoking extension forces,

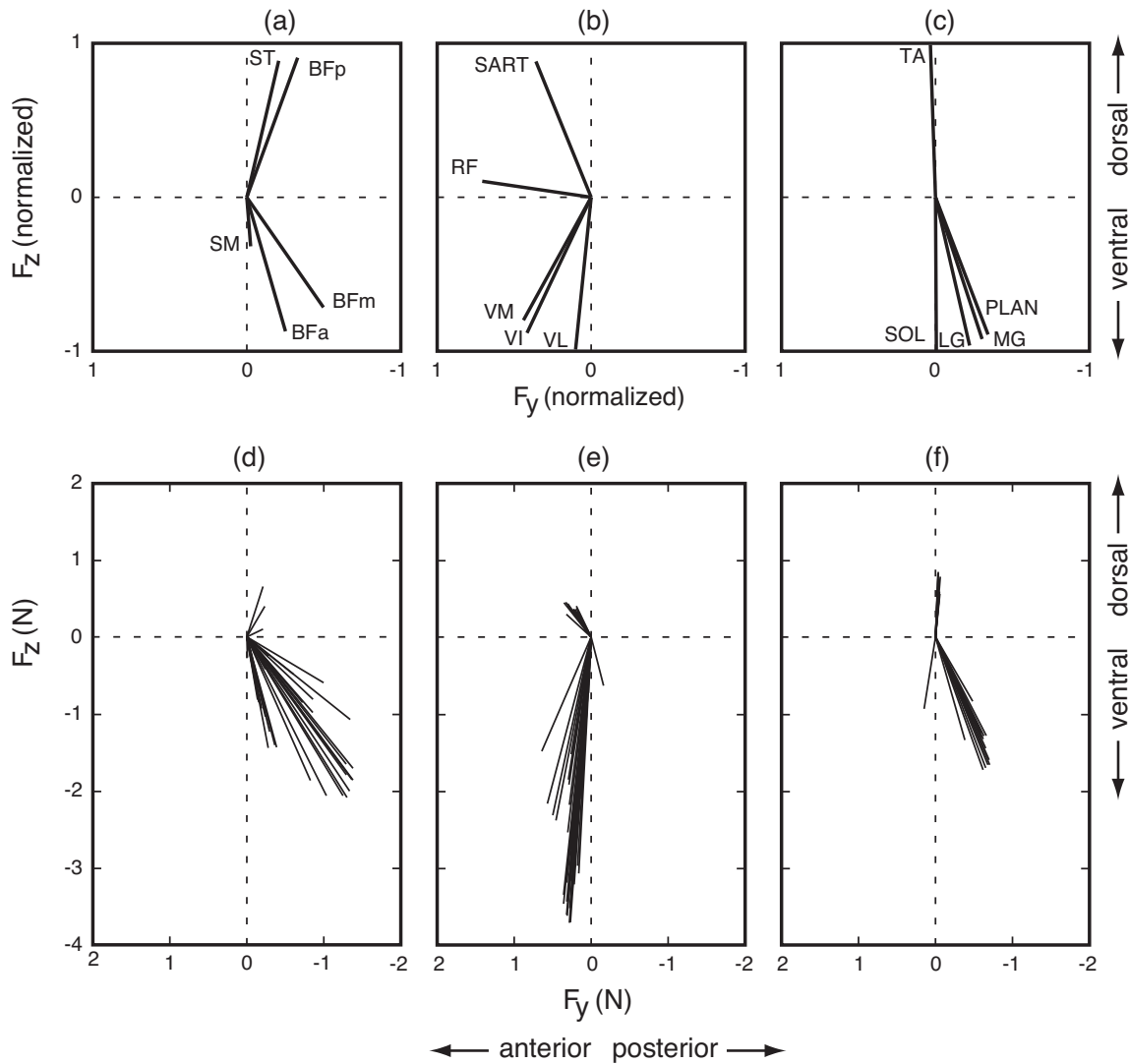


Figure 4.3: Force Vectors Evoked by Intramuscular and USEA Stimulation

Intramuscular stimulation (a-c) and intrafascicular stimulation (d-f) evoked forces in similar directions. Sagittal-plane view of forces evoked by intramuscular stimulation showed a clear distinction between flexors and extensors for muscles innervated by (a) the muscular branch of the sciatic nerve, (b) the femoral nerve, and (c) the sciatic nerve. The best-fit line of the 3-D forces from IM recruitment curves were normalized to unit length and averaged across animals. The sagittal-plane projections of the 3-D unit vectors are shown. Data from only 2 animals were used for RF, SM, and VM. Individual electrodes of USEAs implanted in the (d) muscular branch of the sciatic nerve, (e) the femoral nerve, and (f) the sciatic nerve of 1 animal evoked forces in directions similar to those evoked by IM stimulation of the individual muscles. Each line represents the sagittal plane projection of the best-fit line of the 3-D forces evoked by an individual USEA electrode. The USEA vectors shown are not normalized to unit length.

and 28 electrodes fell outside of both IM distributions (Figure 4.4). The number of USEA electrodes falling within either IM distribution was greater than would be expected from a random uniform distribution, thus indicating that the flexion and extension forces evoked by USEA electrodes can be classified using evoked endpoint forces (t-test, $t_2 = 5.05$, $p < 0.05$). On average, each USEA implant had 16 ± 11 electrodes that activated flexion forces and 30 ± 15 electrodes that activated extension forces (mean \pm SD, 9 USEAs). EMG data recorded during recruitment curves showed a similar distribution of electrodes that activated flexor and extensor muscles. Flexor muscles were activated by 14.1 ± 6.6 electrodes per array, and extensor muscles were activated by 34.8 ± 8.0 electrodes. Across all 9 USEA implants, 10.5 ± 7.5 electrodes activated each muscle, as assessed by the EMG responses recorded at force plateau or saturation (Table 4.2). The good agreement between force and EMG data supports endpoint force as a viable means to characterize muscle activation of an entire limb produced by stimulation via electrodes implanted in three different nerves.

Excitation Overlap of Electrode Pairs

In 1 animal, 12 electrodes from each implant that evoked robust forces were selected for overlap testing, which resulted in 66 electrode pairs per implant for a total of 198 pairs. For the 198 total electrode pairs tested, the overlap ranged from 1% to 96% with a median of 12%. Disregarding forces from the first 100 ms of stimulation eliminated most of the fluctuations in force due to limb motion, and allowed for identification of low- and high-overlap electrode pairs (Figure 4.5). For 193 of the 198 pairs, the forces evoked by single electrode stimulation and the paired refractory tests were well fit ($p < 0.05$) by the vector model of excitation overlap as expressed by equations (4.1)–(4.3) ($r^2 = 0.81 \pm 0.18$).

Discussion

This study presents a simple noninvasive technique for identifying several key properties of the muscle excitation evoked by several hundred intrafascicularly implanted electrodes. This technique would allow for electrode and stimulus parameter selection for use in a lower limb motor neuroprosthesis. In each preparation, three

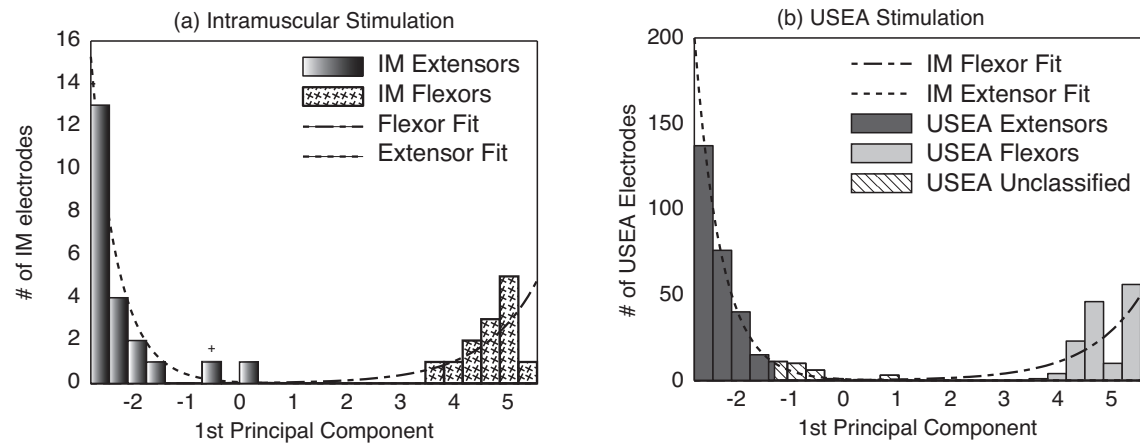


Figure 4.4: Classification of USEA Electrodes Using IM-Evoked Forces

USEA electrodes were classified as evoking flexion or extension using the MANOVA analysis performed on the IM-evoked forces. (a) The forces evoked by IM stimulation of flexor (patterned bars) and extensor (shaded bars) muscles were mapped to the first principal vector and fit with exponential distributions (dashed lines). The + symbol denotes that one flexor muscle and one extensor muscle fell into this bin. (b) The forces evoked by 440 individual USEA electrodes were mapped onto the same principal vector. The IM-evoked exponential distributions from (a) are duplicated in (b) and were used to classify each USEA electrode as evoking flexion (light bars), extension (dark bars), or neither (crosshatched bars), on the basis of whether they fell within the 95% probability region of either IM-evoked distribution.

Table 4.2: Number of Electrodes Activating each Muscle

Muscle	Action	Mean # Electrodes
MG	APF/KF	8.7
LG	APF/KF	12.7
PLAN	APF/KF	7.3
SOL	APF	1.3
TA	ADF	6.7
VM	KE	16.0 ^a
VI	KE	13.7
VL	KE	10.0
RF	KE/HF	14.5 ^a
SART	HF/KE	19.0
BFa	HE	9.3
BFm	HE/KF	9.0
BFp	KF/HE	10.7
SM	HE/KF	18.0 ^a
ST	KF/HE	6.0

^aData are from 2 animals.

Other data are from 3 animals

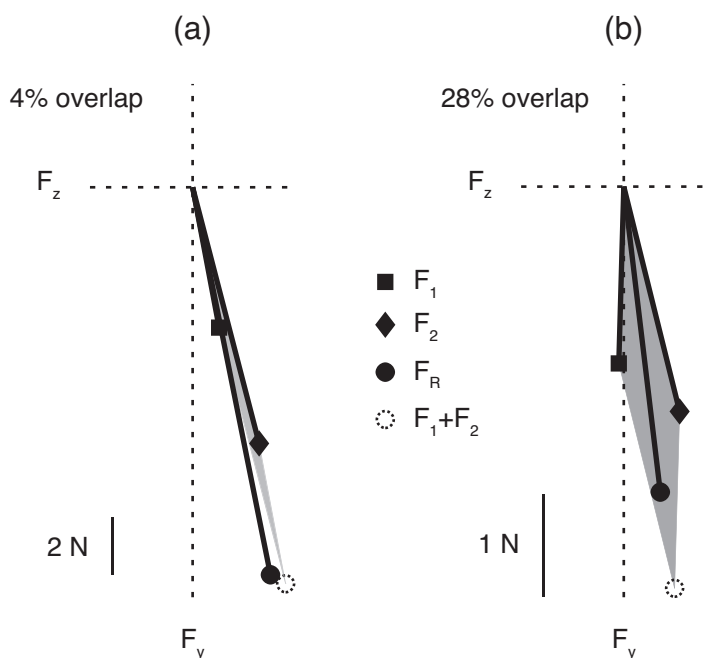


Figure 4.5: Excitation Overlap Using Force Vectors

Examples of low and moderate excitation overlap as assessed using refractory tests of electrode pairs. F_1 and F_2 are the mean forces produced by stimulation via each single electrode at 40 Hz for 500 ms, excluding the first 100 ms. The difference between the algebraic sum of the two single-electrode evoked force vectors, F_1+F_2 , and the actual force produced during the refractory test, F_R , is used to calculate the percentage of overlap (equation (4.4) in Materials and Methods). Overlap calculations were performed on 3-D vectors; only the sagittal plane forces are shown here for clarity. (a) Low overlap example. Two electrodes implanted in the sciatic nerve excite nearly unique sets of motor units that both generated plantar-flexion forces (overlap = 4%). (b) Moderate overlap example. Two electrodes in the muscular branch excited a pool of motor units that generated hip-extension forces. The force produced during the refractory test was somewhat smaller than the algebraic sum of the forces produced by the two electrodes alone (overlap = 28%).

Utah Slanted Electrode Arrays were implanted into feline hind limb nerves and were capable of evoking torques around the hip, knee, and ankle. The muscle-activation properties of each of the 288 implanted electrodes (96 wired electrodes per array) were characterized using a single 3-D force sensor placed under the paw. Characterization using evoked endpoint force was noninvasive, required only minimal mechanical setup, and was performed using automated data collection and analysis routines. This technique allows for selection of groups of electrodes that could be used to evoke fatigue-resistant limb movements.

Although the primary objective of this study was to present a noninvasive means to characterize the muscle responses evoked by individual electrodes in multiple USEA implants, the data presented here also represent the most comprehensive description to date of the repertoire of muscle activations possible using intrafascicular electrode arrays implanted in feline hind limb nerves. Previous studies used muscle tendon force or EMG to document the use of USEAs to activate individual muscles innervated by the sciatic nerve [9, 21] and the muscular branch of the sciatic nerve [13]. Unlike tendon force or EMG, the endpoint forces presented in this study predict the limb motions that will be possible using intrafascicular stimulation via different electrodes. Lemay and colleagues [30] demonstrated that isometric endpoint force direction predicts limb movement direction during intraspinal microstimulation. Muscle activation evoked by intraspinal stimulation can be modulated by limb position and thus can affect endpoint force direction, but this effect is primarily contained to the limits of the limb range of motion [31]. Although during intraspinal stimulation the exact direction of endpoint force is dependent on limb position, the general pattern of flexion or extension is conserved, and resembles the force patterns evoked from direct muscle or nerve stimulation [30, 32, 33].

For an FES system to produce the cyclic swing and stance phases required for gait, both flexion and extension torques must be generated about the hip, knee, and ankle. USEA implantations in the femoral nerve, sciatic nerve, and muscular branch of the sciatic nerve were able to evoke both flexion and extension forces at each joint, with one exception. In 1 animal, dorsi-flexion forces at the ankle were

not generated by the USEA in the sciatic nerve. Because intramuscular stimulation of tibialis anterior produced robust dorsi-flexion forces in this animal, the lack of USEA-evoked dorsi-flexion forces was most likely the result of incomplete coverage of the nerve by the USEA due to incomplete or noncentered USEA implantation. Previous studies of muscle recruitment by the USEA implanted in the cat sciatic nerve showed reliable dorsi-flexor activation [21, 24, 34]; thus, the lack of evoked dorsi-flexion forces suggests that no electrodes penetrated into the peroneal fascicle during implantation in this animal, but this is an unusual outcome.

On average, 16 electrodes per implant evoked flexion forces and 30 electrodes evoked extension forces. Appreciable increase in time-to-fatigue over a single stimulation channel has been shown by interleaving stimulation across just two electrodes [6, 9], with even greater endurance improvements when interleaving stimulation across four electrodes [7]. Recent work using interleaved stimulation of three groups of 6 or more electrodes to evoke sit-to-stand transitions in anesthetized felines produced movements that were slower to fatigue than those evoked by simultaneous stimulation of the same electrodes [35]. The electrodes and stimulus parameters used in the aforementioned study were identified using endpoint forces as described herein. The numbers of electrodes found in the present study to evoke flexion and extension forces around each joint should not only be sufficient to implement an interleaved stimulation strategy to produce fatigue-resistant stance, but to produce fatigue-resistant flexion and extension cycles for gait.

In this study, we extended the refractory technique to three dimensions to quantify the excitation overlap for 198 pairs of electrodes using 3-D endpoint force. The refractory technique relies on linear addition of muscle forces produced by independent populations of motor fibers to estimate excitation overlap. Although the refractory technique has been widely used to measure excitation overlap between pairs of neural electrodes, most previous studies have used twitch responses evoked from single stimuli [9, 12, 18, 21, 28, 36]. Because a goal of this study was to perform the force characterization using minimal and noninvasive restraint of the limb, motion during electrical stimulation was not completely eliminated and thus the muscle contractions

were not fully isometric. This limb motion made the use of twitch responses unsuitable for the quantification of excitation overlap. One study has shown that rapid deviations in muscle length can cause nonlinearities in muscle force summation as large as 7% of maximum tetanic force [29]. Further, elastic elements in muscles and tendons can cause nonlinear summation even in isometric twitch contractions, but these nonlinearities are largely abolished during tetani [26, 29], which suggests that twitches may not be suitable for overlap quantification even in the isometric case. These nonlinearities tend to reduce the force produced when two groups of muscle fibers are activated together compared with the sum of their individual forces, thus overestimating excitation overlap. In the present study, 500-ms tetani were used for refractory tests to allow limb motion and internal muscle shortening to reach a steady state. Force waveforms recorded during these tetani often showed large fluctuations at the onset and offset of stimulation, but a period of relative stability during stimulation. Although the use of tetani may mitigate the nonlinearities associated with muscle movement or internal shortening, the relationship between excitation overlap, as measured using tetani, to the rate of muscle fatigue has not been studied and thus warrants further investigation.

The stimulation capabilities of intrafascicular electrodes have been well documented in acute animal preparations. However, to extend these results to clinical neuroprosthetic systems, many practical challenges must be met. Arguably, the most important of these challenges is ensuring and documenting the long-term stability and efficacy of intrafascicular stimulation for controlling muscle function. The long-term effect of intrafascicular electrode implantation on peripheral nerve tissue is an area of active research [34, 37, 38, 39], and these studies show a persistent but tolerable level of tissue damage. Recent studies have also demonstrated improved long-term functionality of USEAs [35, 40]. Eventually, the efficacy of multi-implant systems using intrafascicular electrodes that are capable of evoking stance and gait will need to be evaluated over months and years, requiring repeated characterization of implant function. The simple and noninvasive instrumentation required to measure endpoint

forces make it an attractive option for documenting the stimulation capabilities of hundreds of electrodes that can activate muscles throughout an entire limb.

Conclusion

Endpoint forces produced during stimulation via intrafascicular electrodes were used to quantify key stimulation properties of each electrode as well as to determine the excitation overlap between electrode pairs. The direction of evoked muscle force and the relationship between stimulus strength and muscle output allow for electrode selection for use in a stance or gait neuroprosthesis.

References

- [1] Vivian K Mushahwar, Patrick L Jacobs, Richard A Normann, Ronald J Triolo, and Naomi Kleitman. New functional electrical stimulation approaches to standing and walking. *J. Neural Eng.*, 4(3):S181–97, Sep 2007.
- [2] P Hunter Peckham and Jayme S Knutson. Functional electrical stimulation for neuromuscular applications. *Annu Rev Biomed Eng*, 7:327–60, Jan 2005.
- [3] Xavier Navarro, Thilo B Krueger, Natalia Lago, Silvestro Micera, Thomas Stieglitz, and Paolo Dario. A critical review of interfaces with the peripheral nervous system for the control of neuroprostheses and hybrid bionic systems. *J Peripher Nerv Syst*, 10(3):229–58, Sep 2005.
- [4] E J Nightingale, J Raymond, J W Middleton, J Crosbie, and G M Davis. Benefits of fes gait in a spinal cord injured population. *Spinal Cord*, 45(10):646–57, Oct 2007.
- [5] T A Thrasher and M R Popovic. Functional electrical stimulation of walking: function, exercise and rehabilitation. *Ann Readapt Med Phys*, 51(6):452–60, Jul 2008.
- [6] K Yoshida and K Horch. Reduced fatigue in electrically stimulated muscle using dual channel intrafascicular electrodes with interleaved stimulation. *Ann Biomed Eng*, 21(6):709–14, Jan 1993.
- [7] Daniel McDonnall, Gregory A Clark, and Richard A Normann. Interleaved, multisite electrical stimulation of cat sciatic nerve produces fatigue-resistant, ripple-free motor responses. *IEEE Trans Neural Syst Rehabil Eng*, 12(2):208–15, Jun 2004.
- [8] C Veraart, W M Grill, and J T Mortimer. Selective control of muscle activation with a multipolar nerve cuff electrode. *IEEE Trans Biomed Eng*, 40(7):640–53, Jul 1993.
- [9] Daniel McDonnall, Gregory A Clark, and Richard A Normann. Selective motor unit recruitment via intrafascicular multielectrode stimulation. *Can J Physiol Pharmacol*, 82(8-9):599–609, Jan 2004.
- [10] Z P Fang and J T Mortimer. A method to effect physiological recruitment order in electrically activated muscle. *IEEE Trans Biomed Eng*, 38(2):175–9, Feb 1991.
- [11] N Nannini and K Horch. Muscle recruitment with intrafascicular electrodes. *IEEE Trans Biomed Eng*, 38(8):769–76, Aug 1991.
- [12] K Yoshida and K Horch. Selective stimulation of peripheral nerve fibers using dual intrafascicular electrodes. *IEEE Trans Biomed Eng*, 40(5):492–4, May 1993.

- [13] Brett R Dowden, Andrew M Wilder, Scott D Hiatt, Richard A Normann, Nicholas A T Brown, and Gregory A Clark. Selective and graded recruitment of cat hamstring muscles with intrafascicular stimulation. *IEEE Trans Neural Syst Rehabil Eng*, 17(6):545–52, Dec 2009.
- [14] D R McNeal and B R Bowman. Selective activation of muscles using peripheral nerve electrodes. *Med Biol Eng Comput*, 23(3):249–53, May 1985.
- [15] Katharine H Polasek, Harry A Hoyen, Michael W Keith, and Dustin J Tyler. Human nerve stimulation thresholds and selectivity using a multi-contact nerve cuff electrode. *IEEE Trans Neural Syst Rehabil Eng*, 15(1):76–82, Mar 2007.
- [16] M A Schiefer, K H Polasek, R J Triolo, G C J Pinault, and D J Tyler. Selective stimulation of the human femoral nerve with a flat interface nerve electrode. *J. Neural Eng.*, 7(2):26006, Apr 2010.
- [17] Matthew D Tarler and J Thomas Mortimer. Selective and independent activation of four motor fascicles using a four contact nerve-cuff electrode. *IEEE Trans Neural Syst Rehabil Eng*, 12(2):251–7, Jun 2004.
- [18] Matthew D Tarler and J Thomas Mortimer. Linear summation of torque produced by selective activation of two motor fascicles. *IEEE Trans Neural Syst Rehabil Eng*, 15(1):104–10, Mar 2007.
- [19] W M Grill and J T Mortimer. Non-invasive measurement of the input-output properties of peripheral nerve stimulating electrodes. *J Neurosci Methods*, 65(1):43–50, Mar 1996.
- [20] W M Grill and J T Mortimer. Stability of the input-output properties of chronically implanted multiple contact nerve cuff stimulating electrodes. *IEEE Trans Rehabil Eng*, 6(4):364–73, Dec 1998.
- [21] A Branner, R B Stein, and R A Normann. Selective stimulation of cat sciatic nerve using an array of varying-length microelectrodes. *J Neurophysiol*, 85(4):1585–94, Apr 2001.
- [22] Kabilar Gunalan, David J Warren, Justin D Perry, Richard A Normann, and Gregory A Clark. An automated system for measuring tip impedance and among-electrode shunting in high-electrode count microelectrode arrays. *J Neurosci Methods*, 178(2):263–9, Apr 2009.
- [23] Scott D Hiatt, Andrew M Wilder, K Shane Guillory, Brett R Dowden, Richard A Normann, and Gregory A Clark. 1100-channel neural stimulator for functional electrical stimulation using high-electrode-count neural interfaces. *IFESS Abstract*, pages 1–3, Jul 2010.
- [24] Andrew M Wilder, Scott D Hiatt, Brett R Dowden, Nicholas A T Brown, Richard A Normann, and Gregory A Clark. Automated stimulus-response mapping of high-electrode-count neural implants. *IEEE Trans Neural Syst Rehabil Eng*, 17(5):504–11, Oct 2009.

- [25] A Savitzky and MJE Golay. Smoothing and differentiation of data by simplified least squares procedures. *Analytical Chemistry*, 36(8):1627–1639, 1964.
- [26] M C BROWN and P B MATTHEWS. An investigation into the possible existence of polyn neuronal innervation of individual skeletal muscle fibres in certain hind-limb muscles of the cat. *J Physiol (Lond)*, 151:436–57, Jun 1960.
- [27] W L Rutten, H J van Wier, and J H Put. Sensitivity and selectivity of intraneural stimulation using a silicon electrode array. *IEEE Trans Biomed Eng*, 38(2):192–8, Feb 1991.
- [28] Amin Mahnam, S Mohammad Reza Hashemi, and Warren M Grill. Measurement of the current-distance relationship using a novel refractory interaction technique. *J. Neural Eng.*, 6(3):036005, Jun 2009.
- [29] TG Sandercock. Nonlinear summation of force in cat soleus muscle results primarily from stretch of the common-elastic elements. *Journal of Applied Physiology*, 89(6):2206, 2000.
- [30] MA Lemay, D Grasse, and WM Grill. Hindlimb endpoint forces predict movement direction evoked by intraspinal microstimulation in cats. *Neural Systems and Rehabilitation Engineering, IEEE Transactions on*, 17(4):379–389, 2009. femur free.
- [31] MA Lemay and WM Grill. Modularity of motor output evoked by intraspinal microstimulation in cats. *Journal of Neurophys*, 91(1):502, 2004.
- [32] MA Lemay, M Bhowmik-Stoker, GC McConnell, and WM Grill. Role of biomechanics and muscle activation strategy in the production of endpoint force patterns in the cat hindlimb. *Journal of Biomechanics*, 40(16):3679–3687, 2007. femur fixed.
- [33] Yoichiro Aoyagi, Vivian K Mushahwar, Richard B Stein, and Arthur Prochazka. Movements elicited by electrical stimulation of muscles, nerves, intermediate spinal cord, and spinal roots in anesthetized and decerebrate cats. *IEEE Trans Neural Syst Rehabil Eng*, 12(1):1–11, Mar 2004.
- [34] Almut Branner, Richard B Stein, Eduardo Fernandez, Yoichiro Aoyagi, and Richard A Normann. Long-term stimulation and recording with a penetrating microelectrode array in cat sciatic nerve. *IEEE Trans Biomed Eng*, 51(1):146–57, Jan 2004.
- [35] Richard A Normann, Brett R Dowden, Mitchell A Frankel, Andrew M Wilder, Scott D Hiatt, Noah M Ledbetter, David J Warren, and Gregory A Clark. Coordinated, multi-joint, fatigue-resistant feline stance produced by utah slanted electrode arrays in hind limb nerves. *J Neural Eng*, (In Review), 2011.
- [36] Sean Snow, Kenneth W Horch, and Vivian K Mushahwar. Intraspinal microstimulation using cylindrical multielectrodes. *IEEE Trans Biomed Eng*, 53(2):311–9, Feb 2006.

- [37] Stephen M Lawrence, Jytte O Larsen, Kenneth W Horch, Ron Riso, and Thomas Sinkjaer. Long-term biocompatibility of implanted polymer-based intrafascicular electrodes. *J Biomed Mater Res*, 63(5):501–6, Jan 2002.
- [38] Natalia Lago, Ken Yoshida, Klaus P Koch, and Xavier Navarro. Assessment of biocompatibility of chronically implanted polyimide and platinum intrafascicular electrodes. *IEEE Trans Biomed Eng*, 54(2):281–90, Feb 2007.
- [39] Xiujun Zheng, Jian Zhang, Tongyi Chen, and Zhongwei Chen. Recording and stimulating properties of chronically implanted longitudinal intrafascicular electrodes in peripheral fascicles in an animal model. *Microsurgery*, 28(3):203–9, Jan 2008.
- [40] Gregory A Clark, Noah M Ledbetter, David J Warren, and Reid R Harrison. Recording sensory and motor information from peripheral nerves with utah slanted electrode arrays. *Conf Proc IEEE Eng Med Biol Soc*, 2011.

CHAPTER 5

CONCLUSION

Taken as a whole, the research presented in this dissertation demonstrates the fine control of the neuromuscular system that is possible with intrafascicular electrode arrays. The ability to selectively activate and deactivate individual muscles, motor units, and neural circuits enables a neuroprosthetic system to begin to approach the flexibility and precision of the intact nervous system. The work presented here has advanced the capabilities of the USEA from evoking fatigue-resistant contractions at a single joint to selectively activating muscles throughout an entire limb, and sets the stage for producing coordinated multijoint movements. This dissertation will conclude with a summary of the major findings, followed by a discussion of the limitations of the work, and finally a description of further research that would advance the capabilities of intrafascicular arrays towards clinical applications.

Summary of Major Findings

Chapter 2 extends the investigation of the selective stimulation capabilities of the USEA to the hamstring muscle group. USEAs implanted in the muscular branch of the sciatic nerve were able to selectively activate each muscle of the hamstring muscle group, including the three separate neuromuscular compartments of biceps femoris. Because the different biarticular hamstring muscles either preferentially flex or extend the limb (at the knee or hip, respectively), the ability to selectively activate each one independently will allow for control of these different actions to evoke functional movements. Activation of these muscles was graded with increasing stimulus strength and provided ample dynamic range that will allow for fine control of muscle force.

Chapter 3 demonstrates for the first time that intrafascicular electrodes are capable of selectively blocking muscle activation. High-frequency alternating currents have

been used for decades to completely abolish conduction through a nerve [1]. Although nonselective block has been achieved with intrafascicular electrodes [2], and partial block has been demonstrated with cuff electrodes [3], there has previously been no control over which parts of the nerve are blocked and thus which muscles are rendered inactive. By the delivery of high-frequency sinusoids through individual electrodes of the USEA, a specific subset of fibers in a nerve could be blocked while allowing the remainder of the nerve to function normally. Sinusoids delivered through different electrodes allowed for controlled deactivation of different muscles. The ability to selectively interrupt activity in fiber subpopulations within a nerve will provide new therapeutic options for conditions such as spasticity and neurogenic bladder.

Chapter 4 presents the use of evoked 3-D endpoint force as a noninvasive method for identifying electrodes and stimulus parameters that produce flexion and extension around each joint, as well as quantifying the degree to which each electrode excites an independent set of motor units. A USEA-based clinical FES system will include arrays implanted into several different nerves of each leg, and before any movements can be evoked, subsets of electrodes must be chosen that produce each desired action. Endpoint force enabled quantification of the effects of stimulation regardless of which muscle in the limb was activated, which allowed for rapid testing of all implanted electrodes with minimal mechanical setup. This method has already been proven effective in selecting electrodes and stimulus parameters to evoke coordinated multijoint sit-to-stand transitions in acute and chronic animal preparations [4].

Technological Developments

Taken as a whole, execution of the above research aims required stimulation via several thousand USEA electrodes, and concurrent monitoring of the evoked muscular responses. To make this experimentation feasible, it was necessary to expand our stimulation and neuromuscular monitoring capabilities. Prior to this research, it was necessary to manually connect a desired electrode to the stimulation unit, manually control the stimulation parameters, and muscle tendon force was the only output metric we had the capability to measure.

A software-controlled stimulation and recording system was developed to enable automated data collection and generation of arbitrary stimulus patterns [5, 6]. By integrating a custom-built 1100-channel stimulation unit with a Cerebus data acquisition system (Blackrock Microsystems, Salt Lake City, UT, USA), stimulus parameters could be algorithmically controlled based on the responses evoked by previous stimuli. The Cerebus system provided a means to record many different muscle output responses such as EMG, joint torque, and endpoint forces. This integrated system allowed stimulus-response curves to be collected for all electrodes on a USEA without user intervention. By removing the user from repetitive data collection, the system collected data using objective criteria making data sets more consistent between electrodes and across preparations.

The software-controlled stimulation system was designed to deliver arbitrary stimulation patterns to sets of electrodes. This capability was used to execute the refractory tests used in Chapter 4 to measure excitation overlap. Although not described in this dissertation, the multi-electrode stimulation capabilities were used to generate fatigue-resistant, coordinated limb extension for sit-to-stand transitions in cat using interleaved multi-electrode stimulation [4].

Limitations

Chapter 2 demonstrates that a USEA in the muscular branch of the sciatic nerve is capable of selectively exciting the muscles of the hamstring group. A limitation of this study is that EMG was the only metric of muscle activation. EMG provides a reliable metric of which muscle or muscles are activated by stimulation, but it does not provide a direct metric of the force or torque produced [7]. Because this study was carried out in preparation for evoking functional movements in the cat hind limb, it would be advantageous to have force or torque measurements to determine if USEA electrodes in the muscular branch of the sciatic nerve are capable of evoking sufficient torques for sit-to-stand transitions and gait. However, Chapter 2 demonstrates maximal EMG responses during some USEA stimulation, indicating maximal muscle activation. Because stance and walking require joint torques well below maximum [8], the muscle

activation evoked by USEA stimulation should be sufficient to create functional movements.

Chapter 3 presented for the first time that high-frequency alternating currents (HFAC) delivered via intrafascicular electrodes could selectively block evoked muscle activation. Perhaps the greatest limitation to this study was the lack of complete block threshold data. Ideally, Chapter 3 would present thresholds for the two observed mechanisms of block for many electrodes, averaged across all animals in the study. The nerve responds with intense tonic firing when HFAC amplitudes are just below the block threshold [9], and results in maximal tetanic activity in the muscles the nerve innervates. These tetani eventually led to severe muscle fatigue and limited the total number of trials possible in each preparation, which prevented systematic threshold measurement of both block mechanisms across many electrodes.

Although achieving block of action potential conduction was a goal of the study, conduction block was only observed in 1 animal and required seemingly very high HFAC voltages. For intrafascicular conduction block to become a viable clinical FES tool, it is imperative that the effects of this level of HFAC on the tissue and electrode be investigated. Electrodes in tissue rely on two types of charge transfer—capacitive and faradaic [10]. Capacitive charge transfer does not produce toxic ionic species in the tissue, and the ability of an electrode to transfer charge capacitively is frequency dependent. Therefore, the effects of HFAC on tissue are likely frequency dependent and warrant further experimental investigation.

The USEA has been shown to evoke highly selective muscle activation. Chapter 3 suggests that the ability of the USEA to block muscle contractions is somewhat less selective. McDonnall and colleagues report that, on average, 30% of electrodes tested could selectively activate a single muscle to maximum force [11], whereas only 18% of the electrodes tested in the block study presented in Chapter 3 were able to selectively block a single muscle without activating any other muscles.

Because the threshold for tonic activation is just below the threshold for block, many electrodes tested were unable to block activation of one or more muscles without activating others. This implies that it may not be possible to block a subset of fibers

within a fascicle without activating other fibers within the same fascicle. Systematic investigation into this hypothesis could determine the selectivity limits of block using intrafascicular electrodes, and would have important implications for which clinical applications are most suitable for this technique.

Chapter 4 presented a noninvasive means to characterize the muscle responses evoked throughout the limb by three electrode arrays. The minimal mechanical restraint of the limb allowed each electrode to be classified as evoking limb flexion or limb extension using automated stimulation routines and limited setup. However, the simplicity of the mechanical restraint came at the cost of a lower signal-to-noise ratio. The restraint did not fully immobilize the limb, and correspondingly, there were substantial oscillations present in the force responses measured in response to the single stimuli delivered throughout the study. Although low-pass filtering greatly reduced these oscillations, the remaining oscillations contaminated the recordings and potentially limited the accuracy of electrode classification and stimulus-response characterization.

Future Work

The ability to block conduction through a portion of a nerve is a promising option for patients with spasticity. It is now well documented that HFAC can block action potential conduction in animals, and Chapter 3 of this dissertation demonstrates that block can be selective. However, it still remains to be demonstrated that HFAC can ameliorate the motor deficits caused by spasticity in human patients. The next step in block research is to test whether HFAC can abolish spastic muscle tone in humans. Animal studies of block use a simple experimental paradigm where HFAC is delivered to a peripheral nerve between the innervated muscle and an upstream electrode that excites the entire nerve. The pathophysiology of spasticity is much more nuanced than this experimental setup, and can vary depending on the cause of spasticity [12].

Because HFAC has not been tested in humans for spasticity management—and because it would be an invasive procedure involving delivery of electric currents—HFAC experiments would need to be included in a procedure where surgical exposure and ablation of neural tissue is already planned. I recently had the opportunity

to observe a selective dorsal rhizotomy (SDR) procedure, and this procedure would be an exciting avenue with which to test the ability of HFAC to abolish spastic muscle contractions. Because spasticity is thought to occur from hyper-excitability of the stretch reflex, the goal of the SDR procedure is to identify and disrupt spastic circuits by cutting selected dorsal rootlets. Dorsal rootlets innervating a region of spasticity are exposed and stimulated to test if they evoke a spastic motor response. A clinician monitors the response of the limb to the stimulation via palpitation and EMG recordings. Stimulation of rootlets that are part of a normal reflex circuit will result in a brief motor response. Stimulation of rootlets that are part of a spastic circuit will result in a prolonged and powerful motor response.

The surgical exposure of the dorsal rootlets and the diagnosis of spastic versus normal motor responses make the SDR procedure an ideal situation for initial testing of HFAC for spasticity management. Once a rootlet is identified that is part of a spastic circuit, a second set of electrodes could be used to deliver HFAC to the proximal portion of the rootlet to see if it abolished the spastic motor response. Although SDR is an attractive setting for testing the ability of HFAC to abolish spastic motor responses, the ideal clinical application of HFAC for spasticity may not involve electrode implantation onto spinal rootlets. Because the exposure and microdissection of spinal rootlets is a complex and time-consuming procedure, it may be simpler to target peripheral nerves as a location of HFAC delivery for spasticity management. However, if HFAC were effective at blocking spasticity in the SDR setting, it would provide experimental justification for exploring other avenues of HFAC delivery in human subjects.

One major limiting factor for the use of USEAs in clinical FES systems is the need for transcutaneous delivery of stimulus currents. Presently, the leads of the USEA are routed to a bone-mounted connector that spans the skin [13]. Transcutaneous wires or connectors pose an infection risk [14], and SCI patients place a high priority on cosmesis [15]; therefore, a fully implantable stimulation system is highly desirable. An FES system for upper limb control has been developed that includes fully implanted electrodes and a stimulation unit that is controlled by an external module [16]. This

system provided improved function and was well accepted by users, with over 90% of the patients using the system regularly for several years [17]. A wireless recording system for the USEA is under development [18], and a version of this system has been used to record wirelessly from awake, behaving, nonhuman primates [19]. A wireless stimulation system is under development as well [20]; however, a fully implantable stimulation system for the USEA does not yet exist and remains a key obstacle for a USEA-based clinical FES system.

The complexity and unpredictability of movement involved in daily life demand an FES system with feed-back control. Current FES systems use various forms of open-loop finite-state control strategies to produce sit-to-stand transitions and gait [21, 22]. Although closed-loop techniques are being developed to achieve unsupported standing in paraplegic patients [23], current open-loop systems rely on upper body support for balance. Yoshida and Horch demonstrated that closed-loop control of FES stimulation is possible using intrinsic sensory feed back [24], and work has continued to improve estimations of muscle length and limb position using activity recorded from sensory neurons [25, 26, 13].

Because intrafascicular electrode arrays provide access to many motor unit populations, they have the potential to improve the performance of current FES systems. However, the performance potential of this highly-selective access has been limited by the lack of a control strategy that can combine activation of many muscles using interleaved stimulation to generate graceful, fatigue-resistant movements. A recent study demonstrated a proportional multi-input single-output control strategy that could accurately track desired isometric force profiles using interleaved stimulation of USEA electrodes [27]. Although isometric force control is not novel, this study demonstrated closed-loop control of interleaved stimulation for the first time. Extension of this work to dynamic multi-joint movements would greatly advance the USEA towards clinical FES implementation.

In conclusion, intrafascicular electrode arrays provide comprehensive and selective access to the neuromuscular system that could greatly enhance the performance of current FES systems. The work presented in this dissertation has leveraged the

selectivity of the Utah Slanted Electrode Array to excite muscles throughout an entire limb and also block activation of selected muscles. The ability to noninvasively characterize the muscle responses evoked by several hundred implanted electrodes has set the stage for evoking coordinated, multijoint, fatigue-resistant movements.

References

- [1] JA Tanner. Reversible blocking of nerve conduction by alternating-current excitation. *Nature*, 195:712–3, Aug 1962.
- [2] D Michael Ackermann, Emily L Foldes, Niloy Bhadra, and Kevin L Kilgore. Conduction block of peripheral nerve using high-frequency alternating currents delivered through an intrafascicular electrode. *Muscle Nerve*, 41(1):117–9, Jan 2010.
- [3] K L Kilgore and N Bhadra. Nerve conduction block utilising high-frequency alternating current. *Med Biol Eng Comput*, 42(3):394–406, May 2004.
- [4] Richard A Normann, Brett R Dowden, Mitchell A Frankel, Andrew M Wilder, Scott D Hiatt, Noah M Ledbetter, David J Warren, and Gregory A Clark. Coordinated, multi-joint, fatigue-resistant feline stance produced by utah slanted electrode arrays in hind limb nerves. *J Neural Eng*, (In Review), 2011.
- [5] Andrew M Wilder, Scott D Hiatt, Brett R Dowden, Nicholas A T Brown, Richard A Normann, and Gregory A Clark. Automated stimulus-response mapping of high-electrode-count neural implants. *IEEE Trans Neural Syst Rehabil Eng*, 17(5):504–11, Oct 2009.
- [6] Scott D Hiatt, Andrew M Wilder, K Shane Guillory, Brett R Dowden, Richard A Normann, and Gregory A Clark. 1100-channel neural stimulator for functional electrical stimulation using high-electrode-count neural interfaces. *IFESS Abstract*, pages 1–3, Jul 2010.
- [7] A C Guimaraes, W Herzog, M Hulliger, Y T Zhang, and S Day. Emg-force relationship of the cat soleus muscle studied with distributed and non-periodic stimulation of ventral root filaments. *J Exp Biol*, 186:75–93, Jan 1994.
- [8] Lisa N MacFadden. *Musculoskeletal Modeling for Intrafascicular Multielectrode Stimulation of the Feline Hindlimb*. PhD thesis, University of Utah, 2009.
- [9] B R Bowman and D R McNeal. Response of single alpha motoneurons to high-frequency pulse trains. firing behavior and conduction block phenomenon. *Appl Neurophysiol*, 49(3):121–38, Jan 1986.
- [10] Daniel R Merrill, Marom Bikson, and John G R Jefferys. Electrical stimulation of excitable tissue: design of efficacious and safe protocols. *J Neurosci Methods*, 141(2):171–98, Feb 2005.
- [11] Daniel McDonnall, Gregory A Clark, and Richard A Normann. Selective motor unit recruitment via intrafascicular multielectrode stimulation. *Can J Physiol Pharmacol*, 82(8-9):599–609, Jan 2004.
- [12] Sherif M Elbasiouny, Daniel Moroz, Mohamed M Bakr, and Vivian K Mushahwar. Management of spasticity after spinal cord injury: current techniques and future directions. *Neurorehabil Neural Repair*, 24(1):23–33, Jan 2010.

- [13] Gregory A Clark, Noah M Ledbetter, David J Warren, and Reid R Harrison. Recording sensory and motor information from peripheral nerves with Utah slanted electrode arrays. *Conf Proc IEEE Eng Med Biol Soc*, 2011.
- [14] J Thomas Mortimer and Narendra Bhadra. Peripheral nerve and muscle stimulation. *Neuroprosthetics: Theory and Practice. World Scientific Pub Co Inc*, Nov 2004.
- [15] Kim D Anderson. Consideration of user priorities when developing neural prosthetics. *J Neural Eng*, 6(5):055003, Oct 2009.
- [16] P Hunter Peckham, Kevin L Kilgore, Michael W Keith, Anne M Bryden, Niloy Bhadra, and Fred W Montague. An advanced neuroprosthesis for restoration of hand and upper arm control using an implantable controller. *J Hand Surg Am*, 27(2):265–76, Mar 2002.
- [17] P H Peckham, M W Keith, K L Kilgore, J H Grill, K S Wuolle, G B Thrope, P Gorman, J Hobby, M J Mulcahey, S Carroll, V R Hentz, A Wiegner, and Implantable Neuroprosthesis Research Group. Efficacy of an implanted neuroprosthesis for restoring hand grasp in tetraplegia: a multicenter study. *Arch Phys Med Rehabil*, 82(10):1380–8, Oct 2001.
- [18] Reid R Harrison, Ryan J Kier, Cynthia A Chestek, Vikash Gilja, Paul Nuyujukian, Stephen Ryu, Bradley Greger, Florian Solzbacher, and Krishna V Shenoy. Wireless neural recording with single low-power integrated circuit. *IEEE Trans Neural Syst Rehabil Eng*, 17(4):322–9, Aug 2009.
- [19] Cynthia A Chestek, Vikash Gilja, Paul Nuyujukian, Ryan J Kier, Florian Solzbacher, Stephen I Ryu, Reid R Harrison, and Krishna V Shenoy. HermesC: low-power wireless neural recording system for freely moving primates. *IEEE Trans Neural Syst Rehabil Eng*, 17(4):330–8, Aug 2009.
- [20] Brandon Kimball Thurgood, David J Warren, Noah M Ledbetter, Gregory A Clark, and Reid R Harrison. A wireless integrated circuit for 100-channel charge-balanced neural stimulation. *Biomedical Circuits and Systems, IEEE Transactions on*, 3(6):405 – 414, 2009.
- [21] Lee E Fisher, Michael E Miller, Stephanie N Bailey, John A Davis, James S Anderson, Lori Rhode, Dustin J Tyler, and Ronald J Triolo. Standing after spinal cord injury with four-contact nerve-cuff electrodes for quadriceps stimulation. *IEEE Trans Neural Syst Rehabil Eng*, 16(5):473–8, Oct 2008.
- [22] Anirban Dutta, Rudi Kobetic, and Ronald J Triolo. Gait initiation with electromyographically triggered electrical stimulation in people with partial paralysis. *J Biomech Eng*, 131(8):081002, Aug 2009.
- [23] Hamid-Reza Kobravi and Abbas Erfanian. A decentralized adaptive fuzzy robust strategy for control of upright standing posture in paraplegia using functional electrical stimulation. *Medical Engineering & Physics*, Jul 2011.

- [24] K Yoshida and K Horch. Closed-loop control of ankle position using muscle afferent feedback with functional neuromuscular stimulation. *IEEE Trans Biomed Eng*, 43(2):167–76, Feb 1996.
- [25] Milan Djilas, Christine Azevedo-Coste, David Guiraud, and Ken Yoshida. Interpretation of muscle spindle afferent nerve response to passive muscle stretch recorded with thin-film longitudinal intrafascicular electrodes. *IEEE Trans Neural Syst Rehabil Eng*, 17(5):445–53, Oct 2009.
- [26] J Rigosa, D J Weber, A Prochazka, R B Stein, and S Micera. Neuro-fuzzy decoding of sensory information from ensembles of simultaneously recorded dorsal root ganglion neurons for functional electrical stimulation applications. *Journal of Neural Engineering*, 8(4):046019, Jun 2011.
- [27] Mitchell A Frankel, Brett R Dowden, V John Mathews, Richard A Normann, Gregory A Clark, and Sanford G Meek. Multiple-input single-output closed-loop isometric force control using asynchronous intrafascicular multi-electrode stimulation. *IEEE Trans Neural Syst Rehabil Eng*, 19(3):325–32, Jun 2011.